



This is to certify that the
 thesis entitled
 MICROFILTRATION PROCESS FOR ENHANCED PRODUCTION
 OF rDNA RECEPTOR CELLS OF *ESCHERICHIA COLI*

presented by

KEVIN WARREN ANDERSON

has been accepted towards fulfillment
 of the requirements for

M.S. degree in Chemical
Engineering

Eric A. Brulke

Major professor

Date December 22, 1983



RETURNING MATERIALS:

Place in book drop to
remove this checkout from
your record. FINES will
be charged if book is
returned after the date
stamped below.

--	--	--

MICROFILTRATION PROCESS FOR ENHANCED PRODUCTION
OF rDNA RECEPTOR CELLS OF *ESCHERICHIA COLI*

By

Kevin Warren Anderson

A THESIS

Submitted to
Michigan State University
in partial fulfillment of the requirements
for the degree of

MASTER OF SCIENCE

Department of Chemical Engineering

1983

Copyright by
KEVIN WARREN ANDERSON
1984

ABSTRACT

MICROFILTRATION PROCESS FOR ENHANCED PRODUCTION
OF rDNA RECEPTOR CELLS OF *ESCHERICHIA COLI*

By

Kevin Warren Anderson

Escherichia coli HB101 was cultured in a micro-filtration fermentor system to five times the density obtained in a control batch system. A synthetic glucose-salts medium was fed continuously into the aerated culture, and spent medium and products were continuously removed at the same rate through the microfiltration unit so that culture volume remained constant.

The influence of hydraulic residence time and feed composition on the unsteady state growth of cells, consumption of nutrients and production of acids was studied.

The culture exhibited changes in aerobic metabolism from aerobic fermentation to respiration depending on the glucose concentration in the culture. When glucose was in excess, aerobic fermentation occurred and mixed acids accumulated. When glucose was limiting or exhausted, a respiratory metabolism predominated with low acid production rates.

ACKNOWLEDGMENTS

I wish to express my appreciation to Dr. Eric A. Grulke for his help and guidance throughout my graduate studies and research and to Dr. Philipp Gerhardt from the Department of Microbiology for his guidance and use of his facilities.

I wish to thank Drexelbrook Engineering Co. for their donation of a liquid level transmitter for use on this project and Mr. Dale Hauk of Gelman Sciences for assistance in the use of their products. I am further grateful to Dr. C. A. Reddy of the Department of Microbiology for use of equipment in his lab and Sue Cuppett of the Department of Food Science for advise on gas chromatography. I also acknowledge advise given by Dr. Donald K. Anderson and Dr. K. Jayaraman, both of the Department of Chemical Engineering, on process control applied in this investigation for which I am grateful.

I acknowledge financial support from grant DAR 79-10236 (to Dr. Philipp Gerhardt) from the U. S. National Science Foundation.

TABLE OF CONTENTS

	<u>Page</u>
1. List of Tables	vi
2. List of Figures	vii
3. Nomenclature	ix
3.1 Nomenclature used in Literature Review	ix
3.2 General Nomenclature	x
4. Introduction	1
5. Literature Review	3
5.1 Kinetics of Microbial Growth	3
5.1.1 Lag Phase	4
5.1.2 Exponential Growth Phase	5
5.1.2.1 Unstructured Models	6
5.1.2.2 Structured Models	9
5.1.3 Stationary Phase	12
5.1.4 Death Phase	13
5.2 Growth Kinetics of <i>Escherichia coli</i>	14
5.3 Membrane Enhancement of Microbial Cultivation	15
5.3.1 Dialysis	16
5.3.2 Microfiltration	16
5.4 Liquid Level Control	20
6. Materials and Methods	23
6.1 Organism and Culture Conditions	23
6.2 Analytical Methods	24
6.2.1 Optical Density	24
6.2.2 Viable Cell Counts	24
6.2.3 Cell Dry Weight	25
6.2.4 Ammonia	25
6.2.5 Glucose	30
6.2.6 Volatile Fatty Acids	31
6.2.7 Non-Volatile Acids	34
6.3 Experimental Microfiltration System and Procedure	39
6.4 Liquid Level Control	45
6.4.1 Control Loop Analysis	47

	<u>Page</u>
7. Results and Discussion	51
7.1 Experimental Results and Discussion	51
7.1.1 Control Batch Cultivation:	
Experiment 1	52
7.1.2 Microfiltration Cultivation	60
7.1.2.1 Long Residence Time Micro-	
filtration: Experiment 2	62
7.1.2.2 Moderate Residence Time	
Microfiltration: Experi-	
ment 3	70
7.1.2.3 Short Residence Time Micro-	
filtration: Experiment 4	76
7.2 Mathematical Model and Computer	
Simulation	82
7.2.1 Mathematical Model	82
7.2.2 Kinetic Parameter Estimation	85
7.2.3 Computer Simulation	90
7.2.3.1 Batch Growth Simulation	91
7.2.3.2 Experiment 2 Simulation	91
7.2.3.3 Experiment 3 Simulation	96
7.2.3.4 Experiment 4 Simulation	105
8. Conclusion	111
8.1 Equipment Considerations	111
8.2 Metabolic Considerations	112
8.3 Cell Productivity Considerations	113
8.4 Modeling Considerations	113
9. Recommendations	115
10. Appendices	116
Appendix I: Standard Data	116
Appendix II: Sample Calculations	123
Appendix III: Numerical Data	126
Appendix IV: Level Control Loop Start-Up	
Procedures and Schematic Diagram	131
Appendix V: Computer Program and Output	134
11. Literature Cited	141
12. Materials Bibliography	146

LIST OF TABLES

<u>Table</u>		<u>Page</u>
1	Non-Volatile Acid Identification	38
2	Summary of Microfiltration Experiments	51
3	Early Exponential Growth Phase Specific Growth Rates (hr^{-1})	86
4	Kinetic Parameters for the Mathematical Model	90
A1	Computation of Non-Volatile Acid Concentrations	125
A2	Numerical Data for Experiment 1	127
A3	Numerical Data for Experiment 2	128
A4	Numerical Data for Experiment 3	129
A5	Numerical Data for Experiment 4	130
A6	Computer Program and Simulated Results	134

LIST OF FIGURES

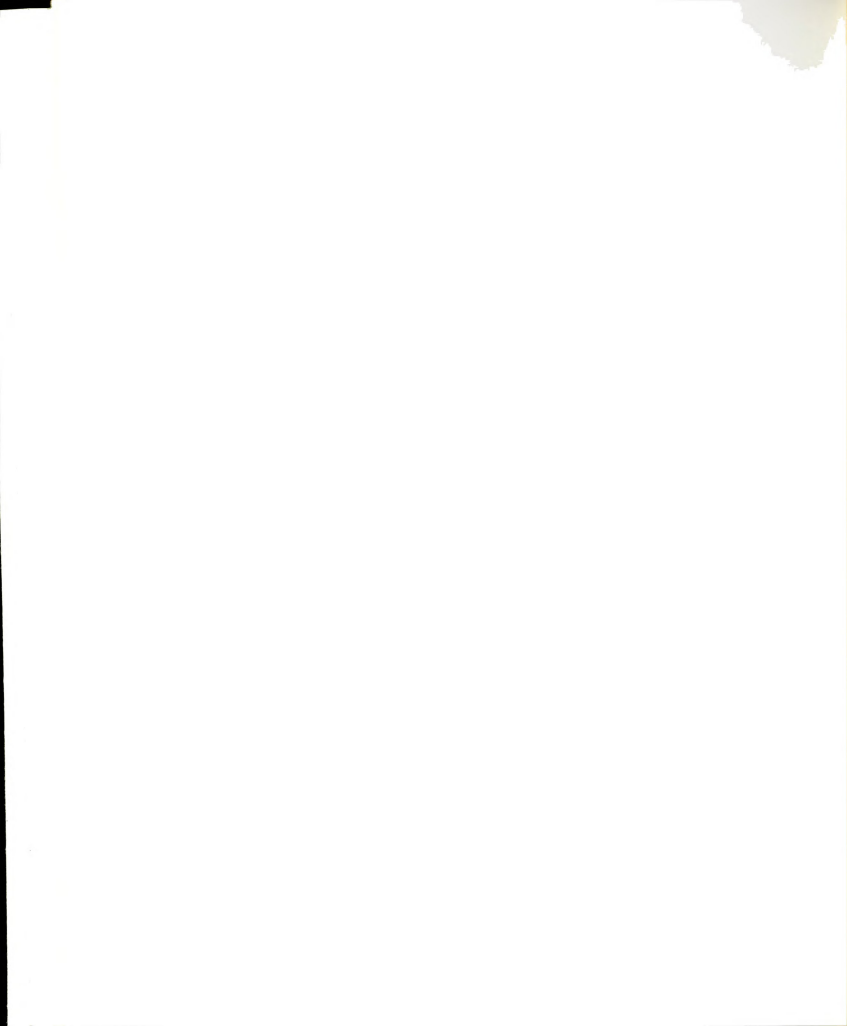
<u>Figure</u>		<u>Page</u>
1	Comparison of the Dialysis Culture System and the Microfiltration System	18
2	Cell Dry Weight vs. Optical Density at 600 nm (O.D. ₆₀₀) Standard Curve	26
3	Ammonium Ion Absorption Spectrum	29
4	Volatile Fatty Acid Chromatograms	33
5	Non-Volatile Acid Chromatograms	37
6	Experimental Process Flow Diagram and Photograph	41
7	Photograph of the Acroflux Capsule	44
8	Level Control Loop Diagram	46
9	Level Control Block Diagram	48
10	Pump Speed (R) vs. Controller Output Current (I_D)	50
11	Results of Experiment 1	54
12	Proposed Modification of the TCA Cycle to a Branched Pathway for Exponentially Growing <i>E. coli</i> Under Aerobiosis (adapted from Amarsingham and Davis, 1965)	58
13	Cut-Away View of the Modified Gelman Acroflux Capsule	61
14	Results of Experiment 2	65
15	Metabolic Shifts in <i>E. coli</i> under Aerobic Conditions	69
16	Results of Experiment 3	72
17	Results of Experiment 4	78

<u>Figure</u>		<u>Page</u>
18	Cell Dry Weight (X_f) vs. Viable Cells (N_f) Concentrations from Experiment 1	87
19	Computer Simulation of Experiment 1	93
20	Computer Simulation of Experiment 2	98
21	Computer Simulation of Experiment 3	102
22	Computer Simulation of Experiment 4	107
A1	Glucose Standard Curves	117
A2	Ammonium Ion Standard Curves	119
A3	Standard Curves for Acetic Acid	120
A4	Standard Curve for Propionic Acid	121
A5	Non-Volatile Acid Standard Curves for Experiment 4	122
A6	Level Control Loop Schematic Diagram	132

NOMENCLATURE

3.1 Nomenclature used in Literature Review

<u>Symbol</u>		<u>Units</u>
a	maintenance metabolism parameter	hr ⁻¹
A	constant	gl ⁻¹ hr ⁻²
ATP	concentration of adenosine tri-phosphate	mole l ⁻¹
b	quantitative index of the Pasteur effect	dimensionless
B	constant	hr ⁻¹
C	constant in equation 11	gl ⁻¹ hr ⁻¹
C	constant	mole g ⁻¹
C _L	percent saturation of O ₂	dimensionless
C ₁	constant	mole g ⁻¹
C ₂	constant	mole mole ⁻¹
E _d	activation energy for death	kcal mole ⁻¹
F _d	filtrate flow rate	l hr ⁻¹
F _f	feed rate to fermentor	l hr ⁻¹
F _f	purge rate	l hr ⁻¹
F _r	feed rate to reservoir	l hr ⁻¹
-k _d	specific death rate	hr ⁻¹
-k _{d0}	standard specific death rate	hr ⁻¹
K _i	inhibition constant	g l ⁻¹
K _i	oxygen saturation constant	dimensionless
K _L	substrate saturation constant	g l ⁻¹
K _S	product inhibition constant	l g ⁻¹
n ₁	exponent in equation 8	dimensionless
N	viable cell number	cells l ⁻¹
N ₀	initial viable cell number	g l ⁻¹
P	product concentration	g l ⁻¹
P _{max}	maximum product concentration allowing growth	g l ⁻¹
r	rate of growth	g l ⁻¹ hr ⁻¹
r ^g	rate of product formation	g l ⁻¹ hr ⁻¹
-r ^p	rate of substrate utilization	g l ⁻¹ hr ⁻¹
R ^s	universal gas constant	k cal mole ⁻¹ K ⁻¹
S	substrate concentration	g l ⁻¹
t	time	hr
t _{lag}	lag time	hr
T	temperature	K
V _f	fermentor volume	l
V _G	velocity of glycolysis	hr ⁻¹
V _{GM}	maximum velocity of glycolysis	hr ⁻¹
V _{GM}	reservoir volume	l
V _R	velocity of respiration	mole g ⁻¹ hr ⁻¹



SymbolUnits

V_{RM}	maximum velocity of respiration	$\text{mole g}^{-1} \text{hr}^{-1}$
X	cell dry mass concentration	g l^{-1}
X_0	initial cell dry mass concentration	g l^{-1}
Y	cell growth yield	g l^{-1}

Greek Letters

α	product yield	g cell^{-1}
β	product formation by maintenance metabolism	$\text{g cell}^{-1} \text{hr}^{-1}$
μ	specific growth rate	hr^{-1}
μ_{max}	maximum specific growth rate	hr^{-1}

Other Subscripts

G	glycolytic quantity
R	respiratory quantity

3.2 General Nomenclature

A_f	ammonium ion concentration in feed	g l^{-1}
A_f^0	ammonium ion concentration	g l^{-1}
A_f	cross sectional area of fermentor (equation 23)	cm^2
\hat{F}_d	deviation of filtrate flow rate from steady state rate	l hr^{-1}
F_f	nutrient feed rate	l hr^{-1}
\hat{F}_f	deviation of feed rate from steady state rate	l hr^{-1}
G	controller transfer function	mA mA^{-1}
G_C	filter transfer function	rpm hr^{-1}
G_f	motor and pump transfer function	mA rpm^{-1}
G^m	process transfer function	in hr l^{-1}
G^p	controller output current	mA
\hat{I}_D	deviation of controller output current from steady state current	mA
K	proportional gain	mA mA^{-1}
K_C	substrate saturation constant	g l^{-1}
K_S	transmitter gain	mA cm^{-1}
\hat{L}^T	deviation in fermentor liquid level from steady state	cm
L_{set}	deviation in fermentor liquid level from set point	cm
m_C	single cell mass	g
N_f^C	viable cell count as colony forming units	cells ml^{-1}



Symbol

		<u>Units</u>
P_f	acetic acid concentration in fermentor	$g\ l^{-1}$
P_{f_0}	acetic acid concentration in feed	$g\ l^{-1}$
$-r_{f_0}^A$	rate of ammonium ion utilization	$g\ l^{-1}hr^{-1}$
r^g	rate of growth	$g\ l^{-1}hr^{-1}$
r^p	rate of product formation	$g\ l^{-1}hr^{-1}$
$-r^s$	rate of glucose utilization	$g\ l^{-1}hr^{-1}$
R^s	pump speed	rpm
\hat{R}	deviation in pump speed from steady state speed	rpm
s	Laplace transform independent variable	
S_f	residual glucose concentration in fermentor	$g\ l^{-1}$
S_{f_0}	glucose concentration in the feed	$g\ l^{-1}$
t	time	hr
X_f	cell dry weight concentration	$g\ l^{-1}$

Greek Letters

α_A	ammonium ion consumption coefficient	$g\ g^{-1}$
α_S	glucose consumption coefficient	$g\ g^{-1}$
β	maintenance metabolism parameter	$g\ g^{-1}hr^{-1}$
γ	acetic acid yield coefficient	$g\ g^{-1}$
τ_D	controller derivative action	hr
τ_I	controller integral action	hr
τ_H	hydraulic residence time	hr
μ_{max}	maximum specific growth rate	hr^{-1}

INTRODUCTION

The large scale production and recovery of new products made available by recombinant DNA technology will create new problems in process design and manufacturing. Desired products may be retained in the cell (intracellular) or released to the environment (extracellular). The new genetic information may handicap the receptor organism, and wild type revertants would have a selective advantage. Nutrient, temperature, and pH requirements of the organism must be satisfied in order to provide a suitable environment for growth. All of these factors are important when considering the production and recovery of these biological products.

The usual method for production of biological products consists of a batch fermentation in large vessels with subsequent recovery steps to purify the desired products. If higher density populations of cells within the fermentor could be obtained, then smaller scale equipment would be required or an existing process could be improved.

Growth is typically limited in the batch fermentor either by depletion of a particular nutrient and/or the accumulation of toxic end products of metabolism. Proposed methods for minimizing these two effects have primarily involved membrane techniques. Dialysis culture involves the simultaneous transfer of nutrients into the fermentor and removal of inhibitory end products under the influence of a concentration gradient across a cell impermeable membrane.

Since diffusion coefficients of solutes in liquids are low, large membrane areas are required to alleviate mass transfer limitations. This problem of dialysis may be overcome by direct addition of fresh medium to the fermentor and bulk removal of spent medium containing metabolic end products by microfiltration.

The objectives of this research were: (1) to determine the technical feasibility of operating a microfiltration fermentor system to enhance the growth of rDNA receptor cells of *Escherichia coli* including the development of a workable liquid level control system; (2) to analyze how the metabolism of the organism responds to the culture conditions encountered in the system; (3) to determine if higher productivity, reflected in higher cell populations, can be achieved relative to batch culture; and (4) formulate a mathematical model describing the unsteady state process of growth with computer simulation of the experimental results.

LITERATURE REVIEW

The literature review encompasses the work done by previous investigators on the objectives set forth in this investigation. These included the kinetic aspects of microbial growth, and specifically that of *Escherichia coli*, membrane enhancement of microbial cultivation, and liquid level control.

5.1 Kinetics of Microbial Growth

The successful mathematical description of a system undergoing chemical reaction requires a thorough understanding of the reaction kinetics. Microbial growth poses a challenge in developing kinetic models valid under all culture conditions. The numerous biochemical pathways and hundreds of reaction intermediates would make analysis of each elementary step and the associated transport processes a formidable if not impossible task.

Many approaches have been taken in kinetic modeling resulting in a variety of classes of models (Kossen, 1979). Typically these models predict only certain phases of growth or apply to a small group of organisms.

The events that occur during the growth of a population of cells can best be described in reference to a batch culture. In general, four different phases are noted: lag phase, exponential growth phase, stationary phase, and death phase.



5.1.1 Lag Phase. When fresh medium is inoculated with cells, exponential growth does not occur immediately. Rather a period of little or no growth occurs which is termed lag phase. If an organism is presented with two or more substrates, growth will occur preferentially on one until depletion. A second lag phase ensues, and then growth occurs on the second substrate (diauxic growth). Chesney (1916) attributed the cause of lag phase to either intracellular or extracellular mechanisms.

The transfer from lag to exponential growth phase is not always abrupt. Lodge and Hinshelwood (1943) proposed the following definition of the lag time, t_{lag} ,

$$t_{lag} = t - \frac{1}{\mu} \ln \frac{N}{N_0} \quad (1)$$

where N_0 is the cell number upon inoculation, N is the cell number at time t in exponential growth phase, and μ is the specific growth rate early in exponential growth phase.

The hypothesis that extracellular mechanisms control lag phase is supported by the reported inverse dependence of lag phase on inoculum size (Penfold, 1914; Lodge and Hinshelwood, 1943). Some substance is required in the medium such as extracellular enzymes or growth factors, before exponential growth can occur. A large inoculum would provide more cells contributing to the pool of that substance in the bulk medium. Lodge and Hinshelwood (1943) proposed that lag phase ended when the "active substance" reached some critical value. The study of lag phase in



Streptococcus sanguis by Repaske, Repaske, and Mayer (1974) showed a dependence on carbon dioxide concentration. Media stripped of carbon dioxide required endogenous carbon dioxide to accumulate to end lag phase. Media supplemented with carbon dioxide eliminated lag phase. Other extracellular substances have been shown important in determining lag time and were reviewed by Pamment and Hall (1978).

The physiological state of the cell has also been found important in determining lag time supporting the intracellular hypothesis of lag phase. Pamment and Hall (1978) found little dependence of lag time on inoculum size in *Saccharomyces cerevisiae* rather the concentration of key glycolytic and respiratory enzymes in the parent cells were important. Pamment, Hall, and Barford (1978) improved on the growth models of Bijkerk and Hall (1977) to include changes in glycolytic and respiratory activity in an attempt to account for lag phase. Similarly Swanson, *et al.* (1966) noted the importance of biochemical products in control of lag phase.

5.1.2 Exponential Growth Phase. Once the cells have made all necessary physiological adjustments to the media, exponential growth begins. The exponential growth phase is characterized by constant relative concentrations of all metabolites in the cell (Monod, 1949) and is termed the period of "balanced growth".

Many kinetic models describing exponential growth phase have been proposed, some of which may predict other phases as well. Two of the classes of models described by Kossen

(1979) are of particular interest; the unstructured and structured models. The unstructured models view the cell as a single compartment. The cell may be divided into two or more compartments giving a structured model.

5.1.2.1 Unstructured Models . These models are widely popular due to their ability to fit experimental data. Yang and Humphrey (1975) found that five different models could fit their data equally well for the growth of *Pseudomonas putida* and *Trichosporon cutaneum* on phenol.

The simplest unstructured model for the growth rate of cell mass in a batch fermentor is given by (see for example Stanier, Adelberg, and Ingraham, 1976),

$$\frac{dX}{dt} = r_g = \mu X \quad (2)$$

where μ is the specific growth rate, X is the cell dry mass concentration, r_g is the growth rate per unit volume and t is time. If μ is constant, then equation (2) can be integrated with the initial condition $X = X_0$ at $t = 0$ to give

$$X = X_0 e^{\mu t}. \quad (3)$$

Equation 3 predicts unbounded increase in cell mass with time. In practice this does not occur usually due to depletion of essential nutrients or accumulation of inhibitory end products. The specific growth rate is also a function of temperature, pH, and the media composition for any particular organism. Numerous unstructured models for the specific growth rate have been developed to account for these effects and were reviewed by Bailey and Ollis (1977).

Monod (1949) proposed that the specific growth rate was a function of limiting substrate concentration, with all other essential nutrients in excess, given by

$$\mu = \mu_{\max} \left(\frac{S}{S+K_s} \right). \quad (4)$$

Temperature and pH effects are contained in the term μ_{\max} (the maximum specific growth rate) and K_s is the substrate saturation constant equal to the substrate concentration supporting growth at half the maximum rate. This equation is similar to the Michaelis-Menten equation for first order enzyme reactions or the Langmuir adsorption isotherm.

The effect of ethanol on the growth of baker's yeast resembles noncompetitive enzyme inhibition (Aiba, Shoda, and Nagatani, 1968). Coulman, Stieber, and Gerhardt (1977) adapted the rate expression for noncompetitive enzyme inhibition to describe the effect of lactic acid on *Lactobacillus bulgaricus* to give

$$\mu = \mu_{\max} \left(\frac{S}{S+K_s} \right) \left(\frac{K_i}{K_i+P} \right) \quad (5)$$

where P is the inhibitory product concentration and K_i is the inhibition constant.

This model has also been applied to growth on inhibitory substrates (Andrews, 1968; Yang and Humphrey, 1975; and others). Assuming $K_i \gg K_s$, equation (5) becomes

$$\mu = \frac{\mu_{\max}}{1 + K_s/S + S/K_i} \quad (6)$$

for inhibitory substrates.

Aiba *et al.* (1968) and Levenspiel (1980) proposed other forms to include product inhibition. The definitions of the symbols are given in the literature review.

$$\text{Aiba, et al.: } \mu = \mu_{\max} \left(\frac{S}{S+K_S} \right) e^{-K_1 P} \quad (7)$$

$$\text{Levenspiel : } \mu = \mu_{\max} \left(\frac{S}{S+K_S} \right) \left(1 - \frac{P}{P_{\max}} \right)^n \quad (8)$$

These models require knowledge of the substrate and product concentrations as functions of time and hence are models for the intrinsic rates of substrate utilization and product formation.

Monod (1949) found that the total yield of cells in a batch culture was linearly related to the amount of limiting nutrient consumed and was independent of the concentration of nutrient. If the yield is also independent of the growth rate, then the rate of substrate utilization, $-r_s$ (the rate of formation of any component is taken as +), is given by

$$-r_s = \frac{1}{Y} \frac{dX}{dt} \quad (8)$$

where Y is the cell growth yield.

If the limiting substrate is the carbon and energy source, then non-growth associated reactions would consume some of the substrate. Motility requirements, repair of cellular damage, and other mechanisms that tend to increase the entropy of the cell require additional expenditure of energy. Marr, Nilson, and Clark (1963) included a term, independent of the growth rate, to account for this maintenance requirement (a) in equation (9).

$$-r_s = \frac{1}{Y} \left(\frac{dX}{dt} + aX \right) \quad (9)$$

The rate of formation of products, r_p , with inhibitory effects on the growth kinetics have been studied. Leudeking and Piret (1959) found the rate of lactic acid formation in cultures of *Lactobacillus delbrueckii* to be described by

$$r_p = \alpha \frac{dN}{dt} + \beta N \quad (10)$$

where α is the product yield and β is the product formation by maintenance metabolism where both depend on pH.

Holzberg, Finn, and Stienkraus (1967) studied the kinetics of ethanol formation in *S. cerevisiae* and found that during exponential growth,

$$r_p = A \frac{\ln N}{\mu} - BP - C \quad (11)$$

where A, B, and C are arbitrary constants.

The unstructured models fail to describe the transient phenomena that occur in other reactor situations such as the continuous stirred tank reactor (Mateles, Ryu, and Yasuda, 1965; Endo, Nagamune and Inoui, 1981). This deficiency is inherent in the unstructured models because they assume no physiological changes occur within the cell during growth so the concept of balanced growth does not always apply.

5.1.2.2 Structured Models. In reality the cell is composed of many biochemical pathways with finely tuned control mechanisms that optimize its chance for survival in its environment. Studies by Beck and von Myenberg (1968) with



S. cerevisiae in batch and continuous culture have shown that large variations in the activities of certain enzymes occur during growth. Clearly structured models that account for these changes would be more appropriate in describing the kinetics of microbial growth.

Several attempts have been made to develop structured models to include the metabolic pathways and their control mechanisms in the growth of *S. cerevisiae* (Peringer, *et al.*, 1973; Bijkerk and Hall, 1977). These models successfully describe experimental data and can give some additional insight into the physiological nature of the microbial cell.

Peringer, *et al.* (1973) studied the aerobic growth of *S. cerevisiae* and developed a model assuming an equilibrium between the rate of ATP production and consumption. They proposed that the rate of synthesis of biomass is proportional to the rate of synthesis of ATP, thus

$$\frac{d[\text{ATP}]}{dt} = C \frac{dX}{dt} \quad (12)$$

where the symbols are defined in the literature review. ATP may be synthesized by the glycolytic pathway and/or oxidative phosphorylation by the cytochrome chain.

The specific rate of ATP synthesis by these individual pathways were assumed to be proportional to their respective velocities, that is for glycolysis

$$\frac{1}{X} \left[\frac{d[\text{ATP}]}{dt} \right]_G = C_1 V_G \quad (13)$$

and for respiration,

$$\frac{1}{X} \left[\frac{d[\text{ATP}]}{dt} \right]_R = C_2 V_R. \quad (14)$$

Then the total specific rate of ATP synthesis is given by the sum of two pathways:

$$\frac{1}{X} \left[\frac{d[\text{ATP}]}{dt} \right] = \frac{1}{X} \left[\frac{d[\text{ATP}]}{dt} \right]_G + \frac{1}{X} \left[\frac{d[\text{ATP}]}{dt} \right]_R \quad (15)$$

or using equations (12)-(14), the rate of cell mass synthesis is given by

$$\frac{C}{X} \frac{dX}{dt} = C_1 V_G + C_2 V_R. \quad (16)$$

Expressions for V_G and V_R were developed by analysis of the mechanisms involved in glycolysis and respiration. Their analysis gave for the velocity of glycolysis

$$V_G = V_{Gm} \frac{S}{S+K_S} \frac{1}{1+bC_L} \quad (17)$$

and for the velocity of respiration

$$V_R = V_{Rm} \frac{S}{S+K_S} \frac{C_L}{K_L+C_L}. \quad (18)$$

The model can be made to give expressions for the specific growth rate and the growth yield, hence

$$\mu = \frac{S}{S+K_S} \frac{C_1}{C} V_{Gm} \frac{1}{1+bC_L} + \frac{C_2}{C} V_{Rm} \frac{C_L}{K_L+C_L} \quad (19)$$

$$Y = \frac{C_1}{C} + C_2 \frac{V_{Rm}}{V_{Gm}} \frac{C_L}{K_L+C_L} (1+bC_L) \quad (20)$$

In a later work the authors extended the model to include diversion of substrate into biomass and the concept of maintenance metabolism (Peringer *et al.*, 1974).

Another approach to modeling the growth process was proposed by Bijkerk and Hall (1977) and gave excellent results in describing the data of Beck and von Meyenberg (1968). They assumed the cell mass was divided into two parts; the first was involved in the uptake of substrate and its conversion to biomass and energy, the second was involved in division and replication. The energy producing part was further subdivided into the processes of glycolysis and respiration. The model was later modified by Pammet, Hall, and Barford (1978) to include the lag phases that occur during growth.

5.1.3 Stationary Phase. When waste products accumulate to inhibitory levels or an essential nutrient is depleted in the medium, microbial cells cease to grow. Synthesis of different cellular components occurs at different rates as growth enters stationary phase, hence stationary phase cells have a different composition than exponentially growing cells.

The kinetics of stationary phase cultures are important in some industrial processes. The synthesis of secondary metabolites such as antibiotics occurs primarily in stationary phase (Gaden, 1959). Wilson and coworkers inserted a cellulase gene from *Thermomonospora* into *E. coli* HB101 via vector plasmid pBR 322 and found that expression of the

cellulase gene did not occur until growth had stopped in the host organism (Faber, 1983). Holzberg, Finn, and Steinkraus (1967) found different kinetic expressions for alcohol production in a wine yeast applicable in exponential and stationary phases.

5.1.4 Death Phase. After depletion of cellular nutrient reserves the final fate of a cell is death. Few studies on the kinetics of death phase have been made, probably because industrial operations are terminated before this point. In general, the death rate of viable cells is given by the first order equation

$$\frac{dN}{dt} = -k_d N \quad (21)$$

where the initial condition is taken as the time and the number of viable cells at the end of stationary phase and $-k_d$ is the specific death rate. The rate constant k_d is a function of temperature and takes the Arrhenius form (Bailey and Ollis, 1977)

$$k_d = k_{d_0} e^{-E_d/RT} \quad (22)$$

where k_{d_0} is the standard specific growth rate, E_d is the activation energy for death, R is the gas law constant, and T is temperature. These kinetics are important in sterilization of media and process components.

5.2 Growth Kinetics of *Eschericia Coli*

The facultative anaerobic bacterium *E. coli* has been the focus of study by many investigators. The ability for this organism to grow on simple defined media or complex media under aerobic or anaerobic conditions has yielded much information on microbial metabolism. Ingraham, Maaloe and Neidhardt (1983) used *E. coli* as the model organism for their comprehensive book on the growth of bacterial cells. Doelle, Ewings, and Hollywood (1982) reviewed the regulation of glucose metabolism in bacterial systems and compared *E. coli* with other organisms. An understanding of the regulation of metabolic pathways is essential as they are intimately coupled with the growth process of the organism.

Associated with aerobic growth of *E. coli* on glucose is the production of numerous organic endproducts. Acetic acid is produced in large amounts (Amarasingham and Davis, 1965) with lactic acid, pyruvic acid, succinic acid, propionic acid and isobutyric acid also reported (Landwall and Holme, 1977). The proportions of these acids produced are likely to be dependent on the strain of *E. coli* used and culture conditions. Doelle, Ewings, and Hollywood (1982) attributed endproduct formation to an oversupply of NADH_2 .

Glucose was found to repress the respiratory enzymes succinate dehydrogenase and cytochrome a (Hollywood and Doelle, 1976) under aerobic conditions. Thus energy production is primarily done by the partial oxidation of glucose

to acetic acid by glycolysis with the other TCA cycle enzymes taking a biosynthetic role.

Marr, Nilson, and Clark (1963) studied the maintenance metabolism of *E. coli* and described several methods for evaluating the maintenance parameter, a , in equation (9). They obtained values of 0.025 hr^{-1} and 0.028 hr^{-1} , depending on the method used, for *E. coli* strain PS at 30°C .

5.3 Membrane Enhancement of Microbial Cultivation

Many ways have been used to produce dense cultures of microorganisms, with the goal of increasing productivity of cellular products per unit volume of fermentor or simplifying product recovery (Sortland and Wilke, 1969). The general strategy is to provide a sterile feed stream containing the necessary nutrients for growth to the fermentor system. Cells are separated from the effluent stream and returned to the fermentor. The cell-free effluent leaves the system depleted in nutrients and contains metabolic waste products.

The availability of low-cost semipermeable membranes have made membrane separations popular in laboratory and pilot scale reactor designs. Brock (1983) devoted a book to the subject of membranes and their uses in microbiology. Membrane separations have been applied to cell cultivation in primarily two configurations: dialysis and microfiltration.



5.3.1 Dialysis. Dialysis involves the passive exchange of solute molecules through a semipermeable membrane by diffusion. The driving force for the exchange is provided by a concentration gradient with no convective flow across the membrane.

Application of dialysis in the cultivation of microorganisms and modes of operation were reviewed by Schultz and Gerhardt (1969). In general, two reservoirs are separated by a dialyzer (Figure 1A). One reservoir serves as the fermentor; the other contains nutrients required for growth by cells. The contents are continuously pumped passed each side of the membrane in the dialyzer where solute exchange occurs. Thus there are additional nutrients available for cell growth; metabolic byproducts, which may be inhibitory, are removed and cells remain in the reactor circuit.

Subsequent study of the dialysis system showed that solute exchange can become limiting due to low permeability of membranes and/or lack of membrane area (Landwall and Holme, 1977; Stieber and Gerhardt, 1981). Improvements in membrane technology to alleviate low permeabilities would result in further improvements in the dialysis culture process.

5.3.2 Microfiltration. Cell-free effluent may be obtained by using a membrane as a microfilter. In contrast to dialysis where passive diffusion was the transport process for solute exchange, convection of the soluble fraction of the culture through the membrane, driven by a pressure gradient, is the primary transport mechanism in microfiltration.

Figure 1. Comparison of the Dialysis Culture System and the Microfiltration System. Symbols are defined in the literature review.

- (A) Dialysis is characterized by the passive diffusion of solutes across a membrane between the fermentor and reservoir circuits. Various methods of operating the dialysis system were described by Schultz and Gerhardt (1969).

- (B) In the microfiltration system, feed is introduced directly into the fermentor. Cell-free effluent is removed through a membrane by convection under the influence of a pressure gradient developed by a pump. Cell-containing effluent may be removed from the fermentor by a purge stream.

Sterile nutrient feed is added directly to the fermentor while the effluent is forced through the membrane pores by external pumping (Figure 1B). Bacterial cells are immobilized within the fermentor and external filtration loop.

Microfiltration cultivation has previously been applied in two modes. The membrane may be located directly in the fermentor (Sortland and Wilke, 1969; Pirt and Kurowski, 1970; and, Dostálek and Häggstrom, 1982) or in an external loop (Watson and Berry, 1979; Rogers, *et al.*, 1982; and Charley, *et al.*, 1983). Both of these operating modes have produced cultures many times more dense than obtainable in batch cultures. Sortland and Wilke (1969) produced cultures of *Streptococcus faecalis* 45 times more dense than in batch culture using a microfiltration system.

Membrane fouling has been a major problem in microfiltration systems. Several methods have been employed to alleviate this problem. Backflushing the filter with filtrate has been popular in an attempt to maintain filtration rates (Tanny, Mirelman and Pistole, 1980, and Dostálek and Häggstrom, 1982). More notably is the design of microfiltration systems to generate turbulence near the surface of the membrane. Conventional filtration with the flow of the suspension perpendicular to the filter allows nonpermeable material to build up on the filter media. By providing flow tangent to the filter surface, cells and other debris are continually washed away and remain in suspension.

Henry and Allred (1972) found that the shear rate at the filter surface was the dominant parameter in determining permeate fluxes in the filtration of bacterial suspensions. Sortland and Wilke (1969) designed a filtration rotor that rotated at 600 rpm inside the fermentor. Watson and Berry (1979) used a magnetic stirring bar in their apparatus to generate tangential flow. Gelman Sciences (Ann Arbor, Michigan) developed a microfiltration capsule (Acroflux capsule) with a narrow space between the membrane and outer wall. High flow rates through the channel and the presence of a turbulence promoting support screen aid in washing cells from the filter membrane.

Charley, *et al.* (1983) tested several microfiltration devices made by different manufacturers and found problems in operating these for long periods of time. They reported improved results using the Amicon Corporation hollow fiber system (Danvers, Maryland) incorporating an ultrafiltration membrane.

Microfiltration has recently become a popular operation with applications in microbiology not only in bacterial cultivation, but in harvesting of biological materials. Interest in developing microfiltration equipment by membrane manufacturers has resulted in many improvements in available equipment at economical prices.

5.4 Liquid Level Control

The application of continuous flow systems in the cultivation of microorganisms introduces new control problems

not associated with batch cultures. The residence time of material in the reactor is dependent on the liquid level so adequate control of the liquid level is essential.

Several simple methods have been used for level control in laboratory and pilot scale continuous stirred tank reactor systems. Herbert, Elsworth, and Telling (1956) used an overflow tube installed in the fermentor wall at the desired liquid level. Yang and Humphrey (1975) used a U-shaped overflow tube with an effluent pump running at a slightly higher volumetric rate than the feed pump to remove fermentation broth and entrapped air. Stieber and Gerhardt (1979) purged nitrogen into the fermentor to aspirate the effluent through a straight tube extending through the top of the fermentor to the desired liquid level. These methods provide satisfactory control as long as foam formation is kept at a minimum.

Additional complications result when more sophisticated reactor systems are employed such as dialysis culture and partial or total cell recycle schemes. These cultivation methods involve a physical separation of cells from the fermentation broth to yield an essentially cell-free effluent.

Sortland and Wilke (1969) developed an apparatus for removing a cell-free effluent by microfiltration to study the anaerobic growth of *S. faecalis* in dense culture. In this case the fermentation broth occupied the entire reactor volume with no vapor space above the broth. The hydrostatic pressure in the reactor, generated by peristaltic feed pumps, was allowed to fluctuate to provide the driving force for microfiltration. Thus, reactor volume remained constant.

In the case where a gas such as air is sparged into the broth to satisfy aerobic growth requirements in a recycle system, a vapor space above the broth is needed to disengage entrained broth before the gas leaves the reaction vessel. Dostálek and Häggstrom (1982) developed a filter fermentor for the aerobic growth of several organisms. Their control system was composed of level sensing electrodes and pressure transducers to provide on/off activation of effluent and filter backflush pumps.

MATERIALS AND METHODS

6.1 Organism and Culture Conditions

Escherichia coli K12 strain HB101 $F^{-}pro^{-}leu^{-}thi^{-}lacY^{-}recA^{-}$ was used in this investigation. Other genetic markers were described by Bolivar and Backman (1979). This strain and its derivative RR1 $recA^{+}$ were used in DNA recombination work as recipient cells (Bolivar, *et al.*, 1977a; Bolivar, *et al.*, 1977b; Bolivar and Backman, 1979; Faber, 1983) because of their restriction and modification properties (Boyer and Roulland-Dussoix, 1979).

Stock cultures were maintained on Plate Count Agar (4M) however, after repeated subculturing of the organism, some of the genetic markers appeared to have been lost. Other investigators have also noted similar variations in their stock of HB101 (Wilson, David B., Cornell University, personal communication).

Inoculum was prepared in 100 ml of media and incubated at 37°C on a rotary shaker-incubator. The medium was a modification of the M9 minimal medium described by Bolivar and Backman (1979) containing in 1 l of distilled water; 5.54 g $Na_2 HPO_4$, 3 g $KH_2 PO_4$, 0.5 g NaCl, 1.0 g $NH_4 Cl$, 0.25 g $MgSO_4 \times 7 H_2 O$, 0.015 g $CaCl_2 \times 2 H_2 O$, 4 g glucose, 0.025 g thiamine hydrochloride, and 0.2 g each of ℓ -proline and ℓ -leucine. The fermentor was inoculated with exponentially growing cells.

Batch and microfiltration experiments were run aerobically at 37°C and pH 7. In order to attain high cell

densities, the media used in these experiments contained the same components as the inoculum media at twice their concentrations. No inhibitory effects of the higher concentrations of salts were noted. In experiments where these concentrations were varied in the feed medium, their concentrations are noted, however in all experiments the fermentor was initially charged with the double concentrated medium.

6.2 Analytical Methods

Samples of about 15 ml were taken aseptically and the viable cell counts and optical density were measured immediately. The sample was then frozen and stored at -20°C for later analysis of cell dry weight, glucose, ammonium ion and organic acids. Standard curves and sample calculations from raw data are given in Appendices I and II respectively.

6.2.1 Optical Density. Optical densities were measured at 600 nm in cuvettes with a 1 cm lightpath in a grating spectrophotometer (2M). One ml of sample was diluted with distilled water to give a reading in the most accurate range of the spectrophotometer, between an O.D.₆₀₀ of 0.0 and 0.25. Readings were accurate to ± 0.005 units of optical density. The actual optical density was then calculated by multiplying the reading by the dilution factor.

6.2.2 Viable Cell Counts. One ml of the sample was serially diluted in 99 ml sterile saline (0.85% NaCl) dilution blanks to give between 30 and 300 colonies on Plate Count Agar (4M) using the pour plate technique. Plates were read

after 24-48 hrs incubation at 37°C. The average of three plates was taken and the number of viable cells per ml of original culture was calculated. Counts were typically within + 8% of the average but variation as high as + 20% were found occasionally.

6.2.3 Cell Dry Weight. Cell dry weight was calculated from a standard curve of cell dry weight versus optical density (Figure 2). The curve was prepared from samples taken during a batch experiment.

The frozen samples were allowed to thaw at 4°C. Aluminum weighing dishes were predried at 80°C and 15 in Hg vacuum for 12 hours before determining the tare weight. Two 5 ml portions of each sample (one 10 ml sample at low cell densities) were centrifuged at 10,000 x g for 10 min. The centrifugate was saved for later analysis. The pellet was washed once with 10 ml distilled water, centrifuged, and re-suspended in 10 ml distilled water. The suspension was poured on the preweighed aluminum pans and dried at 80°C and 15 in Hg vacuum. The pans were dried to constant weight to determine the dry sample weight.

6.2.4 Ammonia. Concentrations of ammonia were determined by a modification of the Nesslerization colorimetric method described by Johnson (1941). Interference by certain ions (particularly those of Mg, Ca, and Cl) and organic compounds has been found to occur in this method (Franson, 1976; Gerhardt, *et al.*, 1981).



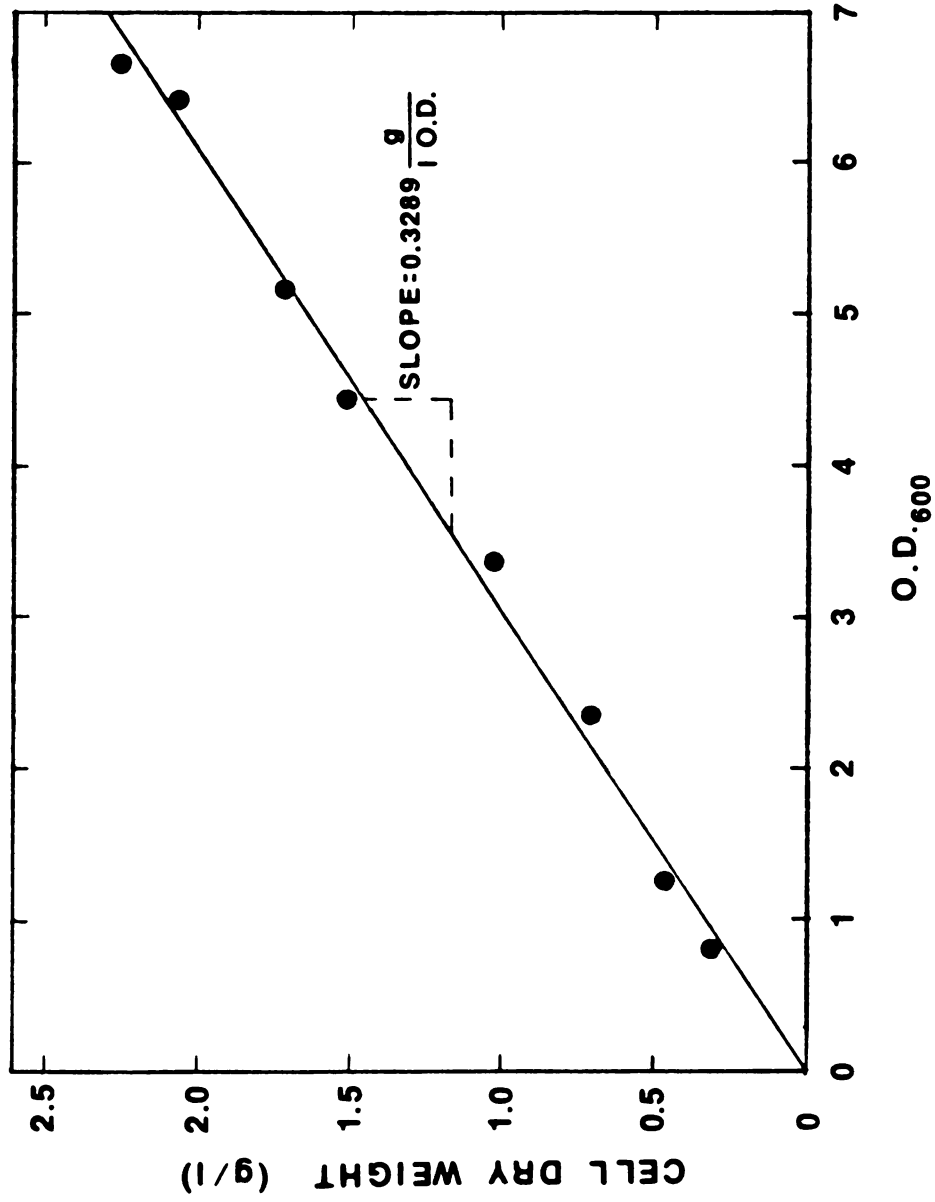


Figure 2. Cell Dry Weight vs. Optical Density at 600 nm (O.D.₆₀₀) Standard Curve

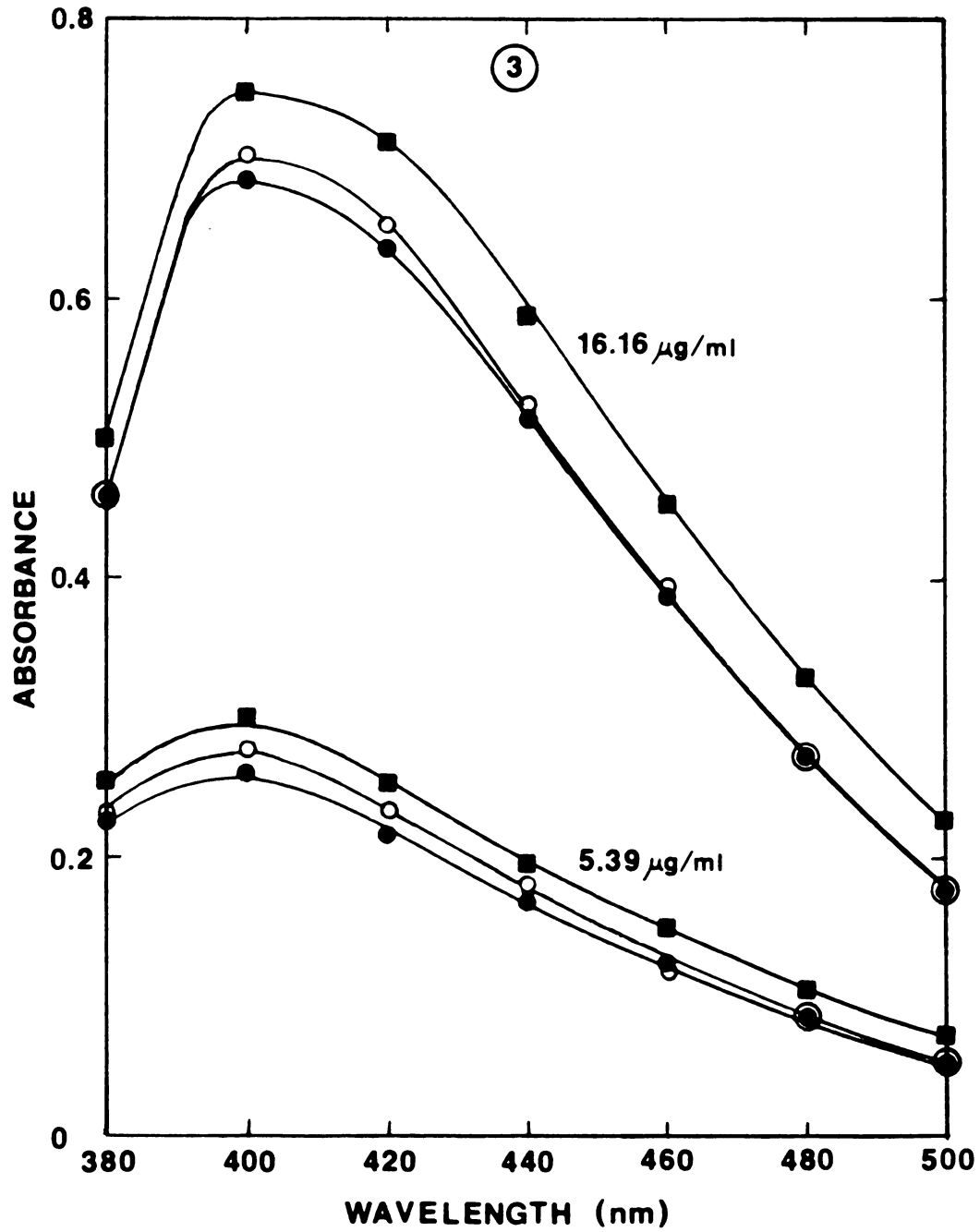
To determine the extent of interference caused by ions and organic components in the media, three solutions were prepared. The first contained 2.0000 g/l NH_4Cl in water; the second contained 2.4706 g/l $(\text{NH}_4)_2\text{SO}_4$ in H_2O and the third contained 2.0000 g/l NH_4Cl in a solution with the same composition as the fermentation media. Thus, each solution contained 0.6735 g/l NH_4^+ . Each solution was then diluted with water to give a final ammonium ion concentration of 16.16 and 5.39 g/ml. Each was nesslerized along with water blanks as described below and the absorption spectrum was recorded between 380 and 500 nm with a grating spectrophotometer (Figure 3). There was a slight difference in the spectra near 400 nm for the solutions containing NH_4Cl and $(\text{NH}_4)_2\text{SO}_4$ prepared in water probably due to dilution error. However, the solution prepared in the fermentation media show significant variation over the entire spectrum.

Samples were typically diluted 1:100 with water such that the ammonium ion concentration was 1.0-15.0 $\mu\text{g/ml}$. To minimize the error due to background interference caused by other ions present in the samples, a diluent was prepared with a composition 1/100 of the fermentation medium without NH_4Cl . A stock solution was prepared in the diluent with 100 $\mu\text{g/ml}$ NH_4Cl (33.67 $\mu\text{g/ml}$ NH_4^+). Standards were prepared by pipeting 1.0, 2.0, 3.0, 4.0, and 5.0 ml of stock solution into test tubes and adding sufficient diluent to bring the volume to 10 ml.

One ml of each standard and diluted sample was placed into test tubes. Two ml of Nessler's reagent and 3.0 ml of

Figure 3. Ammonium Ion Absorption Spectrum.

Three solutions were prepared to determine the interference by chemical species present in the media. They contained NH_4Cl in water (●), $(\text{NH}_4)_2\text{SO}_4$ in water (○), and NH_4Cl in fermentation media (■). These were diluted with water to given ammonium ion concentrations of $16.16 \mu\text{g ml}^{-1}$ and $5.39 \mu\text{g ml}^{-1}$. After Nesslerization their absorption spectra were recorded between 380 and 500 nm.





2N NaOH were added to each tube and the color was allowed to develop for 15 min. The Nessler's reagent contained 4.0 g KI and 4.0 g HgI₂ per liter of water. The absorbance was read at 400 nm in a grating spectrophotometer. The accuracy of the ammonium ion concentration was about +5% but decreased at high concentrations due to dilution error.

6.2.5 Glucose. Glucose concentrations in fermentor samples were determined by the phenol-H₂SO₄ colorimetric method (Dubois, *et al.*, 1955) as modified by Johnson *et al.*, (1956). Interference by α - and β -keto acids, aldehyde and ketones and, in particular, pyruvic acid was shown by Montgomery (1961). Pyruvic acid was previously shown to be a product of *E. coli* growth (Landwall and Holme, 1977) however the low concentrations found in this investigation did not indicate it as an interfering agent.

Standards were prepared from a stock solution containing 100 μ g/ml d-glucose. This was diluted with water to give standards containing 5, 10, 20, 30, 40, and 50 μ g/ml d-glucose. Samples were diluted with water to give a final glucose concentration between 5-50 μ g/ml. Two ml aliquots of the standards, diluted samples, and water (blank) were placed in reaction tubes. One ml phenol reagent (50 g/l phenol in water) and 5.0 ml of concentrated H₂SO₄ were added and the tubes were vortexed. After the tubes cooled for 1 hr the absorbance was read at 490 nm. Glucose concentrations were then determined from a standard curve. Accuracy was within +5% but decreased at high concentration of glucose due to

dilution error. Concentrations less than 5 $\mu\text{g/ml}$ were undetectable.

6.2.6 Volatile Fatty Acids. Fatty acids were analyzed by gas chromatography according to a modification of the procedure described by Supelco, Inc. (1975). Standards were initially prepared from a volatile acid standard mixture (14M). The standard mix contained 1 milliequivalent of the fatty acids $\text{C}_1\text{-C}_7$ per 100 ml water. However, only acetic and propionic acids were found in fermentor samples (Figure 4A). The long elution time of heptanoic acid (30 min) made the use of this standard mix inconvenient. Subsequently a standard mixture of only acetic and propionic acids at 4.026 and 0.985 g/l respectively was prepared, shortening the analysis time to about 6 minutes per standard injected (Figure 4B). This solution was diluted with water to give standard solutions containing the acids at 1/2, 1/4, and 1/8 of the above concentrations.

Two ml aliquots of each fermentor sample and standard were placed in screw cap tubes. These were acidified directly by adding 0.1 ml of 50% H_2SO_4 (v/v in water) and the acids were extracted with 1 ml ethyl ether. These were centrifuged to break the emulsion and the water layer was frozen. The ether layer was then poured into screw-cap tubes containing enough anhydrous Na_2SO_4 to equal about half the volume of ether. This removed any dissolved water in the ether.

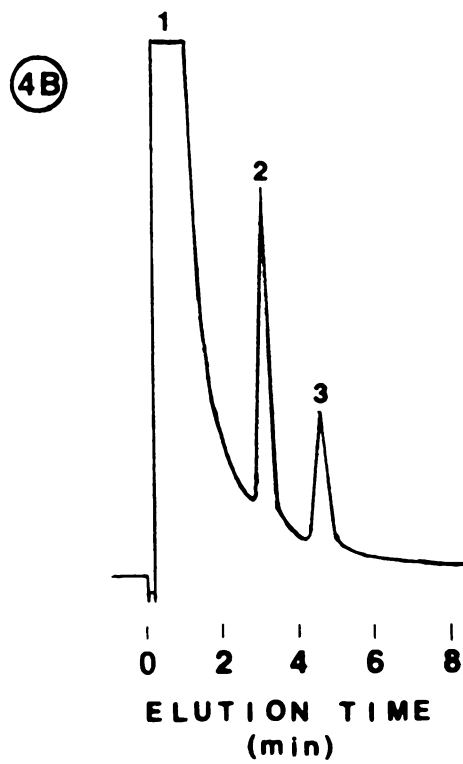
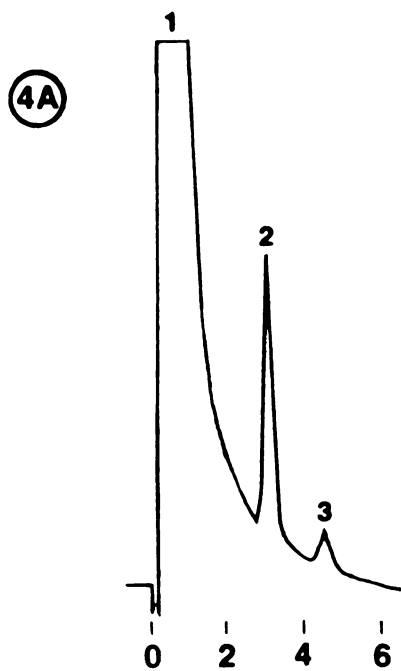
A gas chromatograph (18M) equipped with a thermal conductivity detector was used for the analysis. The injection

Figure 4. Volatile Fatty Acid Chromatograms.

Peaks were identified as 1, solvent (ether); 2, acetic acid (3.04 min); and 3, propionic acid (4.54 min).

(A) Fermentor sample.

(B) Standard mixture of acetic acid (2.013 g l^{-1}) and propionic acid (0.493 g l^{-1}).





temperature was set at 160°C. The detector temperature was 170°C with a bridge current of 200 mA. The carrier gas was helium at a flow rate of 20 ml/min.

The column was a 1/8" O.D. x 6' seamless stainless steel tube packed with 10% SP-1000 on 100/120 Chromosorb W AW (15M). The column oven temperature was 135°C.

Peak areas were determined using a CDS 111 integrator (19M). Chromatograms were recorded with a chart recorder (9M). Fourteen μ l samples of the ether layer were injected into the column twice and the average peak areas were calculated. The concentrations of acids in the original samples were determined from a plot of concentration versus peak area obtained from the standards. Peak areas were within $\pm 5\%$ of average.

6.2.7 Non-Volatile Acids. Non-volatile acids were analyzed by gas chromatography using a procedure described by Supelco, Inc. (1975). Standards were prepared from a non-volatile acid mixture containing 1 milliequivalent in 100 ml of water of pyruvic, lactic, oxaloacetic, oxalic, methyl malonic, malonic, fumaric, and succinic acids (16m). The standard solution was diluted with water to give additional solutions containing 1/2, 1/4, and 1/8 the concentration of each acid.

One ml aliquots of samples and standards were placed in screw cap tubes. Methyl ester derivatives were prepared by adding 0.4 ml of 50% H_2SO_4 (v/v in water) and 2 ml lipopure methanol, vortexing the mixture, and allowing them to sit overnight. One ml of water and 0.5 ml chloroform were added to extract the acid methyl esters. Fourteen μ l of the chloroform

layer was injected into the column twice and the average area calculated. Peak areas were found to be within 5% of average.

Initially the same SP-1000 column was used as in the volatile fatty acid analysis. This gave poor separation of the acids from the solvent peak. Better separation was found using a 6' x 1/8" O.D. stainless steel seamless column packed with 15% DEGS on 80/100 Chromosorb W AW (17M). A chromatogram of the standard solution using this column is shown in Figure 5A. Peaks were identified by injecting individual solutions of the acid methyl esters, prepared as above, and noting their elution times. Results are shown in Table 1. The column temperature was set at 115°C; the injector and detector temperatures were both 155°C. The thermal conductivity bridge current was 200 mA and the helium carrier gas flow rate was 20 ml/min.

The solutions of pyruvic and oxaloacetic acids both gave peaks at 2.41 and 4.48 minutes. Similar problems have been observed by others (Supelco technical service department, personal communication). The spontaneous decomposition of oxaloacetic acid to pyruvic acid has also been noted (Montgomery, 1961). These two acids were assumed to elute as given in Table 1.

Separation of malonic and fumaric acids was poor. However they were not found in any sample chromatogram (Figure 5B). It was noted that using a higher column temperature would reduce the trailing of the malonic/fumaric acid pair but gave poorer separation of pyruvic and lactic acids from the solvent peak.

Figure 5. Non-Volatile Acid Chromatograms.

Peaks are identified in Table 1.

(A) Standard acid solution.

(B) Fermentor sample.

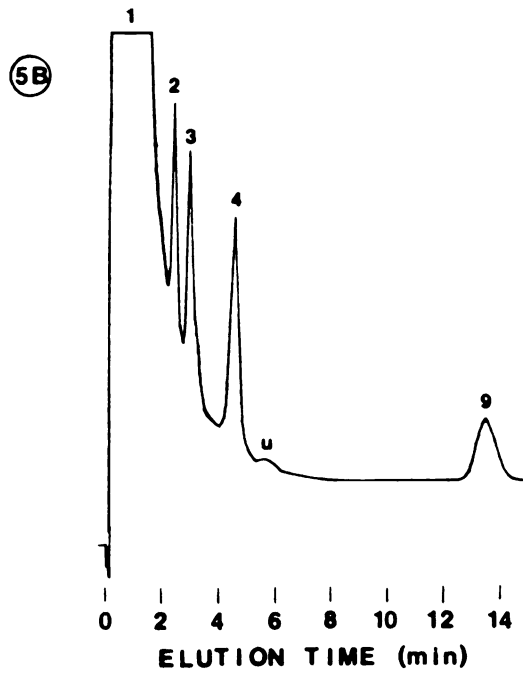
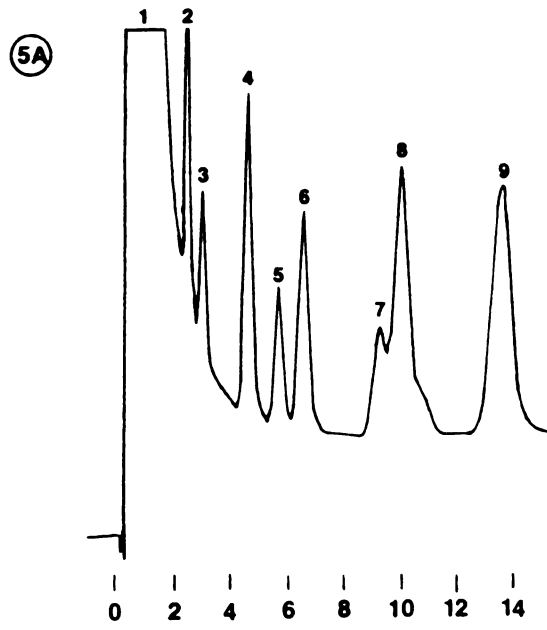


TABLE 1. Non-volatile Acid Peak Identification.
Peak Numbers Correspond to Chromatogram
Peaks in Figure 5.

Peak	Compound ^a	Elution Time (Minutes)
1	solvent (chloroform)	0.48
2	pyruvic acid	2.41
3	lactic acid	2.91
4	oxaloacetic acid	4.48
5	oxalic acid	5.53
6	methyl malonic acid	6.39
7	malonic acid	9.01
8	fumaric acid	9.77
9	succinic acid	13.27
u	unidentified	--

^aacids were analyzed as their methyl ester derivatives.

Acetic and propionic acids were also treated and tested as above but their response was small compared to the non-volatile acids even at high concentrations (4.0 g/l and 1.0 g/l respectively). Acetic acid eluted at the same time as oxaloacetic acid. Similarly propionic acid eluted with oxalic acid. The unidentified peak in the sample chromatogram (Figure 5B) was attributed to propionic acid.

6.3 Experimental Microfiltration System and Procedure

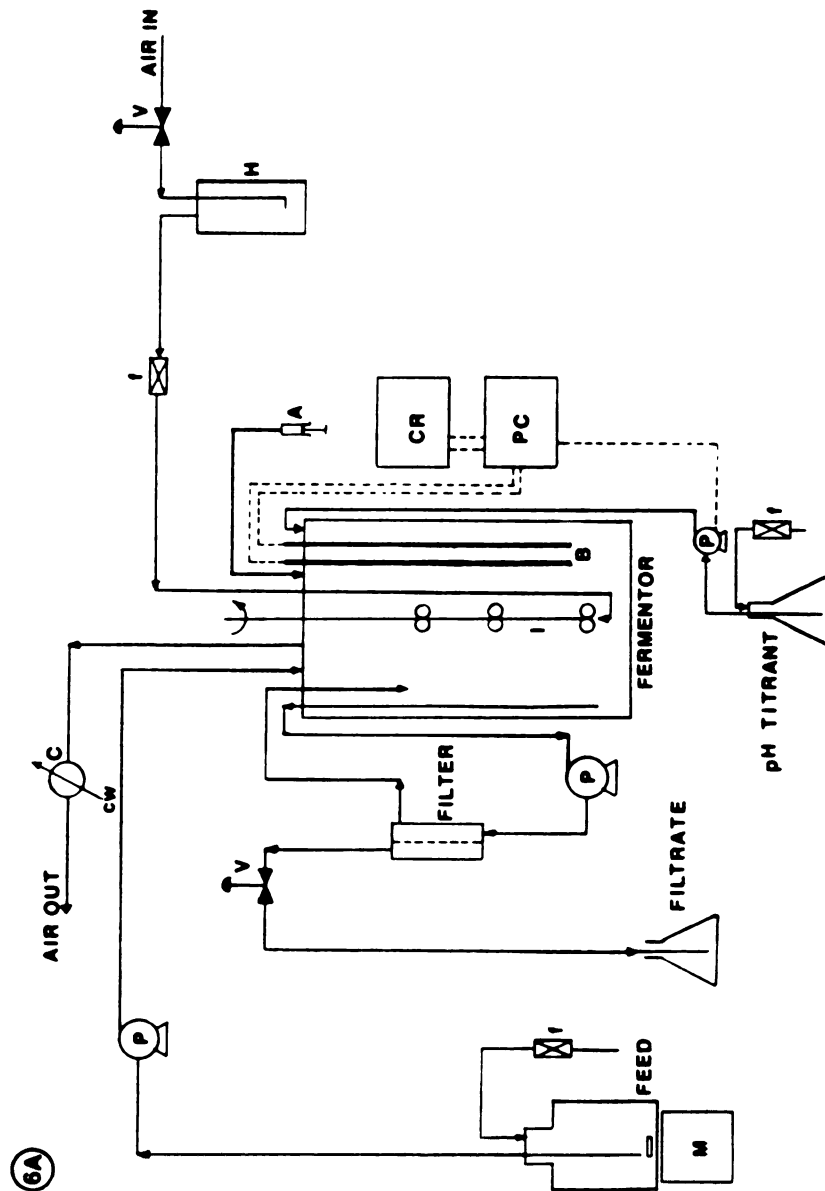
A process flow diagram of the microfiltration system is shown in Figure 6A, and a photograph of the system is shown in Figure 6B. A Microferm Fermentor system equipped with a 5 l fermentor (10M) was used in all experiments. The working volume was 3l but was measured at the end of each experiment. This system included temperature control, agitation, and aeration. The temperature was held at $37 \pm 0.5^{\circ}\text{C}$ by circulating water, the impeller speed was 1000 rpm, and air volumetric rate was $2 \text{ l min}^{-1} \text{ l working volume}^{-1}$ (measured at 70°F and 14.7 psia). Aeration and agitation were assumed sufficient to prevent oxygen limitation.

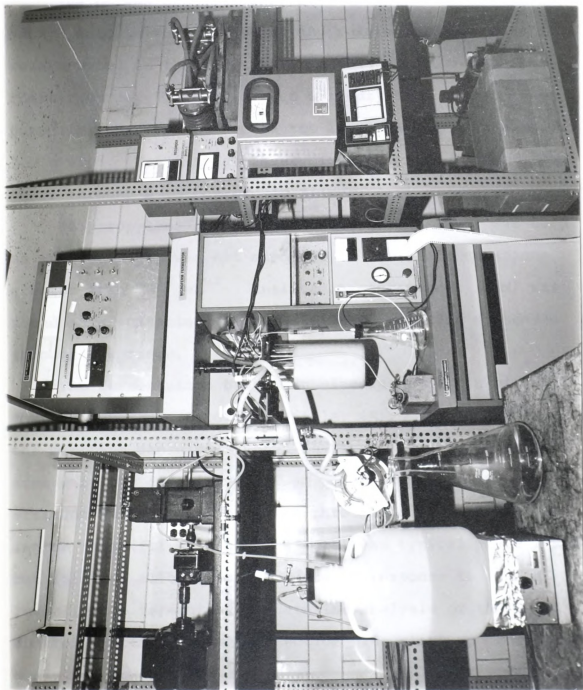
Sterile medium was stored in a 10 l carboy and agitated by a magnetic stirring bar. The carbon was vented to the atmosphere through a filter packed with cotton to prevent contamination. The media was fed directly to the fermentor by a finger-type peristaltic pump (13M) through silicone rubber tubing. Air was humidified by sparging through distilled water and filtered through cotton packing before being sparged



Figure 6. Experimental Process Flow Diagram and Photograph.

- (A) Experimental process flow diagram. Symbols represent, A-antifoam syringe, B-pH measuring and reference electrodes, C-condenser, CR-pH chart recorder, cw-cold water, f-cotton-packed air filter, H-humidifier, I-impeller, M-magnetic stirrer, P-pump, PC-pH controller, V-valve.
- (B) Photograph of the microfiltration system.





6B

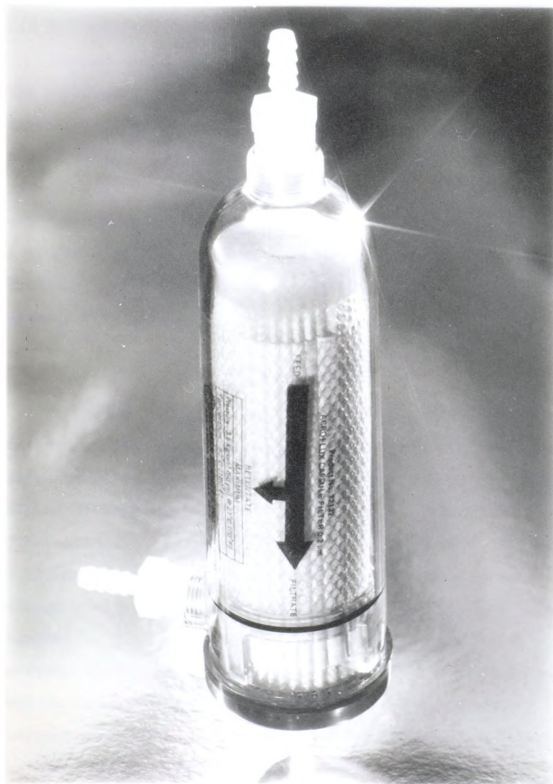
into the fermentor. Gases leaving the fermentor passed through a water-cooled condenser and were vented to the atmosphere.

The pH was controlled by automatic titration with 5M NaOH. Autoclavable measuring and reference electrodes (7M) were mounted in the fermentor. A pH controller and strip chart recorder (11M) activated a rotary-type peristaltic pump (1M) when the pH became too low. pH was maintained at 7.0 ± 0.05 . The titrant reservoir was vented to the atmosphere through a cotton-packed filter.

Polypropylene glycol (molecular weight 2000) was used as antifoam, but was not adequate at cell concentrations greater than 10^{10} ml^{-1} . Antifoam A concentrate (12M) was found more suitable. Either antifoam was added as needed through a syringe.

The fermentation broth was circulated past a microfiltration membrane (Acroflux Capsule, 6M). A photograph of the membrane capsule is shown in Figure 7. The membrane area was 1000 cm^2 with a $0.2 \mu\text{m}$ pore size. Cell-free effluent was removed through a throttling valve. The circulation rate (filter crossflow rate) was typically 3.5 l min^{-1} but this was allowed to fluctuate in response to liquid level in the fermentor. A detailed analysis of the level control system is given in section 6.4; start-up procedures are given in Appendix IV.

In an effort to minimize the effect of removing samples from the fermentor, 15 ml samples were taken at no less than



Courtesy of Gelman Sciences

Figure 7. Photograph of the Acroflux Capsule

1 1/2 hour intervals during a microfiltration experiment. Experiments were continued until the membrane became fouled and filtration rates could no longer be maintained.

Cleaning and storage of the filter was done according to the procedures of Tanny, Mirelman and Pistole (1980). The filter was removed from the system and washed by circulating a 95:5 ethanol-water mixture through the filter capsule for 20 min, then rinsing with distilled water. Severely fouled membrane capsules were washed with a 0.1 N NaOH solution for 1 hr and rinsed with distilled water. Filters were allowed to drain dry for storage and rinsed with sterile distilled water before subsequent use.

6.4 Level Control

A closed loop level control system was developed for the microfiltration system as shown in Figure 8. Feed was supplied at a constant rate and filtrate flow rate was manipulated in response to process changes that would lead to fluctuations in fermentor level (i.e., pH titrant, filter fouling, etc.). Filtration rate has been shown to vary directly with filter differential pressure and shear rate tangent to the filter surface in similar microfiltration devices (Henry and Allred, 1972). Since both of these parameters depend on the circulation rate past the membrane (crossflow pumping rate), the filtrate flow rate may be varied by changing the crossflow pump speed.

The liquid level was monitored by a Teflon insulated probe and transmitter (5M) producing a 4-20 mA current in the



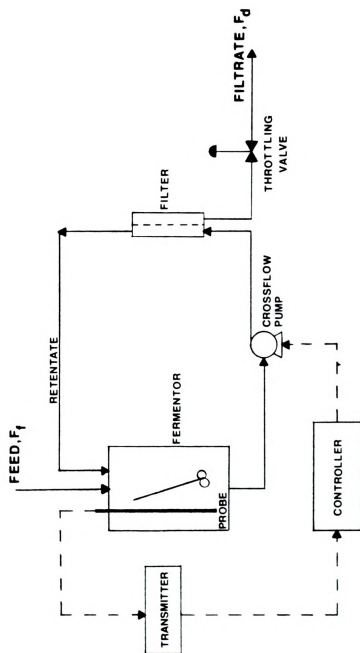


Figure 8. Level Control Loop Diagram



control loop that is proportional to the fermentor level. The retentate inlet was directed away from the probe and the fermentor was sufficiently baffled to prevent vortexing and provide a smooth liquid surface. A strip chart recorder (9M) was used to give a continuous record of fermentor level.

A current output controller (8M) in the control loop generated a 4-20 mA response to the transmitter current. The response current controlled the crossflow pump speed (3M).

Higher filtrate flow rates occurred than were required for the microfiltration system due to the large capacity of the microfilter and crossflow pump. The pump would run at very low speed resulting in a long residence time for cells in the filtration loop. Therefore, a throttling valve was added in the filtrate line to increase the pressure on the filtrate side of the filter membrane resulting in lower filtration rates, higher crossflow pump speed, and a short residence time in the filtration loop.

The level control loop could hold the volume to within $\pm 5\%$ of the total volume, however operation to $\pm 1\%$ was typical.

6.4.1 Control Loop Analysis. The control loop may be represented by the block diagram shown in Figure 9. Transfer functions are given as their Laplace transforms. An overall material balance around the system, assuming constant liquid density, gave for the process transfer function (G_p)

$$G_p = \frac{\hat{L}(s)}{\hat{F}_f(s) - \hat{F}_d(s)} = \frac{1}{\hat{A}_f s} \quad (23)$$

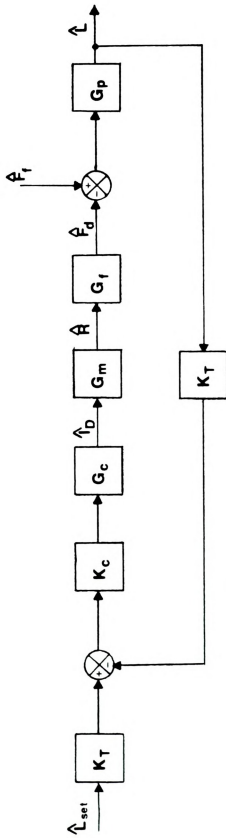


Figure 9. Level Control Block Diagram



The controller is the proportional-integral-derivative type and its transfer function (G_c) was given by

$$G_c = 1 + \tau_D s + \frac{1}{\tau_I s} . \quad (24)$$

The motor response to control current is shown in Figure 10. Its transfer function (G_m) may be approximated by

$$G_m = \frac{\hat{R}}{I_D} = \begin{cases} 64.8 \frac{\text{rpm}}{\text{mA}} & ; \text{ if } I_D > 9.2 \text{ mA} \\ 0 \frac{\text{rpm}}{\text{mA}} & ; \text{ if } I_D \leq 9.2 \text{ mA} \end{cases} \quad (25)$$

The transmitter response to level changes was linear over the active length of the probe and the transmitter gain (K_T) is 0.764 mA cm^{-1} . No measurement lag was observed. The filter transfer function G_f is a complex relation involving the hydrodynamics of the filter capsule system. No attempts were made to determine this function.

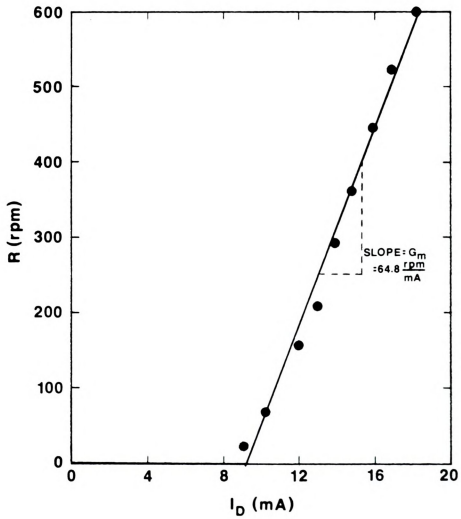


Figure 10. Pump Speed (R) vs. Controller Output Current (I_D)

RESULTS AND DISCUSSION

The results of a control batch and the microfiltration experiments are given in graphical form and are discussed sequentially in Section 7.1. The mathematical model and computer simulation are presented and discussed in Section 7.2.

7.1 Experimental Results and Discussion

The effect of microfiltration cultivation on the growth of *Escherichia coli* was investigated by studying the influence of hydraulic residence time, τ_H (defined as V_f/F_f) and the concentration of glucose in the feed media, S_{f_0} . A summary of these experiments is given in Table 2.

TABLE 2. Summary of Microfiltration Experiments

Experiment	τ_H (hr)	S_{f_0} (g ℓ^{-1})
1	∞ (Batch)	--
2	4.15	8
3	2.94	8
4	1.58	16

The cell dry mass, viable cells, glucose, ammonium ion and acid concentrations were plotted as functions of time. Actual numerical data for each experiment is provided in Appendix III.



7.1.1 Control Batch Cultivation: Experiment 1. A

batch culture was done for later comparison with microfiltration experiments. Figure 11A shows the exponential growth phase through hour 11. The specific growth rate of cell dry weight and viable cells were 0.49 hr^{-1} and 0.50 hr^{-1} respectively during this phase. The specific growth rates were calculated by a least squares fit of the slope from the plots of $\ln X_f$ vs t and $\ln N_f$ vs. t , that is from Equation 2

$$\frac{1}{X_f} \frac{dX_f}{dt} = \frac{d(\ln X_f)}{dt} = \mu \quad (26)$$

and N_f was assumed proportional to X_f .

A gradual decrease in the specific growth rate followed the exponential growth phase, as is characteristic of glucose-limited batch growth of *E. coli* during the transition to stationary phase (Amarsingham and Davis, 1965). The simultaneous depletion of glucose and ammonia is shown in Figure 11B. The medium was believed to have become limiting in glucose; the residual glucose shown was believed to be interference by cellular products present in the sample and reflects the non-specific nature of the analytical method.

Accumulation of acetic and propionic acids are shown in Figure 11C. Succinic acid was also detected but chromatogram peaks were too small to integrate.

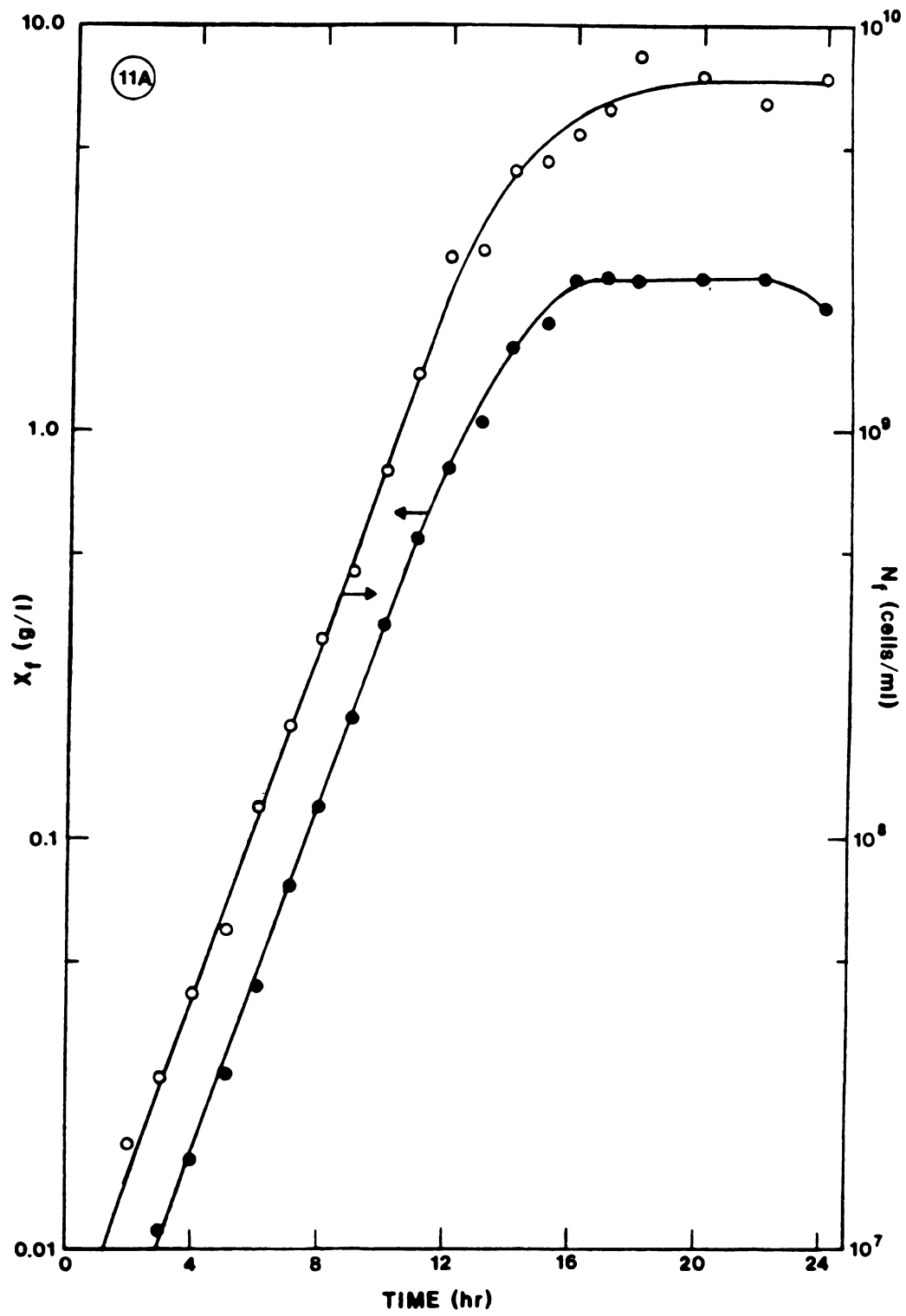
Entry into stationary phase occurred just prior to hour 17. At this time, glucose was depleted, ammonium ion consumption ceased, and the pH began to increase. The fermentor

Figure 11. Results of Experiment 1.

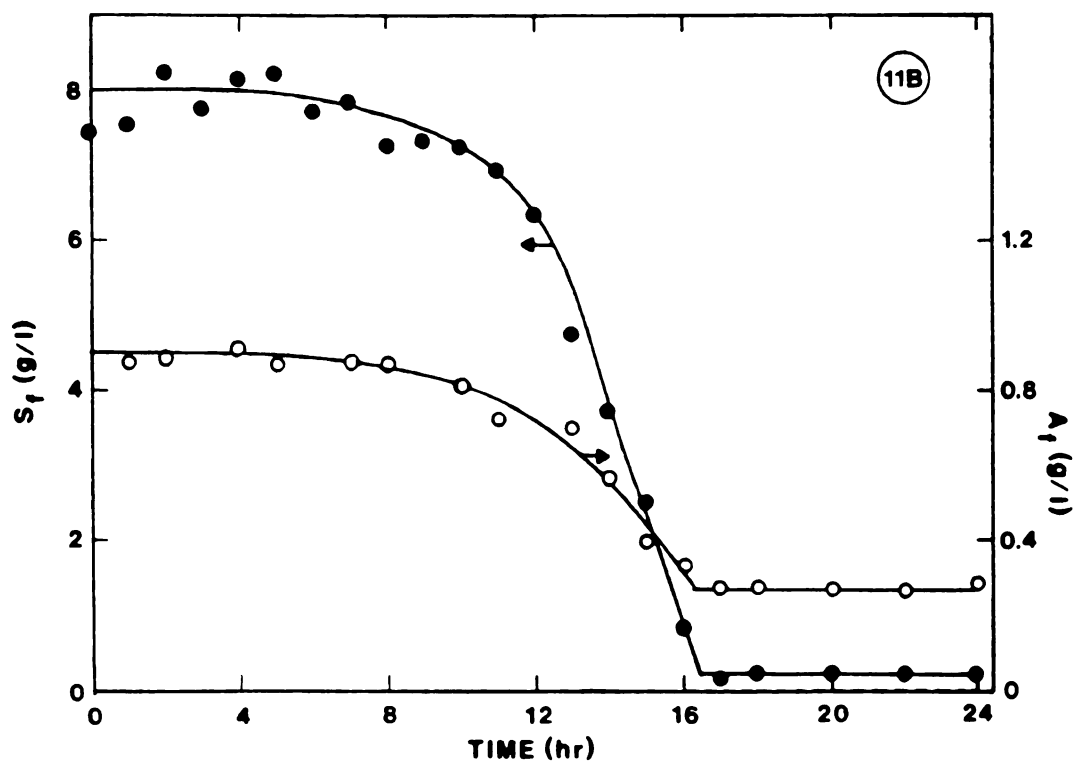
Control batch growth of *E. coli* HB101.

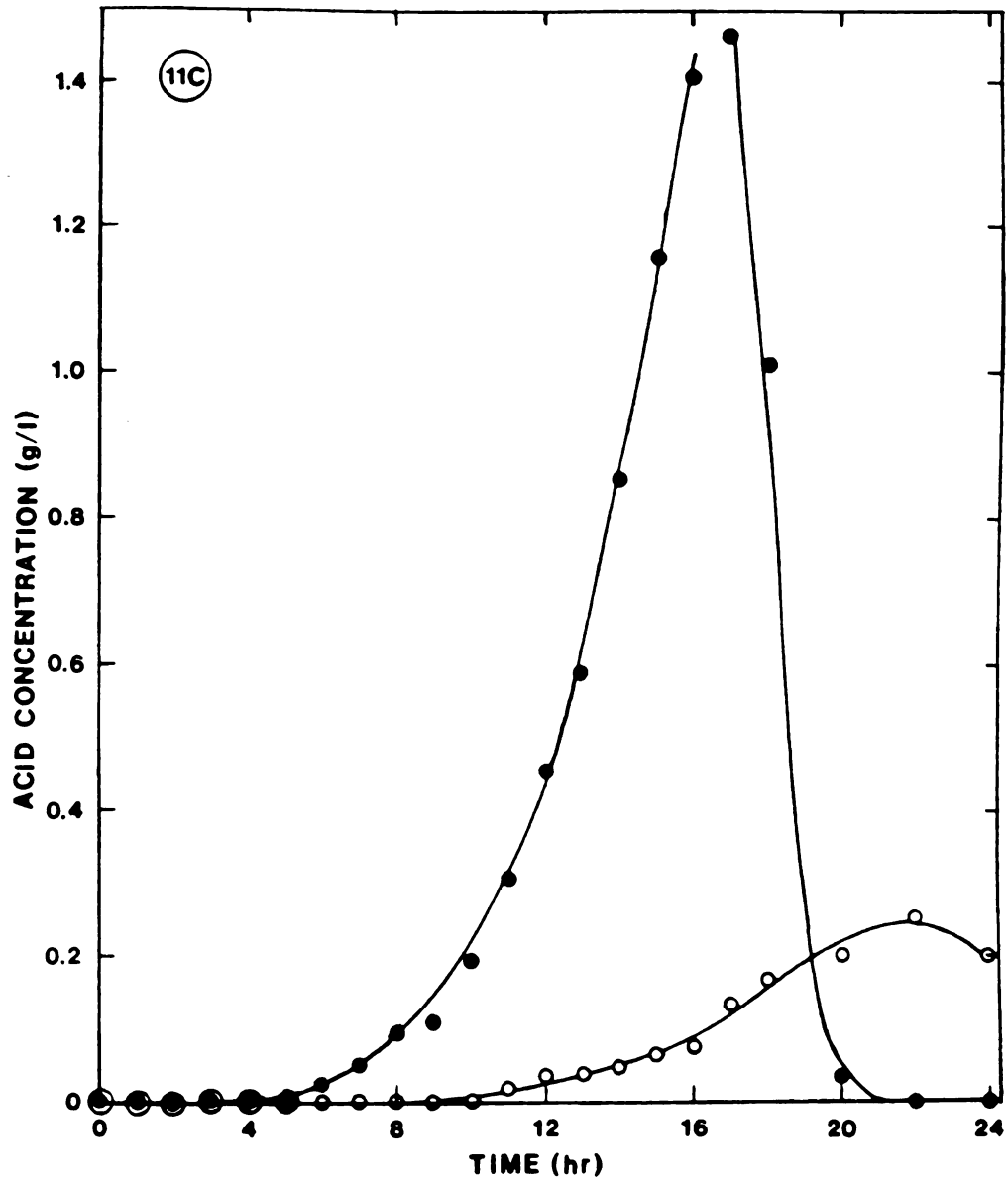
- (A) Cell dry weight concentration (x_f) and viable cell concentration (N_f).
- (B) Residual glucose (S_f) and ammonium ion (A_f) concentrations.
- (C) Volatile acid concentrations. Acetic acid (\bullet) and propionic acid (\circ) concentrations.











broth was subsequently titrated with concentrated HCl to control pH. The rise in pH was attributed to a shift in metabolism from glucose to acetate catabolism as shown by the decrease in acetic acid concentration to undetectable levels. While samples were not taken after 24 hours, the experiment was allowed to continue. The pH strip chart recorder showed additional HCl was required after 24 hours, probably due to propionic acid catabolism. Finally the pH remained stable and no further HCl was used. A slight increase in cell dry weight during the acetic acid catabolism period was noted, however the error in the data may be larger than the indicated increase. The final cell concentration was 2.37 g dry weight per liter or 7.2×10^9 viable cells per ml.

The accumulation of propionate in the medium appears as a peculiar result of glucose metabolism. Previous studies on intracellular enzyme activity has brought forth a plausible explanation for this phenomena. Amarasingham and Davis (1965) found no α -ketoglutarate dehydrogenase activity in *E. coli* cells grown anaerobically or in exponentially growing cells under aerobic condition. This enzyme provides the link between α -ketoglutarate and succinate in the tricarboxylic acid (TCA) cycle (Figure 12). They proposed that, under anaerobic conditions, the TCA cycle operates as a branched pathway. The oxidative branch leads to α -ketoglutarate and the reductive branch leads to succinate. It appears that this modification to the TCA cycle is operating in exponentially growing cells under aerobic conditions as well.

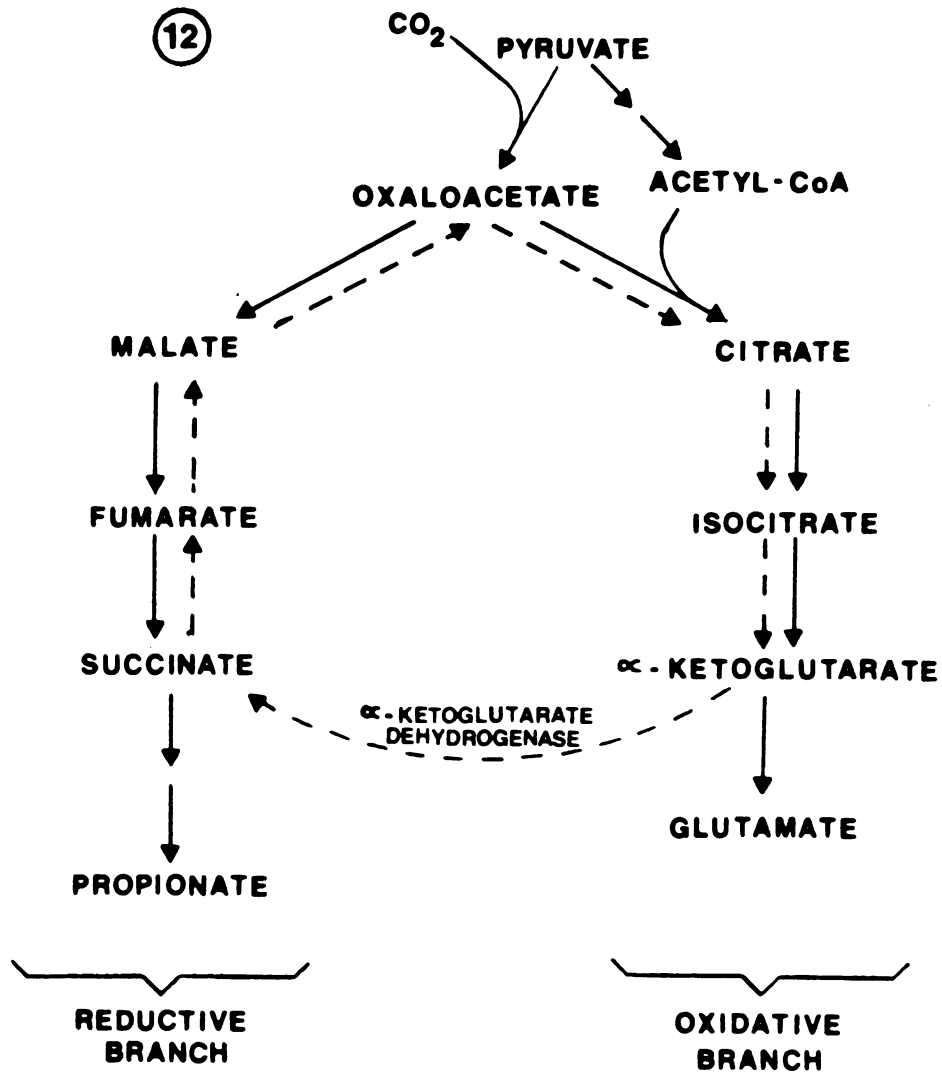


Figure 12. Proposed Modification of the TCA Cycle to a Branched Pathway for Exponentially Growing *E. coli* Under Aerobiosis (adapted from Amarsingham and Davis, 1965).

The intact TCA cycle (--->) is modified to a branched pathway (—>) in the absence of the α -ketoglutarate dehydrogenase system.

This branched mechanism is consistent with the results of the batch experiment. The lack of glutamate in the media indicates that its synthesis from α -ketoglutarate, formed by the oxidative branch, is required. The accumulation of propionic acid as an endproduct is proposed to be the result of the reductive pathway to succinate and finally to propionic acid. A diagram of the proposed mechanism is shown in Figure 12. The lack of data on the activities of key enzymes in these pathways during the course of the experiment makes this proposed mechanism speculative.

The accumulation of acetic acid in the medium by *E. coli*, as in this experiment, was attributed to an oversupply of NADH_2 (Doelle, Ewings, and Hollywood, 1982). The repression of cytochrome a by glucose was also demonstrated (Hollywood and Doelle, 1976) which would prevent electron transport from NADH_2 to oxygen. Thus it appears that acetate may act as a temporary electron reservoir when excess glucose is present with subsequent oxidation of acetic acid when glucose is depleted.

The terminal oxidation of acetic acid requires an active TCA cycle. Amarsingham and David (1965) found that α -ketoglutarate dehydrogenase was induced when sufficient acetate accumulated. The induction of α -ketoglutarate dehydrogenase led to a smooth transition in growth rate during the shift from glucose to acetic acid catabolism.



7.1.2 Microfiltration Cultivation. Culture behavior in the microfiltration system was studied by following the transient growth of *E. coli* using different feed rates (hydraulic residence times) and nutrient feed compositions. Experimental results are compared to the results obtained in the control batch culture.

Cells were allowed to grow in the fermentor as an ordinary batch culture prior to the start of microfiltration. Since the microfiltration capsules were not sterile after their first use, a high density of cells in the fermentor was desirable to prevent overgrowth of contaminants that may have been present. The final samples from each run was streaked for isolation on plate count agar to determine the extent of contamination if any. Few contaminants were found compared to the large number of *E. coli* colonies.

In all runs, microfiltration was started before the cell density reached $0.6 \text{ g } \ell^{-1}$ dry weight in an attempt to wash out acid end products that may be inhibitory to the organism and delay or eliminate the decrease in specific growth rate found in the batch experiment during the transition to acetate catabolism and stationary phase.

The microfiltration system was first tested to assess filtration performance and tune the level control system. Examination of the filter capsule at the end of these tests indicated a heavy build-up of cells between the outer channel wall and housing wall (Figure 13). The outer channel wall was discovered to be slightly permeable to water (Dale

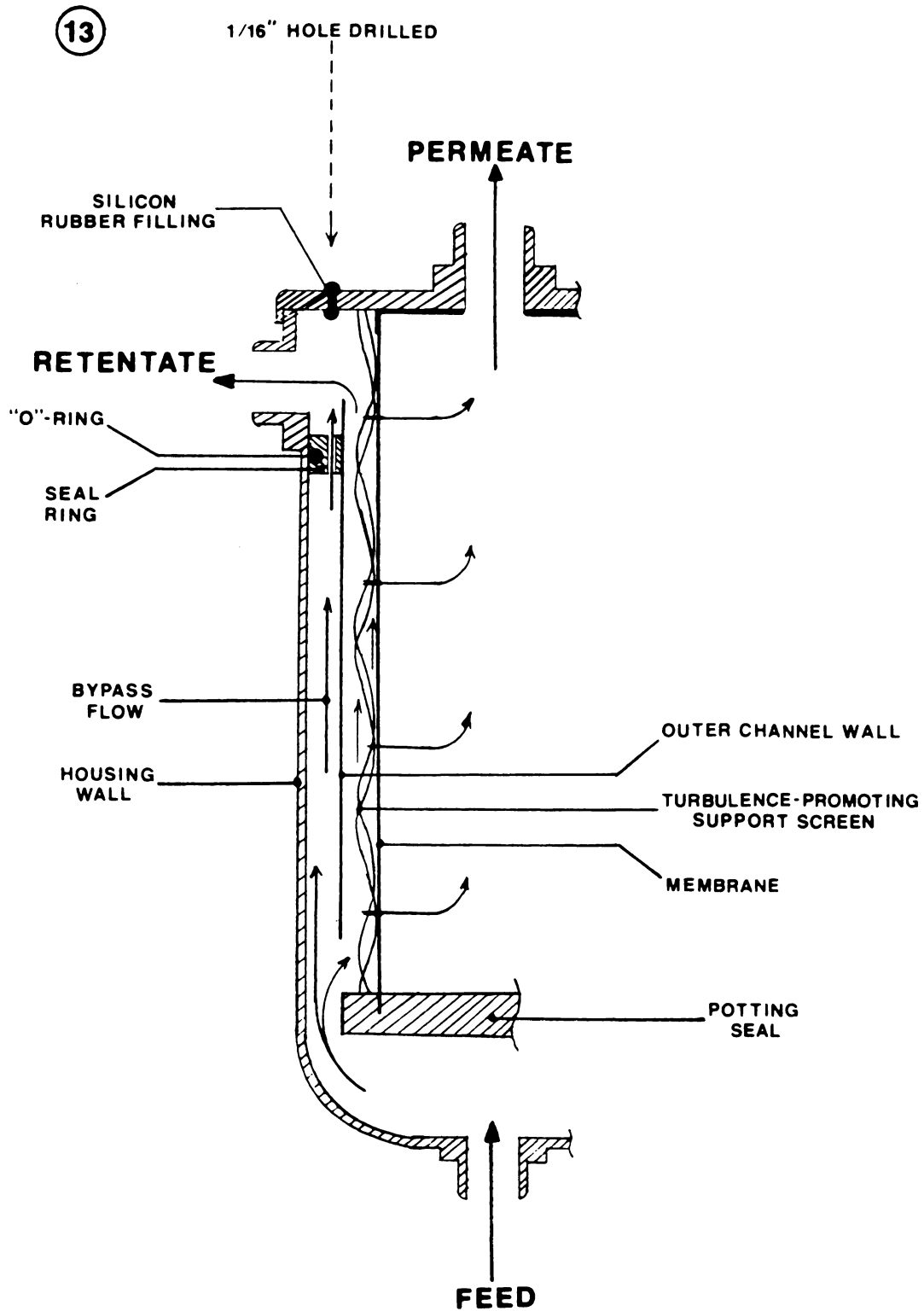


Figure 13. Cut-Away View of the Modified Gelman Acroflux Capsule

Hauk, Gelman Sciences, personal communication) causing a net flow of the fermentation broth into this dead space. The problem was circumvented by drilling 3 x 1/16" I.D. holes through the housing wall from the top, equidistant around the capsule, and through the seal ring. The hole in the housing wall was later filled with silicon rubber cement. This created a bypass around the outer channel wall, eliminating the dead space, allowing the fermentation broth to sweep any deposited cells from the space. The bypass flow did not decrease filtration rates through the membrane noticeably.

The filtrate was clear but took on a yellowish tint as the cell density in the fermentor increased. Viable cell counts in the filtrate were taken during some of the preliminary experiments. Typically less than 100 cell ml^{-1} were found. This was considered negligible compared to the number of cells in the fermentor.

All experiments were continued until the membrane became fouled and filtration rates could no longer be maintained. Attempts to backflush the filter with filtrate were moderately successful, but soon afterwards, the filtration rate again became too low.

7.1.2.1 Long Residence Time Microfiltration: Experiment

2. A long residence time microfiltration experiment was performed in an effort to extend exponential growth beyond that found in the batch experiment and prevent the accumulation of inhibitory acid. A new Acroflux capsule was used for the run.

Microfiltration was started 6 hours after inoculation. The feed rate was 592.5 ml hr^{-1} and the fermentor working volume was 2460 ml giving a hydraulic residence time of 4.15 hours. Results from experiment 2 are shown in Figure 14.

A characteristic drop in the fermentor cell concentration followed the start-up (Figure 14A). This was attributed to adhesion of cells to the filter membrane surface. Tanny, Merelman, and Pistole (1980) observed the same effect, reflected in low cell recoveries (44.5 to 76.1%), when using the filter to harvest small batches of cells. The layer of cells on the membrane is believed to attain a steady-state thickness as turbulence near the surface inhibits further deposition of cells.

The subsequent accumulation of cells in the fermentor continued at a lower specific rate than in the batch portion of the experiment. The final crop of cells was 4.84 g l^{-1} dry weight and 1.4×10^{10} viable cells ml^{-1} representing a two-fold increase over the batch culture.

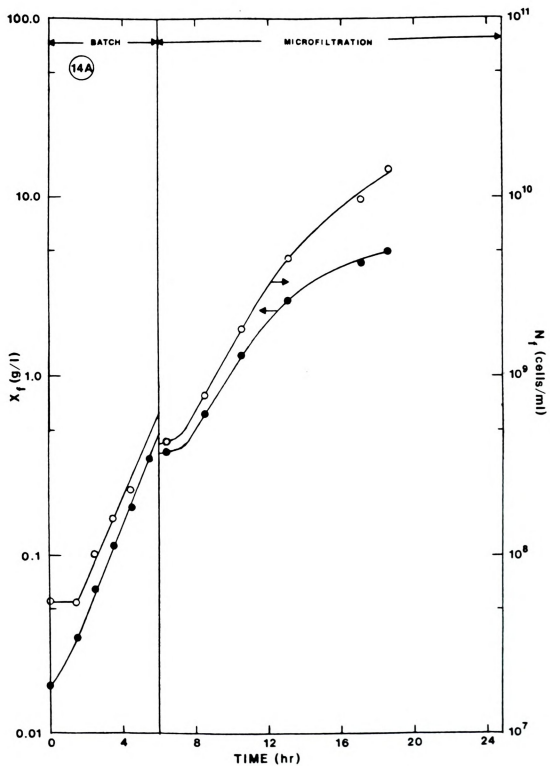
The consumption of glucose and ammonium ion proceeded the same as in Experiment 1 indicating that the rate of utilization of these components by the culture was much faster than the rate at which they were fed (Figure 14B). Growth became glucose-limited as indicated by the depletion of glucose in the fermentor near the end of the experiment. The residual glucose shown is believed to be interference in the glucose analysis.



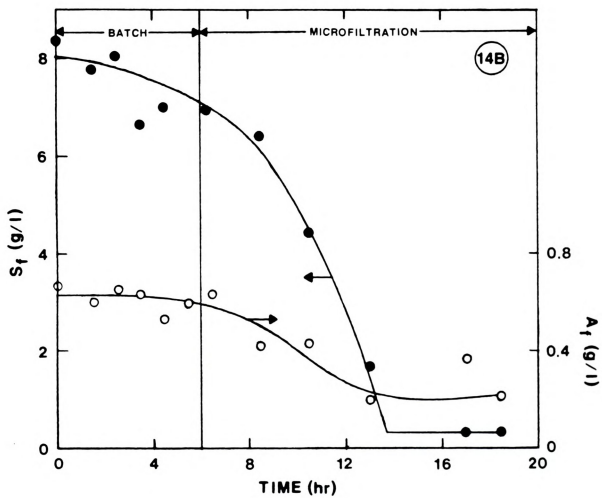
Figure 14. Results of Experiment 2.

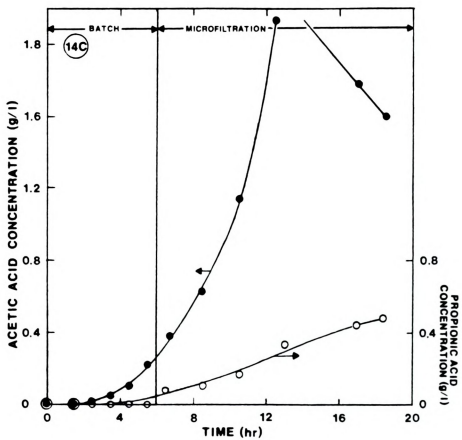
Microfiltration experiment with a hydraulic residence time of 4.15 hr.

- (A) Cell dry weight concentration (X_f) and viable cell concentration (N_f).
- (B) Residual glucose concentration (S_f) and ammonium ion concentration (A_f).
- (C) Acetic and propionic acid concentrations.









Acetic and propionic acid concentrations continued to increase throughout much of the experiment despite the diluting influence of adding fresh media (Figure 14C).

The ultimate decrease in acetic acid was attributed to a shift in metabolism; from an aerobic fermentative metabolism, where acetic acid was the primary fermentation end product (Figure 15A) to a respiratory metabolism with the complete oxidation of glucose to CO_2 and water (Figure 15B) with wash-out of acetic acid by microfiltration. This is in contrast to the decrease in the acetic acid concentration found in Experiment 1 which was due to a shift from glucose to acetic acid catabolism by the culture in the absence of glucose (Figure 15C).

The propionic acid concentration continued to increase even after the acetic acid concentration began to decrease. It is not clear why this should occur based on the mechanism previously described for propionic acid production.

The shift in metabolism from aerobic fermentation to respiration in *E. coli* was previously demonstrated in turbidostat culture (Doelle, Hollywood, and Westwood, 1974). At glucose concentrations greater than $2 \text{ g } \ell^{-1}$, metabolism was characterized by a high specific acid production rate and no α -ketogluta-rate dehydrogenase activity. At low glucose concentrations ($< 1.5 \text{ g } \ell^{-1}$) there was no acid production and α -ketogluta-rate dehydrogenase activity increased to high levels. It appears that the shift to respiration occurs as

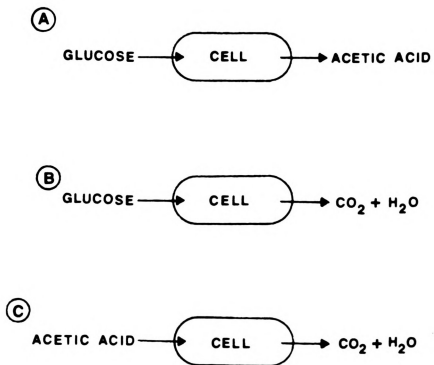
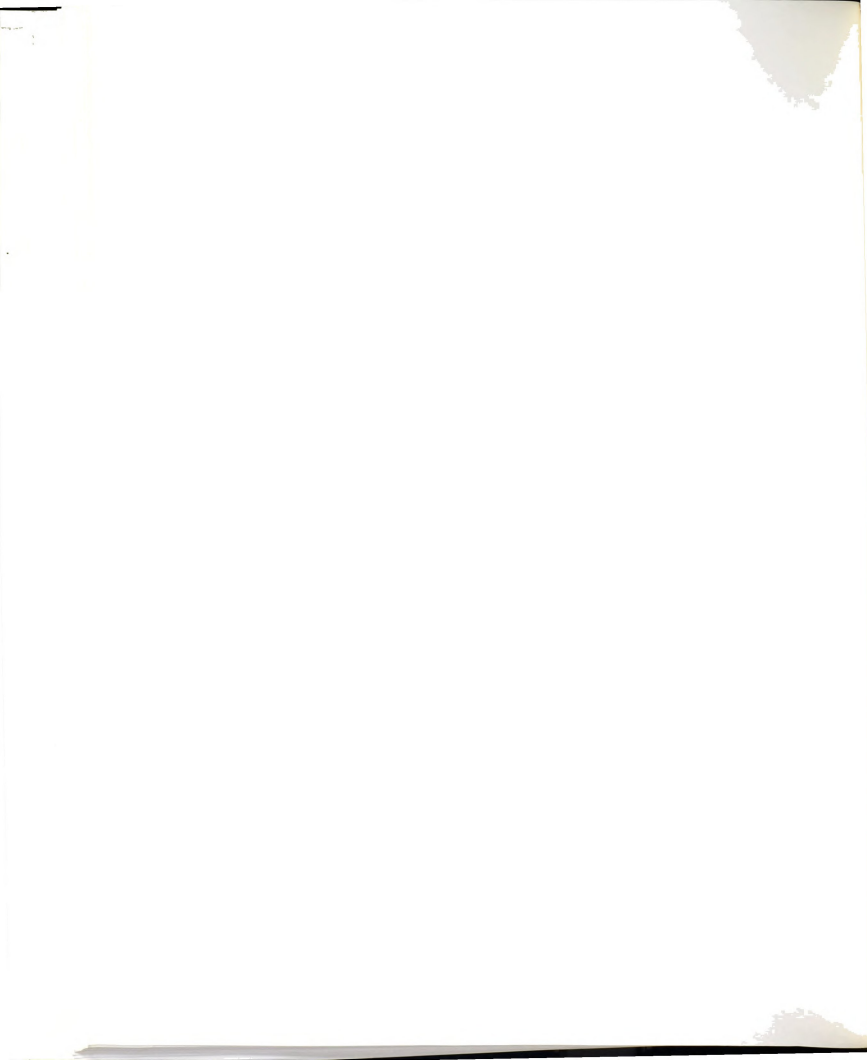


Figure 15. Metabolic Shifts in *E. coli* under Aerobic Conditions.

- (A) Excess glucose in the medium results in the accumulation of acids (particularly acetic acid) as aerobic fermentation end products.
- (B) When glucose becomes growth limiting, acids are not formed and glucose catabolism occurs by respiration.
- (C) If glucose becomes depleted as in Experiment 1, acetic acid is terminally oxidized.



glucose becomes the limiting nutrient indicating a more prudent use of the energy source when it is in limited supply.

In Experiment 2, glucose was depleted between hour 13 and 14. This coincided with the decrease in acetic acid concentration in the fermentor. It was clear that the nutrient feed rate was not fast enough to satisfy the nutrient demand of the culture.

7.1.2.2 Moderate Residence Time Microfiltration:

Experiment 3. A higher feed rate was used in an effort to provide more nutrients for the growing culture. A faster wash-out of acetic acid was expected upon entry into glucose-limited growth than was found in Experiment 2 due to the shorter hydraulic residence time.

In Experiment 3, media was fed at $1008.1 \text{ ml hr}^{-1}$. The fermentor working volume was 2960 ml giving a hydraulic residence time of 2.94 hours.

An Acroflux capsule that had been used for several of the preliminary experiments was used for the experiment. The results are shown in Figure 16. Microfiltration was started at hour 7.3. The growth curves of cell dry weight and viable cell concentrations did not show the decrease encountered with new capsules at start-up. It was concluded that repeated cleaning and deposits of old material on the membrane, and perhaps in the microporous matrix, in some way prevented new material from depositing on the membrane.

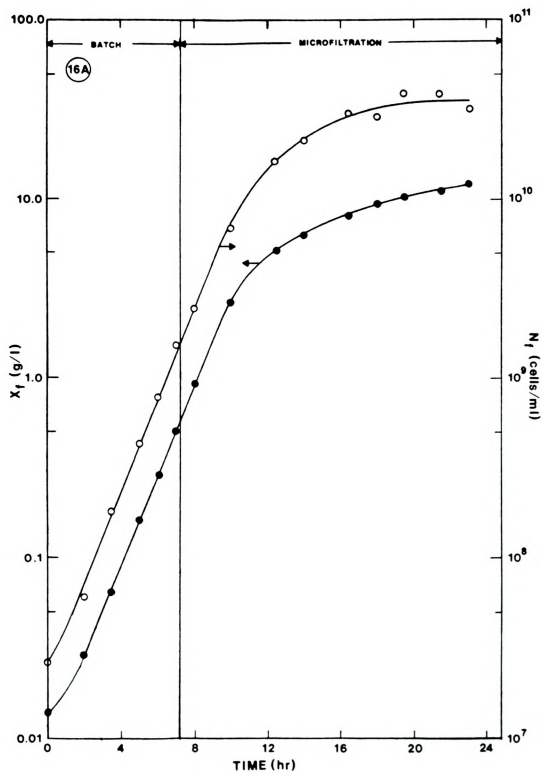


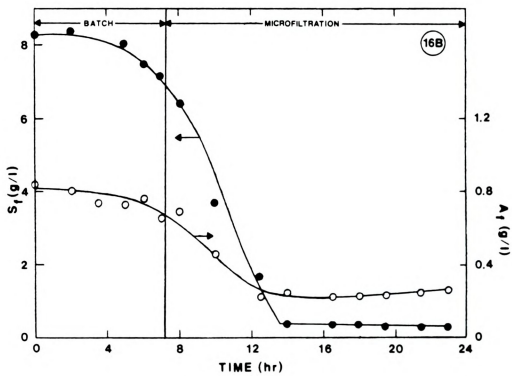


Figure 16. Results of Experiment 3.

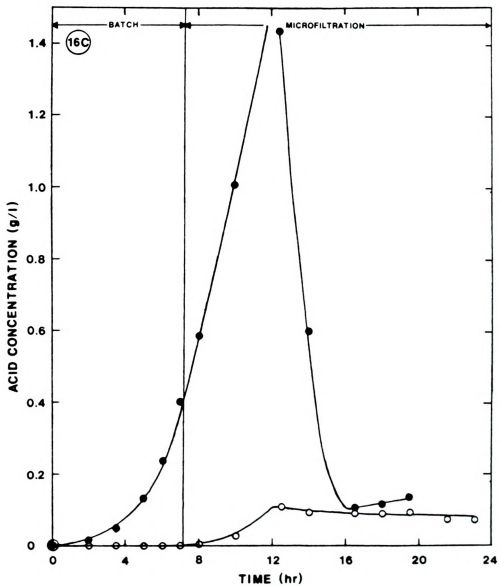
Microfiltration run with a hydraulic residence time of 2.94 hr.

- (A) Cell dry weight (X_f) and viable cell (N_f) concentrations.
- (B) Residual glucose concentration (S_f) and ammonium ion concentration (A_f).
- (C) Volatile acid concentrations. Acetic acid (\bullet) and propionic acid (\circ) concentrations.











Exponential growth continued until hour 10 when the specific growth rate began to decrease (Figure 16A). At hour 14, glucose became growth-limiting as seen by its depletion (Figure 16B). The ammonium ion concentration decreased as growth proceeded but began to increase during the glucose-limited growth phase as would be expected for an excess nutrient.

At the time microfiltration was started, the rate of glucose and ammonium ions entering the fermentor was less than the demand for those components by the culture. This resulted in time-concentration profiles similar to those in Experiments 1 and 2.

Acetic acid accumulated in the fermentor during exponential growth phase but as growth became glucose-limited (between hour 12 and 14) the acid was washed out (Figure 16C). The decrease is much faster than in Experiment 2 due to the shorter hydraulic residence time in the fermentor. Propionic acid production continued throughout the experiment but accumulated to a lower level than in Experiment 2 perhaps due to the shorter residence time.

The final cell dry mass and viable cell concentrations were $12.1 \text{ g } \ell^{-1}$ dry weight and 3.2×10^{10} cells ml^{-1} respectively, or about 5 times that attained in batch culture.

Exponential growth continued at higher cell densities than in the previous two experiments. The nutrient feed rate however was soon unable to satisfy the ever increasing demand for glucose and growth became glucose limited.



7.1.2.3 Short Residence Time Microfiltration with Concentrated Feed: Experiment 4. In an effort to satisfy the demand for glucose which became growth limiting in the previous experiments, the feed was made with 16.0 g ℓ^{-1} glucose and a higher feed rate was used. The NH_4Cl concentration was increased to 4.0 g ℓ^{-1} to ensure that nitrogen remained in excess supply. The other medium components were at the same concentrations as in the previous experiments.

The feed rate was 1773 ml hr^{-1} and the fermentor working volume was 2800 ml giving a hydraulic residence time of 1.58 hours. The results are shown in Figure 17. The same Acroflux capsule was used as in Experiment 2.

Microfiltration was started just after hour 7. Adhesion of cells to the filter was evident in the Experiment but was not as pronounced as in Experiment 2. A decrease in the specific growth rate after start-up was also noted (Figure 17A). By hour 10.75 the filter became fouled and the high filtration rate could not be maintained. The capsule was removed and replaced with a previously used capsule to continue the experiment. The viable cell concentration began to level off at about 10^{10} ml^{-1} after hour 12. It was believed that inhibition by accumulated acid prevented further increases in the viable cells.

A combination of the short residence time and highly concentrated feed led to an increase in glucose and ammonium ion concentration at start-up (Figure 17B). The glucose demand by the culture eventually exceeded the feed supply

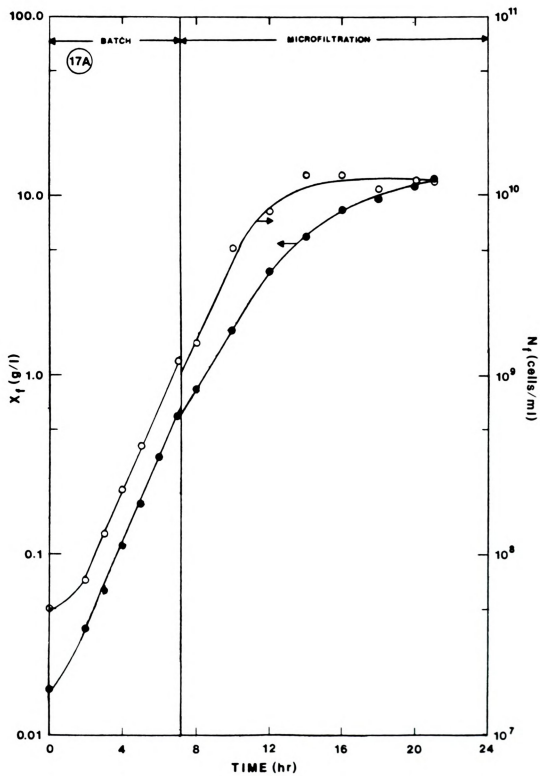




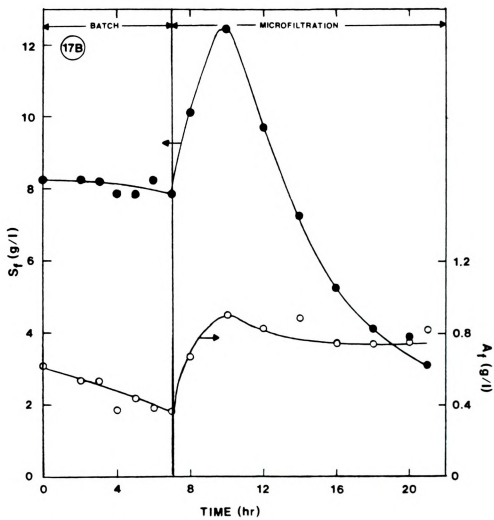
Figure 17. Results of Experiment 4.

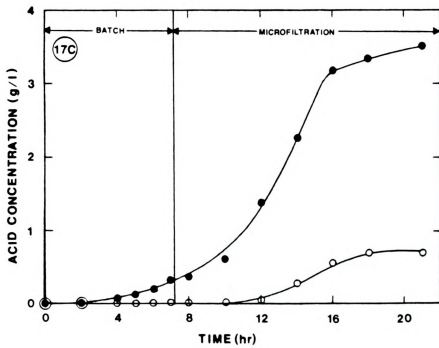
Microfiltration run with a hydraulic residence time of 1.58 hrs. Glucose and NH_4Cl in the feed was increased to 16.0 and 4.0 g l^{-1} respectively.

- (A) Cell dry weight concentration (X_f) and viable cell concentration (N_f).
- (B) Residual glucose (S_f) and ammonium ion (A_f) concentration.
- (C) Volatile acid concentrations. Acetic acid (\bullet) and propionic acid (\circ).
- (D) Non-volatile acid concentrations. Pyruvic acid (\circ), lactic acid (\blacksquare), oxaloacetic acid (\square), and succinic acid (\bullet).

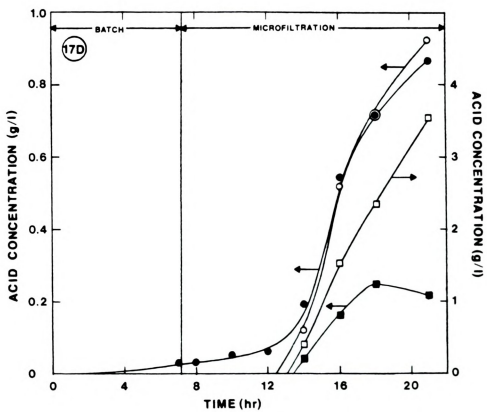












leading to its decline after hour 11. The ammonium ion concentration also increased but remained at high levels throughout the experiment, indicating it was an adequate supply throughout.

Glucose-limited growth did not occur and aerobic fermentation continued throughout the experiment. The utilization of the large amount of glucose in the feed by the culture led to the accumulation of larger amounts of acid than in the previous experiments. Figure 17C shows the accumulation of acetic and propionic acids during the experiment.

Analysis for non-volatile acids, which were only weakly detected in previous experiments (concentrations less than about 0.1 g l^{-1}) showed large amounts of oxaloacetic, lactic, pyruvic, and succinic acids in the medium. It was not clear why these acids should accumulate to high levels or even why they should be produced at all.

The final cell concentration was 12.43 g l^{-1} dry weight and 1.2×10^{10} viable cells ml^{-1} representing a 5 fold increase in cell dry weight and a 2 fold increase in viable cells over the batch culture.

7.2 Mathematical Model and Computer Simulation

7.2.1 Mathematical Model. A mathematical model was developed to describe the transient growth of *E. coli* in the microfiltration system shown in Figure 1B. In all experiments the purge stream flow rate (F_p) was 0 and $F_f = F_d$.

The concentrations of fermentor components modeled were cell dry weight, viable cells, the limiting nutrient, glucose, the excess nutrient, nitrogen (ammonium ion), and the end product acetic acid.

The membrane was assumed to exhibit no selective permeation toward any solute in the liquid fraction of the fermentor broth thus the filtrate has the same composition as the liquid fraction in the fermentor. It was further assumed that the space occupied by the cells was negligible at the cell populations found in these experiments. The highest packed volume of cells found in any sample was less than 8% of the total sample volume.

The component material balances around the system gives for the cell dry weight (X_f),

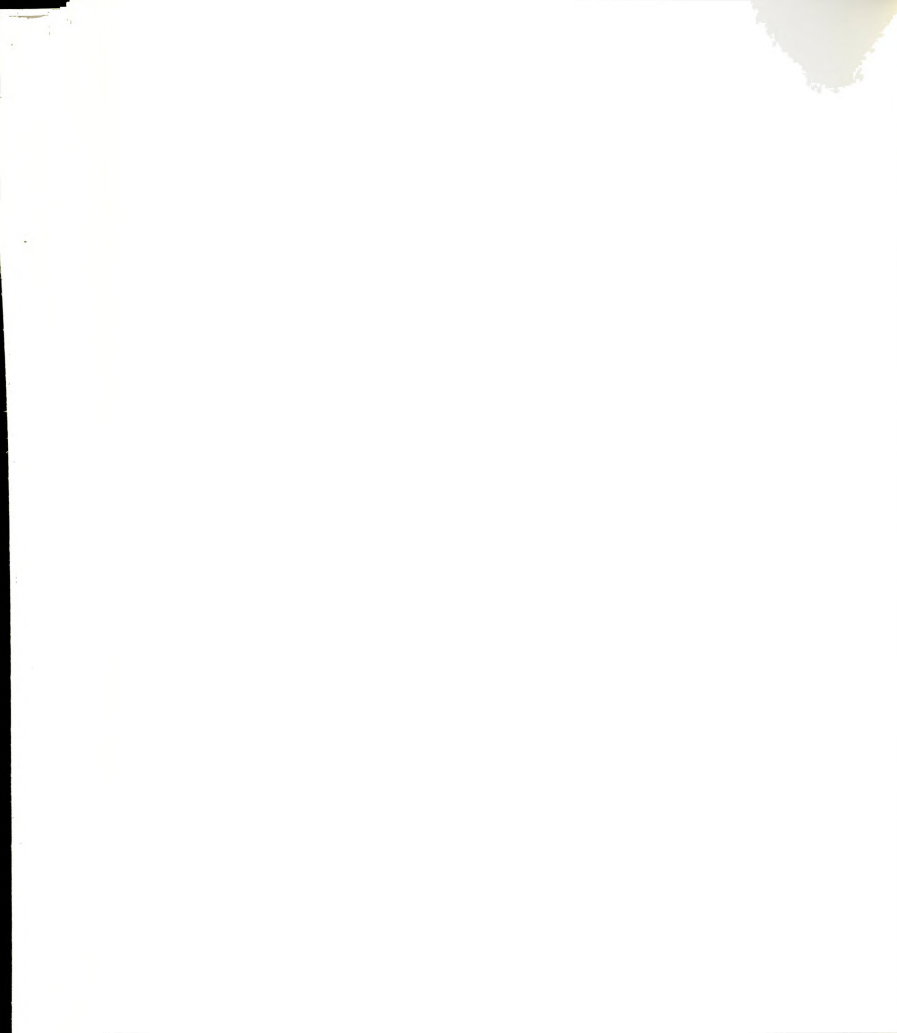
$$\frac{dX_f}{dt} = r_g \quad (27)$$

The viable cells per ml (N_f) were assumed proportional to the cell dry mass concentration,

$$\frac{dN_f}{dt} = 0.001 m_c^{-1} r_g \quad (28)$$

where m_c is the single cell mass and the 0.001 converts l to ml. The glucose concentration (S_f) is given by,

$$\frac{dS_f}{dt} = r_s + \frac{1}{\tau_H} (S_{f_0} - S_f) \quad (29)$$



the ammonium ion concentration (A_f) is

$$\frac{dA_f}{dt} = r_A + \frac{1}{\tau_H} (A_{f_0} - A_f) \quad (30)$$

and the acetic acid concentration (P_f) is

$$\frac{dP_f}{dt} = r_P + \frac{1}{\tau_H} (P_{f_0} - P_f). \quad (31)$$

Unstructured kinetic models were used to describe the intrinsic rates of reaction. The simplest kinetic models were chosen for which kinetic parameters were available or could be determined from the batch experiment. The rate of growth (r_g) is given by the Monod equation; then from equations (2) and (4)

$$r_g = \mu_{\max} \left(\frac{S_f}{S_f + K_S} \right) X_f. \quad (32)$$

Glucose is the sole carbon and energy source for the organism and the rate of glucose utilization ($-r_s$) contains terms for both growth and maintenance. Then equation (9) may be written

$$-r_s = \alpha_s r_g + \beta X_f. \quad (33)$$

The rate of ammonia utilization ($-r_A$) as the nitrogen source is given by

$$-r_A = \alpha_A r_g. \quad (34)$$



The rate of acetic acid production (r_p) is represented as a fraction of the substrate consumed by

$$r_p = \gamma(-r_s). \quad (35)$$

7.2.2 Kinetic Parameter Estimation. Kinetic parameters were estimated from batch data or taken from the literature.

Maximum Specific Growth Rate, μ_{\max} --Glucose is in large excess during the early exponential growth phase. equation (32) then reduces to

$$r_g = \mu_{\max} X_f. \quad (36)$$

Substituting equation (36) into (27) gives

$$\frac{1}{X_f} \frac{dX_f}{dt} = \frac{d(\ln X_f)}{dt} = \mu_{\max}. \quad (37)$$

Comparison of equations (37) and (26) gives

$$\mu = \mu_{\max} \quad (38)$$

during early exponential growth phase.

The early exponential growth phase specific growth rates were variable between experiments (Table 3). The specific growth rate from the batch experiment was taken as the maximum specific growth rate of 0.50 hr^{-1} .



TABLE 3. Early Exponential Growth Phase Specific Growth Rates (hr^{-1})

Experiment	Specific Cell Dry Weight Growth Rate	Specific Viable Cell Growth Rate
1	0.49	0.50
2	0.57	0.48
3	0.57	0.63
4	0.55	0.56

Substrate Saturation Constant, K_s --No experiments were performed to determine this parameter. A value of 0.05 g l^{-1} was selected, however, any reasonable value does not alter the computer outcome significantly.

Single Cell Mass, m_c --Substitution of equation (27) into (28) gives

$$0.001 \frac{dX_f}{dN_f} = m_c. \quad (39)$$

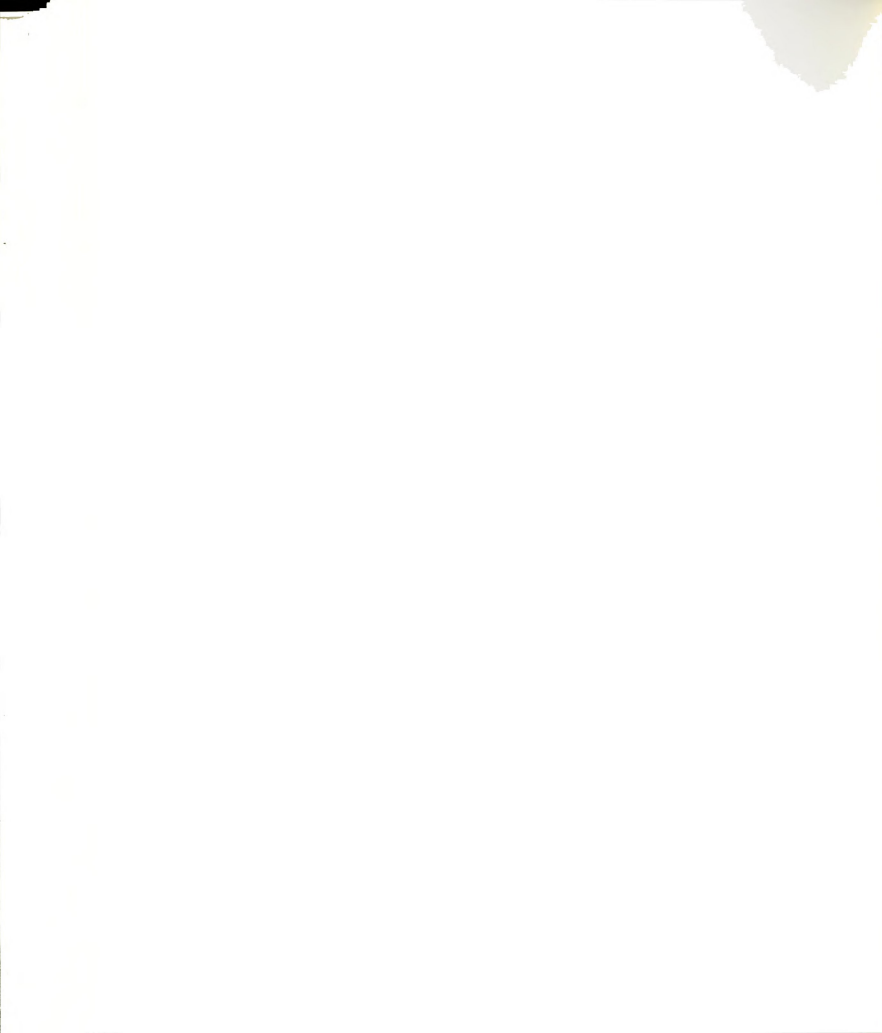
A plot of X_f vs. N_f from the batch data (Figure 18) gives

$$\frac{dX_f}{dN_f} = 3.74 \times 10^{-10} \frac{\text{g ml}}{\text{cells l}}. \quad \text{Then from equation (39)}$$

$$m_c = 0.001 \text{ ml}^{-1} \times 3.74 \times 10^{10} \frac{\text{g ml}}{\text{cells l}} = 3.74 \times 10^{-13} \text{ g cell}^{-1}.$$

Glucose Consumption Coefficient, α_s --Maintenance metabolism was neglected for this calculation. Substitution of equations (33) and (27) into (29) gives for batch growth

$$\frac{dS_f}{dt} = -\alpha_s \frac{dX_f}{dt}. \quad (40)$$



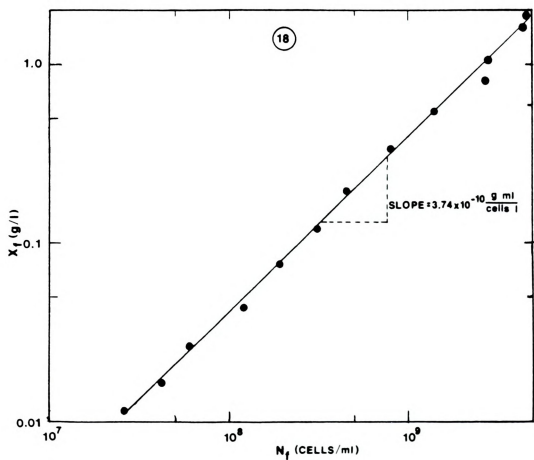


Figure 18. Cell Dry Weight (X_F) vs. Viable Cell (N_F) Concentrations from Experiment 1

This was simplified to

$$-\frac{\Delta S_f}{\Delta X_f} = \alpha_s \quad (41)$$

The initial cell concentration from Experiment 1 was 0.0072 g ℓ^{-1} and the final crop of cells was 2.34 g ℓ^{-1} . The initial glucose concentration was 8.0 g ℓ^{-1} and was 0 (neglecting interference in the glucose analysis) at the end of the experiment.

Then

$$\alpha_s = -\frac{0-8.0}{2.34-0.0072} = 3.43 \text{ g g}^{-1}$$

Maintenance Metabolism Parameter, β --Comparison of

Equations (9) and (33) shows that $\frac{1}{Y} = \alpha_s$ and

$$\frac{a}{Y} = \alpha_s \quad a = \beta \quad (42)$$

Marr, Nilson and Clark (1963) found the value of a to be 0.025 hr^{-1} for *E. coli*. Then using this value in equation (42) gives

$$\beta = \alpha_s a = 3.43 \text{ g g}^{-1} \times 0.025 \text{ hr}^{-1} = 0.086 \text{ g g}^{-1} \text{ hr}^{-1}.$$

Ammonium Ion Consumption Coefficient α_A --This parameter was calculated in a manner analogous to α_s . That is

$$-\frac{\Delta A_f}{\Delta X_f} = \alpha_A \quad (43)$$

The initial ammonium ion concentration was 0.0876 g ℓ^{-1} and the final was 0.276 g ℓ^{-1} . Then from equation 43

$$\alpha_A = - \frac{0.276-0.876}{2.34-0.0072} = 0.26 \text{ g g}^{-1}$$

Acetic Acid Yield Coefficient, γ --Substituting equations (29) and (31) into (35) gives for batch growth

$$\frac{dP_f}{dt} = \gamma \left(- \frac{dS_f}{dt} \right). \quad (44)$$

This was simplified to

$$- \frac{\Delta P_f}{\Delta S_f} = \gamma \quad (45)$$

The initial acetic acid concentration was 0 g l^{-1} and the final concentration was taken as 1.47 g l^{-1} before terminal oxidation began. Then

$$\gamma = \frac{1.47-0}{0-8.0} = 0.183 \text{ g g}^{-1}.$$

A summary of the kinetic parameters are given in Table 4.

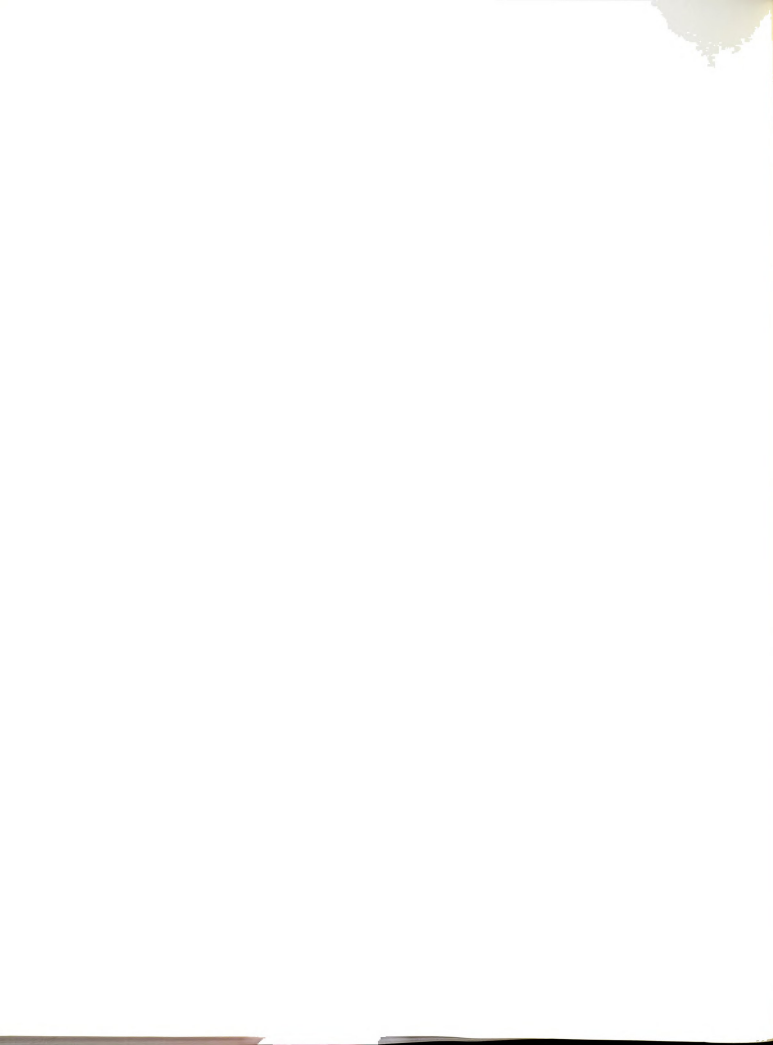


TABLE 4. Kinetic Parameters for the Mathematical Model

Symbol	Value	Probable Error (%)
μ_{\max}	0.50 hr ⁻¹	26
K_S	0.05 g l ⁻¹	90
m_C	3.74×10^{-13} g (cell) ⁻¹	30
α_S	3.43 g g ⁻¹	20
β	0.086 g g ⁻¹ hr ⁻¹	50
α_A	0.26 g g ⁻¹	20
γ	0.183 g g ⁻¹	20

7.2.3 Computer Simulation. The model was used to simulate the transient growth of *E. coli* in the microfiltration system using the parameters estimated from the batch data. Step-wise integration by digital computer using the Second Order Runge-Kutta Method with a step size of 0.01 and 0.001 hours. The error associated with the smaller step size is 100x less than with the larger step size. The same result was obtained with both step sizes. The computer program and output are given in Appendix V.

The kinetic equations do not predict a lag phase; therefore the initial conditions were taken from a point in the experimental data early in exponential growth phase. Physiological changes within the cell, such as the transition from aerobic fermentation to respiration, are not reflected in the unstructured kinetic model.



The maintenance term in Equation (33) can cause Equation (29) to predict negative glucose concentrations. To remedy this unphysical situation, all of the reaction rate terms were set to 0 if the glucose concentration became less than or equal to 0.

The simulated results from each experiment are discussed sequentially.

7.2.3.1 Batch Growth Simulation. The batch growth of cells was closely predicted (Figure 19A). The model did not predict the decrease in specific growth rate after hour 11 since the kinetics did not contain information regarding the shifts in metabolism encountered with this organism.

The consumption of medium components was directly coupled to the rate of growth in the model. The growth rate of cells was predicted faster than was found experimentally, therefore the rate of glucose and ammonium ion consumption was also predicted faster than was found experimentally (Figure 19B).

The accumulation of acetic acid was similarly predicted faster than was seen in the experiment (Figure 19C).

7.2.3.2 Experiment 2 Simulation. The simulation of cell growth in Experiment 2 was only moderately successful. The specific growth of cell dry weight during the batch portion of the experiment was faster than in the simulation. The deposition of cells at the start of microfiltration was not included in the model but was severe in this experiment.

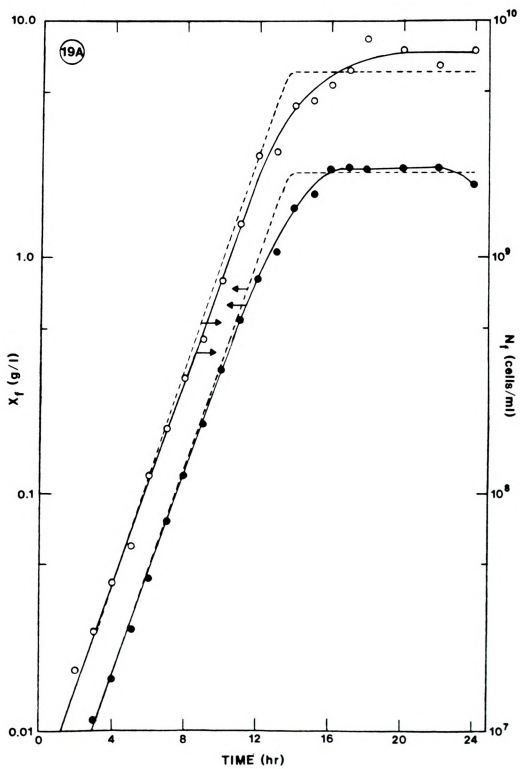


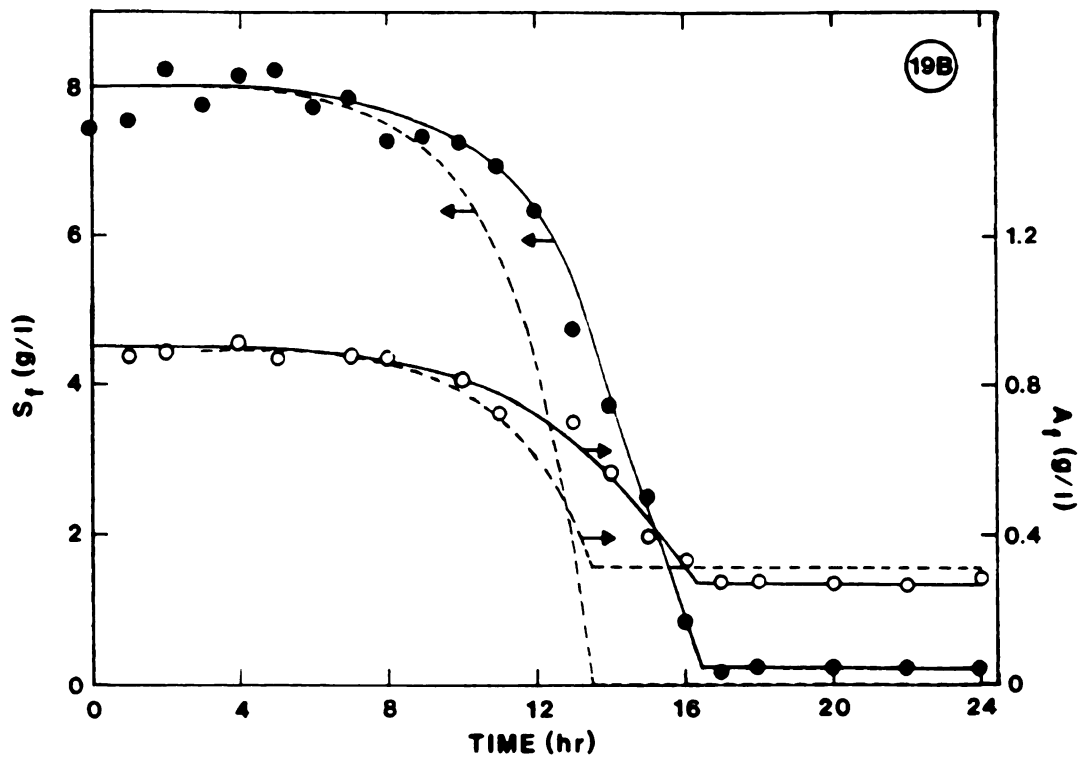


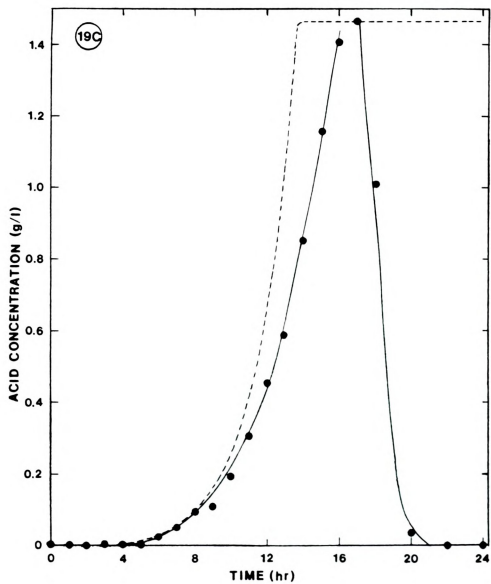
Figure 19. Computer Simulation of Experiment 1.

Simulated results (---) are compared with experimental results (—).

- (A) Cell dry weight (X_f) and viable cell (N_f) concentrations.
- (B) Glucose (S_f) and ammonium ion (N_f) concentrations.
- (C) Acetic acid concentration.







The subsequent growth of cells during microfiltration was at a lower specific rate than in the simulation (Figure 20A).

The predicted consumption of glucose and ammonium ion was faster than in the experiment (Figure 20B). The simulation shows an increase in the ammonium ion concentration as growth becomes glucose limited. This behavior was expected for an excess reactant, however the scatter in the ammonium ion concentration data near the end of the experiment failed to show the increase clearly.

The accumulation of acetic acid was predicted accurately however the concentration increased to higher levels than in the simulation (Figure 20C). This is probably due to uncertainty in the value of γ in equation (35). The model predicts a constant production rate of acetic acid during glucose-limited growth. The data shows, however a decrease in the acetic acid concentration which was attributed to a shift in metabolism from aerobic fermentation to respiration ($r_p \rightarrow 0$) and wash-out of the accumulated acetic acid.

7.2.3.3 Experiment 3 Simulation. The growth of cells in Experiment 3 was faster than in the simulation, however close agreement between the model and the experimental data was found (Figure 21A).

The consumption of glucose and ammonium ion was predicted accurately (Figure 21B). The increase in the ammonium ion concentration during glucose-limited growth, which was expected for an excess reactant, was found in both the simulation and data.

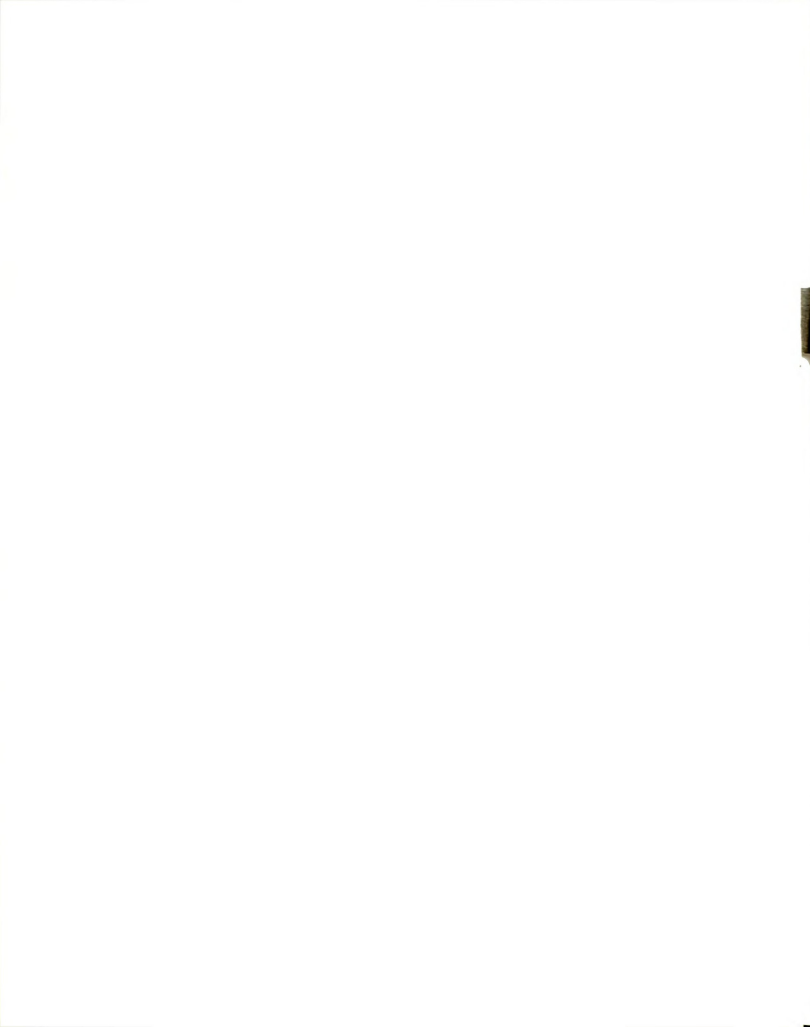
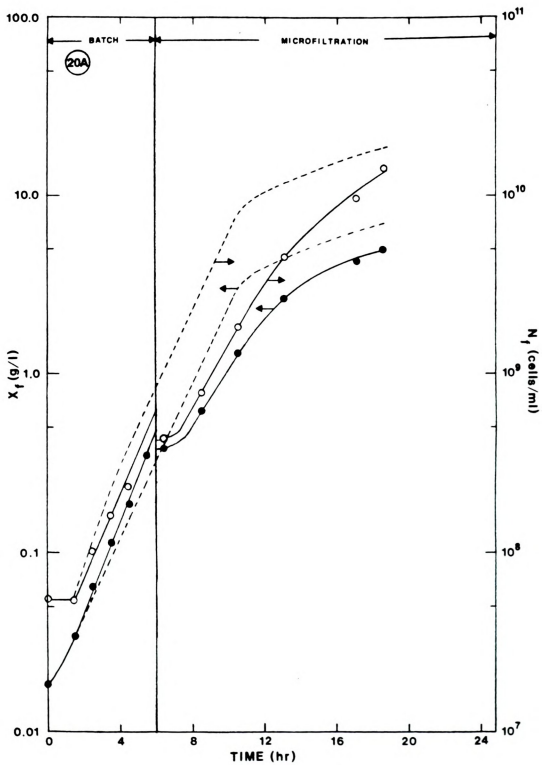


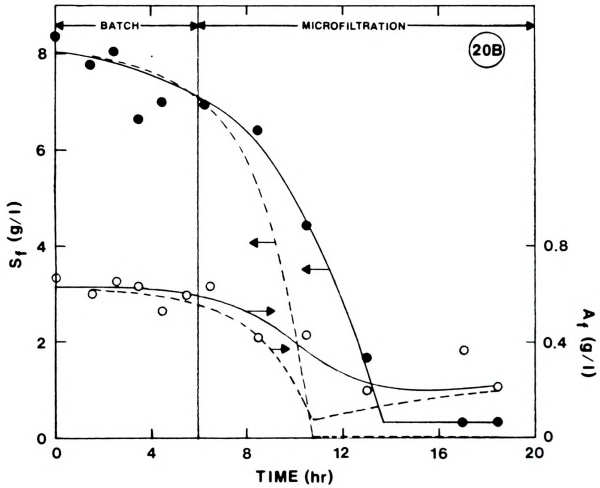
Figure 20. Computer Simulation of Experiment 2.

Simulated results (---) are compared with experimental results (—).

- (A) Cell dry weight (X_f) and viable cell (N_f) concentrations.
- (B) Glucose (S_f) and ammonium ion (A_f) concentration.
- (C) Acetic acid concentration.









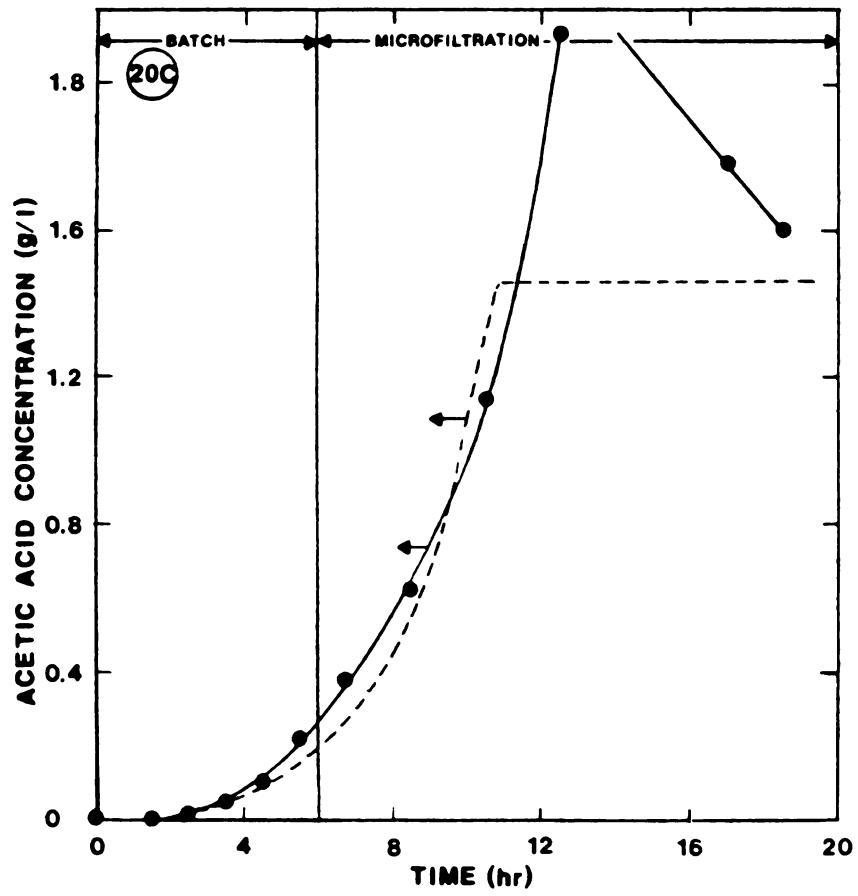
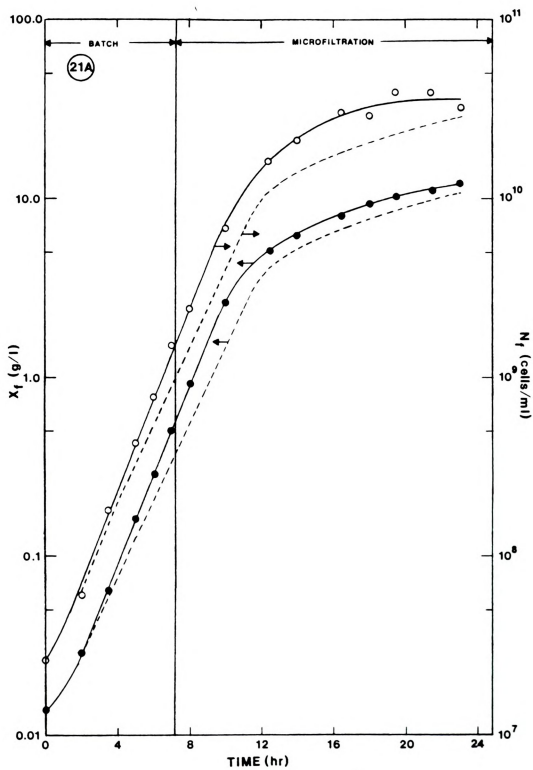


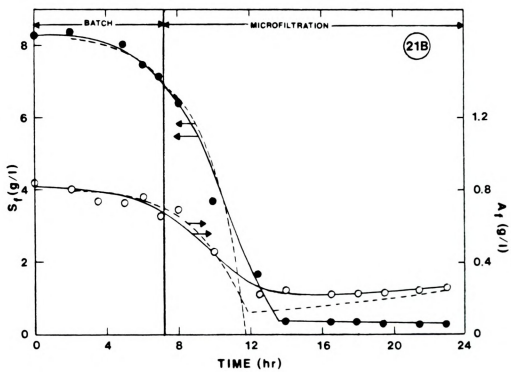
Figure 21. Computer Simulation of Experiment 3.

Simulated results (---) are compared with experimental results (—).

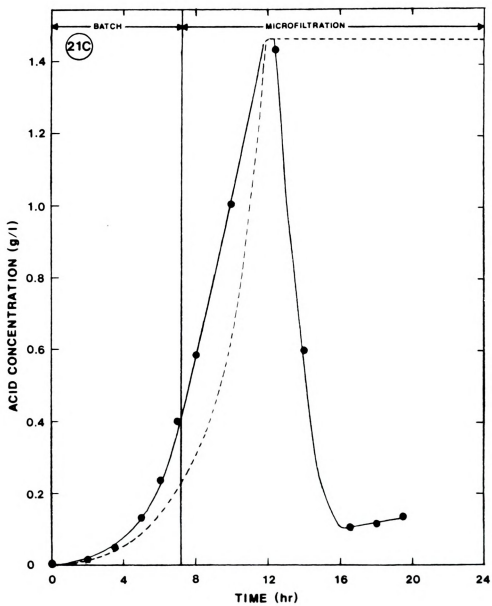
- (A) Cell dry weight (X_f) and viable cell (N_f) concentrations.
- (B) Glucose (S_f) and ammonium ion (A_f) concentrations.
- (C) Acetic acid concentration.











The accumulation of acetic acid shown in Figure 21C was faster than was found in the simulation. The shift from aerobic fermentation to respiration was not included in the kinetics and hence wash-out of acetic acid was not seen in the simulation.

7.2.3.4 Experiment 4 Simulation. The growth of cells in Experiment 4 was predicted accurately through hour 12 (Figure 22A). Thereafter the growth of viable cells stopped even with an excess of glucose in the medium. The large amount of acids that accumulated during this experiment were believed inhibitory to the organism. Acid inhibition was not included in the model hence exponential growth was predicted beyond hour 12.

The increase in glucose and ammonium ion concentration at the start of microfiltration was reflected in the simulation (Figure 22B). Glucose-limited growth was predicted to occur at about hour 13 but glucose was in excess throughout the experiment. This was the result of the inability of the model to predict the decrease in specific growth rate after hour 12. The ammonium ion concentration behavior was also not predicted after hour 12. The low specific growth rate found experimentally imposed a lower demand for ammonium ion as a nutrient after hour 12 whereas the simulation predicted a high demand for this nutrient.

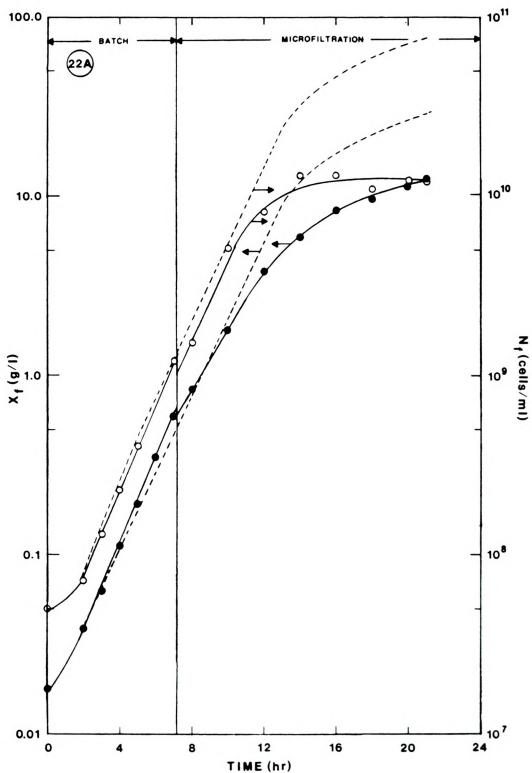
The accumulation of acetic acid was also predicted up to hour 12 (Figure 22C). The high growth rate predicted



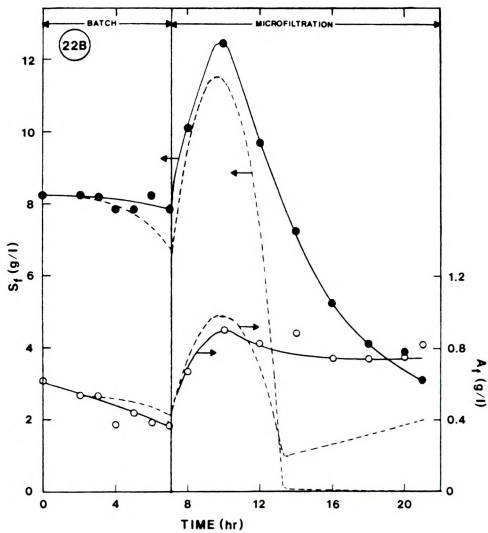
Figure 22. Computer Simulation of Experiment 4.

Simulated results (---) are compared with experimental results (—).

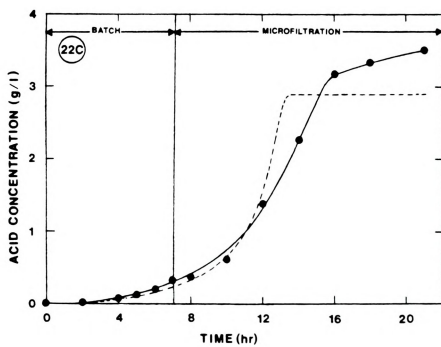
- (A) Cell dry weight (X_f) and viable cell (N_f) concentrations.
- (B) Glucose (S_f) and ammonium ion (A_f) concentrations.
- (C) Acetic acid concentration.











after hour 12 resulted in the acetic acid production rate to be predicted faster than was found in the experiment.

The success of a mathematical model for a system undergoing chemical reaction lies in the understanding of the reaction kinetics and biological systems are no exception. Until recently the only kinetic models in general use were of the unstructured type that only truly apply during balanced growth when all nutrients are in excess. They fail to account for variations in metabolism as was found in this investigation.

CONCLUSION

8.1 Equipment Considerations

Continuous fermentation with microfiltration appears as a promising method for increasing cell population densities and hence metabolite productivity per unit volume of fermentor. The application of microfiltration using microporous membranes has become a popular technique in affecting cell-liquid separations.

Membrane fouling appeared as a major obstacle in running the microfiltration system for long periods of time. Removal of the Acroflux capsule from the system for cleaning proved to be a satisfactory method for rejuvenating the membrane. Backflushing the membrane with filtrate *in situ* was only moderately successful. This problem should be more thoroughly studied before scale-up to an industrial process is attempted.

A closed loop liquid level control system was developed to aid in maintaining constant fermentor working volume. The level transmitter and controller could be used directly on any size process fermentor; only the pumping horsepower need be considered for process scale-up. Similarly the control system could be applied, with modification, to other fermentor designs such as dialysis fermentation.

8.2 Metabolic Considerations

The aerobic metabolism of *E. coli* was found to undergo several changes during the experiments. General trends in the experimental data along with studies on the metabolism of *E. coli* by previous investigators allowed some hypotheses to be formulated regarding these apparent changes.

The key factor affecting these changes was the induction and repression of the α -ketoglutarate dehydrogenase system under the influence of glucose concentration. When glucose was in excess, this enzyme system was repressed and aerobic fermentation proceeded with the simultaneous production of acids, primarily acetic acid; the other TCA cycle enzymes then took on a biosynthetic role. Depletion of glucose in batch culture led to the induction of the enzyme system and terminal oxidation of accumulated acetic acid. In microfiltration experiments, where glucose became growth limiting, the induction of the enzyme system led to a fully respiratory metabolism. Acetic acid that accumulated during glucose-excess growth was washed out by the microfiltration system.

The formation of propionic acid was found as the result of the TCA cycle becoming a branched pathway during glucose-repression of α -ketoglutarate dehydrogenase. Propionic acid was the end product of the reductive branch to succinate. The regulation of propionic acid formation was not understood in this investigation however.



While it is not clear why these metabolic changes should occur, their results were apparent in this study. Further study into these mechanisms is warranted as they are strongly coupled to the growth process of the organism.

8.3 Cell Productivity Considerations

The microfiltration system developed in this investigation produced populations of *Escherichia coli* up to 5 times that obtained in the control batch culture. All experiments were terminated before a stationary or maintenance state of the culture was achieved due to membrane fouling. With better membrane performance, higher populations could be obtained.

High concentrations of glucose in the feed was used in an effort to extend exponential growth phase and produce dense cell populations. This led to high residual glucose concentrations in the fermentor with the production of large amounts of organic acid end products which became inhibitory to further cell growth. The accumulation of these acids could be avoided by maintaining the culture in a state of glucose-limited growth so that a respiratory metabolism prevails. Growth could then continue in a linear fashion to produce high population densities.

8.4 Modeling Considerations

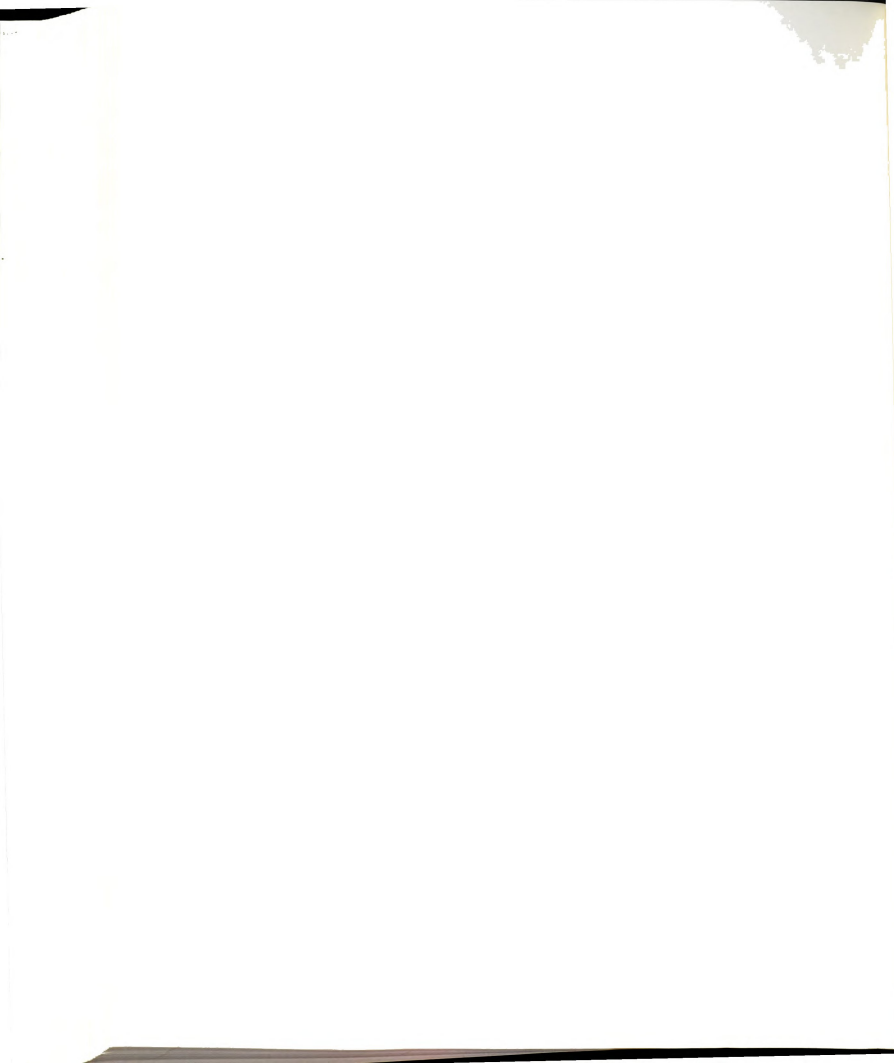
The unstructured kinetic model predicted the general features of the time-concentration profiles found during

glucose excess growth, however, the kinetics did not include parameters for the shifts in metabolism encountered at low glucose concentrations. A structured model would be more appropriate in this case and the elucidation of the metabolic mechanisms of the organism is a first step in formulating these models.



RECOMMENDATIONS

1. Measurement of the activity of certain enzymes involved in metabolism would be helpful in the further understanding of the data.
2. Assessment of the nutritional requirements of the organism and inhibitory effects of end products should be done before any long range study is attempted.
3. Background interference in the glucose and ammonium ion analysis was troublesome and these nonspecific procedures should be dispensed with in favor of techniques such as high performance liquid chromatography (HPLC).
4. Continuous stirred tank reactor (CSTR) cultivation and the transient phenomena that occurs there can be a valuable tool in determining kinetic parameters and studying microbial physiology in general.
5. Further experiments that maintain a low residual glucose concentration in the fermentor and hence a fully respiratory culture, could eliminate product inhibition and produce more dense cultures than obtained in this study.



APPENDICES



APPENDIX I

Standard Data

Standard curves from the analytical procedures are given in graphical form. A least squares fit to a straight line was used to calculate concentrations from the standard data. Lines are drawn on the figures to illustrate calculation procedures (Appendix II).



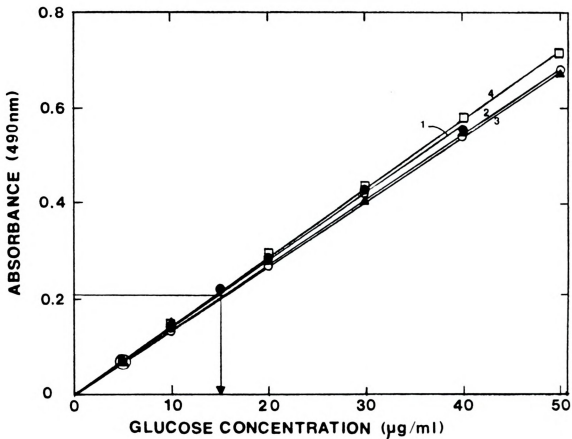
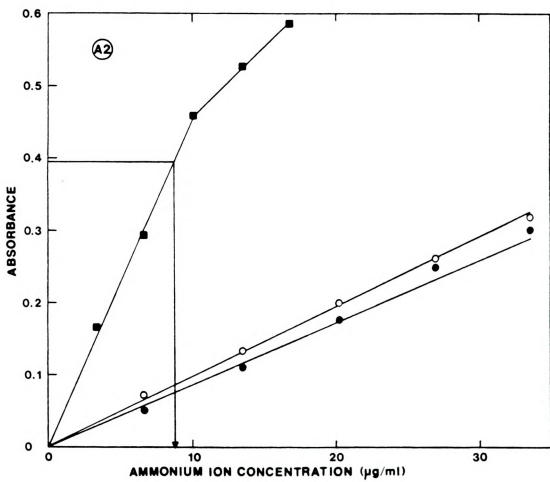


Figure A1. Glucose Standard Curves
Experiment 1 (●), Experiment 2 (▲),
Experiment 3 (○), Experiment 4 (□)

Figure A2. Ammonium Ion Standard Curves.

Experiment 1 (●), Experiment 3 (○), Experiments 2 and 4 (■). The curves for Experiments 1 and 3 were obtained at 490 nm. The curve for Experiments 2 and 4 was obtained at 400 nm by the procedure in Section 6.2.4. Note the increased sensitivity at 400 nm.



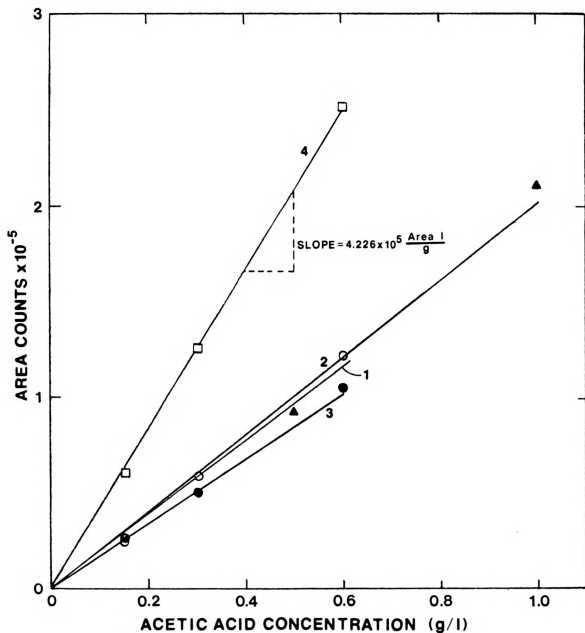


Figure A3. Standard Curves for Acetic Acid
 Experiment 1 (O), Experiment 2 (\blacktriangle),
 Experiment 3 (\bullet), Experiment 4 (\square).
 The signal attenuation to the integrator was 4 in Experiment 4 and 8 in the others resulting in the increased sensitivity.



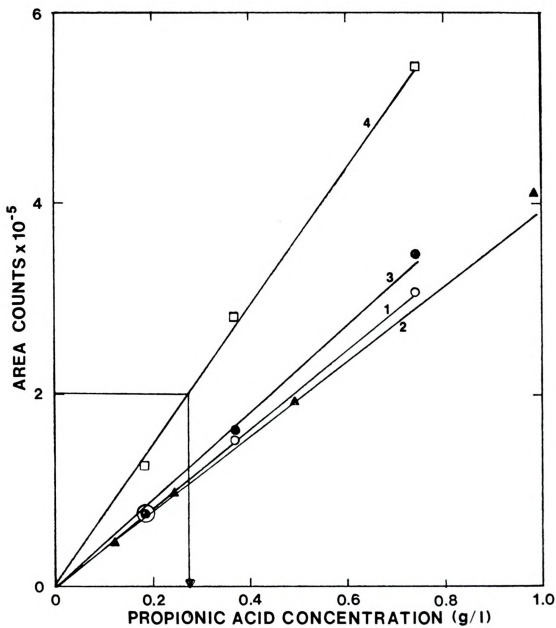


Figure A4. Standard Curves for Propionic Acid
Symbols and attenuation settings are
the same as in Figure A3.

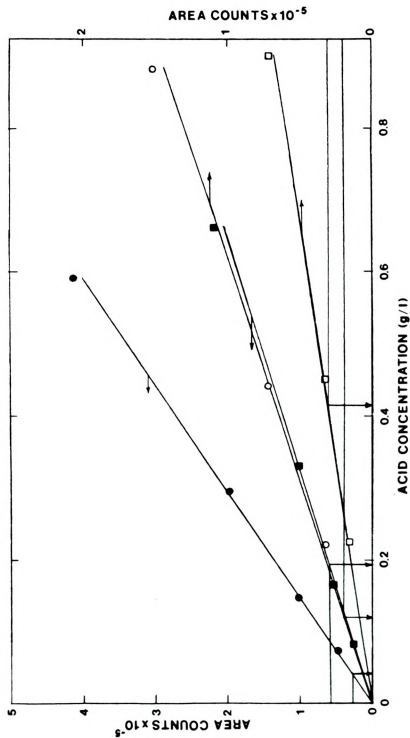
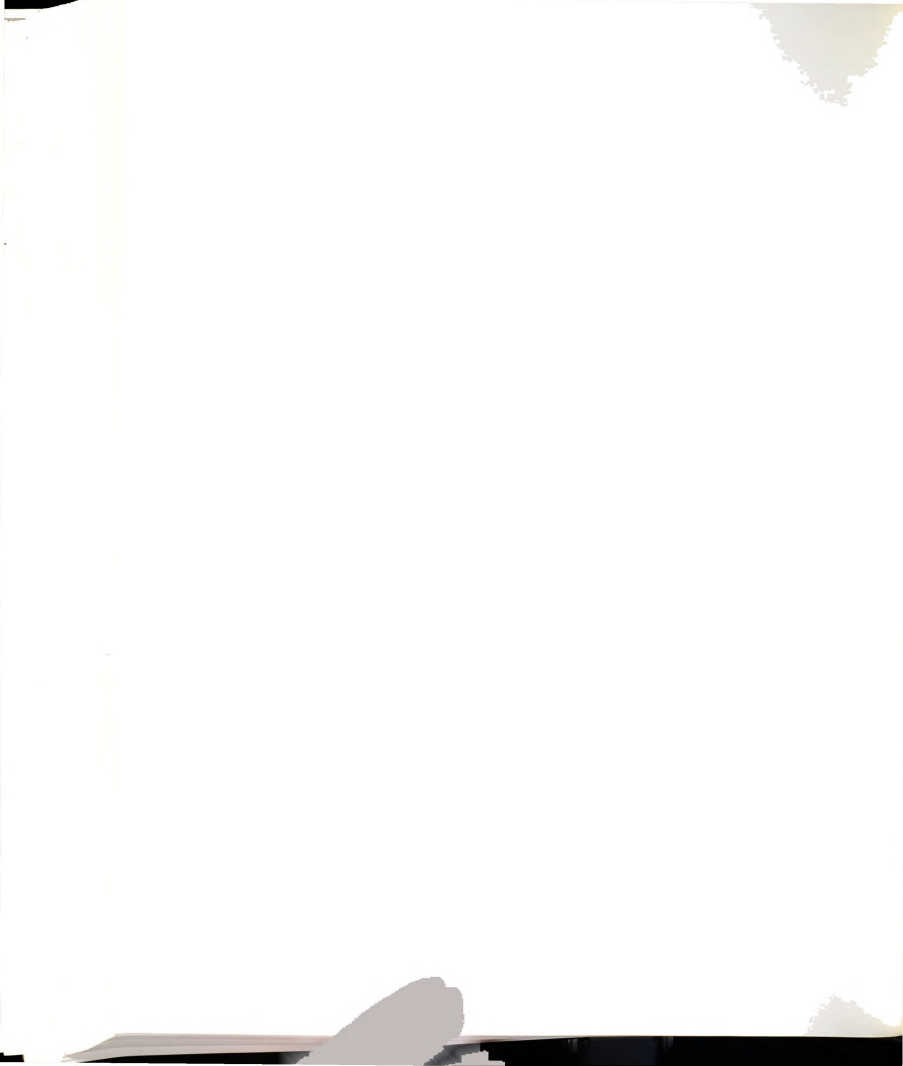


Figure A5. Non-Volatile Acid Standard Curves for Experiment 4
Pyruvic acid (O), Oxaloacetic acid (■), Lactic acid (□),
and Succinic acid (●).



APPENDIX II

Sample Calculations

Examples of calculations from raw data to yield the concentration of various sample components are shown for each analytical technique. Sample 10 of Experiment 4 is used to illustrate these calculations.

OPTICAL DENSITY. One ml of sample was diluted to 100 fold with distilled water. The optical density of the diluted sample was found to be 0.177. The optical density of the original sample was then

$$0.177 \times 100 = 17.7 \text{ O.D.}$$

CELL DRY WEIGHT. The optical density was multiplied by the slope of the standard curve in Figure 2. This gives

$$17.7 \text{ O.D.} \times 0.3289 \frac{\text{g}}{\ell \text{ O.D.}} = 5.821 \text{ g}/\ell.$$

VIABLE CELL COUNTS. The sample was diluted 10^8 fold in saline dilution blanks. The plate counts for the three plates were 132, 132, and 134 for an average of 132.7 colonies (unusually close agreement). The viable cells per ml of original sample was then

$$132 \times 10^8 = 1.3 \times 10^{10} \text{ Cells ml}^{-1}$$

GLUCOSE. One ml of sample was diluted 500 fold. After the diluted sample was treated as described in section 6.2,



the absorbance was measured to be 0.210. From the standard curve in Figure A1, this corresponded to 14.51 $\mu\text{g/ml}$. The glucose concentration in the original sample was

$$14.51 \mu\text{g/ml} \times 500 \times 10^{-3} \frac{\text{ml g}}{\ell \mu\text{g}} = 7.255 \text{ g/l} \approx 7.26 \text{ g/l}.$$

AMMONIUM ION. One ml of sample was diluted 100 fold and Nesslerized as in section 6.2. The absorbance was found to be 0.395. From Figure A2 this corresponds to 8.76 $\frac{\mu\text{g NH}_4^+}{\text{ml}}$. The ammonium ion concentration is then

$$8.76 \frac{\mu\text{g}}{\text{ml}} \times 100 \times 10^{-3} \frac{\text{ml g}}{\ell \mu\text{g}} = 0.876 \text{ g/l} \approx 0.88 \text{ g/l}.$$

VOLATILE FATTY ACIDS. The integrator reported two peaks. The sample was injected twice and the average area was calculated. For acetic acid the areas were 953,128 and 942,674 giving an average of 947,901. The propionic acid areas were 194,608 and 208,472 giving an average of 201,540.

The standard curve for acetic acid did not extend beyond an area of 250,000. Linearity was assumed in calculating the acetic acid concentration for this sample. The slope of the standard curve was $4.226 \times 10^{-5} \frac{\text{AREA COUNT } \ell}{\text{g}}$ giving the acetic acid concentration in the sample as

$$947901 \text{ AREA COUNTS} \div 4.226 \times 10^{-5} \frac{\text{AREA COUNT } \ell}{\text{g}} = 2.24 \text{ g/l}.$$

The propionic acid concentration was read directly from Figure A4 giving 0.276 g/l.



NON-VOLATILE ACIDS. These were handled similarly to the volatile fatty acids. The raw data are shown in table A1 for sample 10. The concentrations were read from Figure A5.

TABLE A1. Computation of Non-Volatile Acid Concentration

Acid	Injection 1	Injection 2	Average Area	Concentration (g/l)
Pyruvic	17,880	16,624	17,252	0.120
Oxaloacetic	58,352	62,520	60,436	0.194
Lactic	34,428	27,912	31,170	0.415
Succinic	25,784	N.R.	25,784	0.0415

N.R.-no integrator report



APPENDIX III

Numerical Data

Numerical data is given in tabular form for each experimental run. Missing data is indicated by a hyphen, —, and was usually the result of lack of enough sample for analysis or some other experimental error. In Experiments 2 through 4 the starting times of microfiltration is noted.

TABLE A2. Numerical Data for Experiment 1. Batch Run ($T_H = \infty$).

Sample	Time (hr)	O.D.-600	Cell Dry Weight (g \bar{x} -1)	Viable Cells (ml-1)	Glucose (g \bar{x} -1)	NH ₄ ⁺ (g \bar{x} -1)	Acetic Acid (g \bar{x} -1)	Propionic Acid (g \bar{x} -1)
0	0	0.022	0.0072	6.8x10 ⁶	7.42	--	0.0	0.0
1	1	0.018	0.0059	9.4x10 ⁶	7.56	0.876	0.0	0.0
2	2	0.022	0.0072	1.8x10 ⁷	8.22	0.892	0.0	0.0
3	3	0.035	0.0115	2.6x10 ⁷	7.78	--	0.0	0.0
4	4	0.050	0.0164	4.2x10 ⁷	8.15	0.916	0.0	0.0
5	5	0.081	0.0266	6.0x10 ⁷	8.22	0.863	0.0	0.0
6	6	0.133	0.0437	1.2x10 ⁸	7.71	--	0.0233	0.0
7	7	0.234	0.0770	1.9x10 ⁸	7.86	0.868	0.0453	0.0
8	8	0.364	0.1197	3.1x10 ⁸	7.27	0.879	0.0904	0.0
9	9	0.592	0.1947	4.5x10 ⁸	7.34	--	0.1084	0.0
10	10	1.016	0.3342	8.0x10 ⁸	7.25	0.815	0.1918	0.0
11	11	1.648	0.5420	1.4x10 ⁹	6.98	0.725	0.3026	0.0179
12	12	2.464	0.8104	2.7x10 ⁹	6.35	--	0.4543	0.0305
13	13	3.20	1.053	2.8x10 ⁹	4.77	0.703	0.5870	0.0352
14	14	4.88	1.605	4.4x10 ⁹	3.75	0.565	0.8503	0.0479
15	15	5.64	1.855	4.6x10 ⁹	2.53	0.398	1.157	0.0611
16	16	7.12	2.342	5.4x10 ⁹	0.86	0.337	1.407	0.0773
17	17	7.20	2.368	6.2x10 ⁹	0.15	0.276	1.496	0.134
18	18	7.08	2.329	8.4x10 ⁹	0.25	0.276	1.010	0.168
19	20	7.20	2.368	7.5x10 ⁹	0.25	0.262	0.033	0.204
20	22	7.23	2.378	6.5x10 ⁹	0.22	0.265	0.0	0.252
21	24	6.08	2.000	7.5x10 ⁹	0.21	0.281	0.0	0.200



TABLE A3. Numerical Data for Experiment 2. Microfiltration Run with $T_H = 4.15$ hr.

Sample	Time (hr)	0.D.+600	Cell Dry Weight (g l ⁻¹)	Viable Cells (ml ⁻¹)	Glucose (g l ⁻¹)	NH ₄ ⁺ (g l ⁻¹)	Acetic Acid (g l ⁻¹)	Propionic Acid (g l ⁻¹)
0	0	0.056	0.0184	5.6x10 ⁷	8.343	0.664	0.0	0.0
1	1.5	0.104	0.0342	5.4x10 ⁷	7.746	0.597	0.0	0.0
2	2.5	0.196	0.0645	1.0x10 ⁸	8.045	0.653	0.0118	0.0
3	3.5	0.336	0.1105	1.6x10 ⁸	6.625	0.637	0.0448	0.0
4	4.5	0.564	0.1855	2.3x10 ⁸	6.998	0.529	0.1023	0.0
5	5.5	1.04	0.3421	--	8.206	0.597	0.2192	0.0
-----Start Microfiltration-----								
7	6.5	1.152	0.3789	4.2x10 ⁸	6.936	0.631	0.3806	0.020
8	8.5	1.88	0.6183	7.7x10 ⁸	6.413	0.418	0.6238	0.025
9	10.5	3.89	1.279	1.8x10 ⁹	4.433	0.429	1.135	0.041
10	13	7.84	2.579	4.4x10 ⁹	1.633	0.198	2.120	0.083
11	17	12.72	4.184	9.3x10 ⁹	0.312	0.368	1.789	0.111
12	18.5	14.7	4.835	1.4x10 ¹⁰	0.335	0.217	1.598	0.121

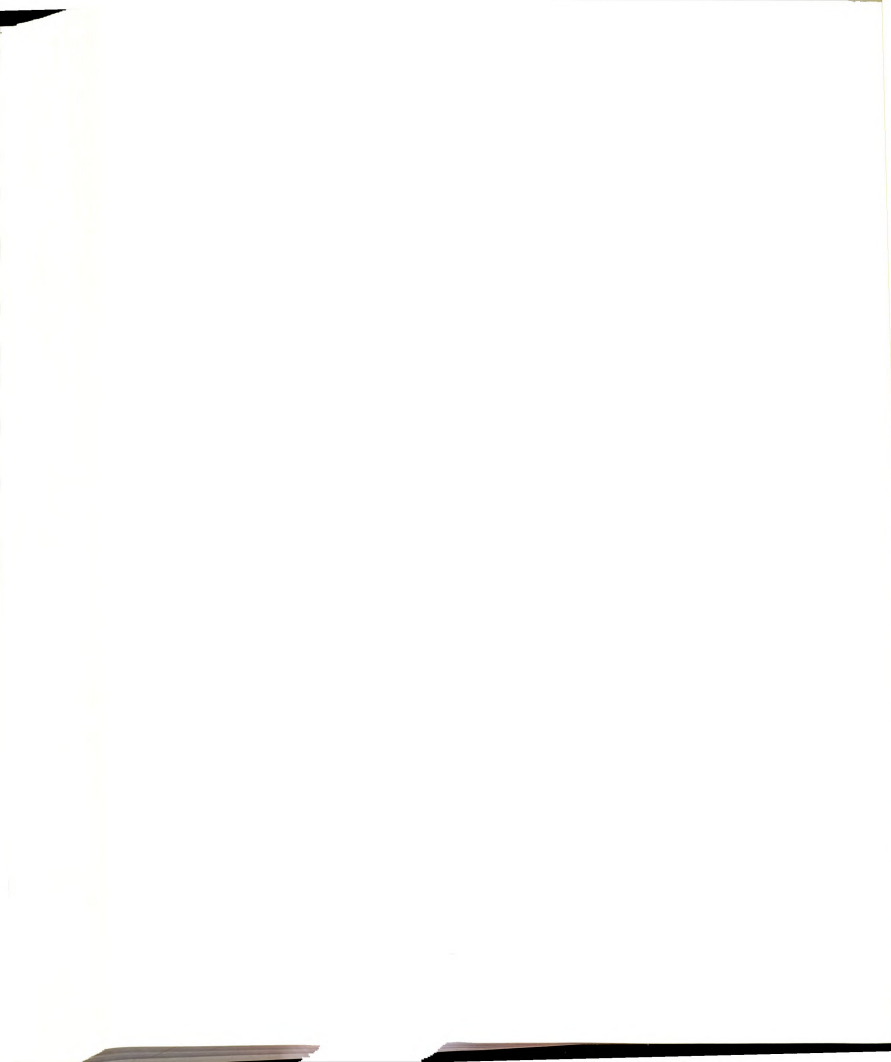


TABLE A4. Numerical Data for Experiment 3. Microfiltration Run with $\tau_H = 2.94$ hr.

Sample	Time (hr)	O.D.-600	Cell Dry Weight (gℓ ⁻¹)	Viable Cells (ml ⁻¹)	Glucose (gℓ ⁻¹)	NH ₄ ⁺ (gℓ ⁻¹)	Acetic Acid (gℓ ⁻¹)	Propionic Acid (gℓ ⁻¹)
0	0	0.042	0.0138	2.6x10 ⁷	8.25	0.836	0.0	0.0
1	2	0.087	0.0286	6.0x10 ⁷	8.40	0.796	0.0141	0.0
2	3.5	0.194	0.0638	1.8x10 ⁸	--	0.730	0.0504	0.0
3	5	0.488	0.1605	4.3x10 ⁸	8.03	0.722	0.1309	0.0
4	6.1	0.868	0.2854	7.7x10 ⁸	7.50	0.759	0.2367	0.0
5	7	1.530	0.5032	1.5x10 ⁹	7.13	0.645	0.4011	0.0052
-----7.3-----Start Microfiltration-----								
6	8.1	2.820	0.9275	2.4x10 ⁹	6.43	0.687	0.5838	0.0077
7	10	8.08	2.658	6.8x10 ⁹	3.68	0.453	1.032	0.0286
8	12.5	15.4	5.065	1.6x10 ¹⁰	1.70	0.220	1.433	0.1058
9	14	18.9	6.216	2.1x10 ¹⁰	0.36	0.241	0.5992	0.0905
10	16.5	24.2	7.959	3.0x10 ¹⁰	0.32	0.217	0.1039	0.0893
11	18	28.4	9.341	2.9x10 ¹⁰	0.32	0.225	0.1140	0.0878
12	19.5	31.2	10.26	3.9x10 ¹⁰	0.27	0.233	0.1338	0.0892
13	21.5	33.6	11.05	3.9x10 ¹⁰	0.28	0.241	--	0.0705
14	23	36.8	12.10	3.2x10 ¹⁰	0.29	0.257	--	0.071

TABLE A5. Numerical Data for Experiment 4. Microfiltration Run with $t_H = 1.58$ hr.

Sample	Time (hr)	0.D.-600	Cell Dry Weight (g $^{-1}$)	Visible Cells (ml $^{-1}$)	Glucose (g g^{-1})	Wt † (g g^{-1})	Acetic Acid (g g^{-1})	Propionic Acid (g g^{-1})	Succinic Acid (g g^{-1})	Lactic Acid (g g^{-1})	Pyruvic Acid (g g^{-1})	Oxaloacetic Acid (g g^{-1})
0	0	0.054	0.0178	5.0x10 ⁷	8.26	0.61	0.0	0.0	0.0	0.0	0.0	0.0
1	2	0.117	0.385	7.2x10 ⁷	8.26	0.53	0.021	0.0	0.0	0.0	0.0	0.0
2	3	0.192	0.0631	1.3x10 ⁸	8.19	0.54	--	--	0.0	0.0	0.0	0.0
3	4	0.336	0.1105	2.3x10 ⁸	7.85	0.37	0.065	0.0	0.0	0.0	0.0	0.0
4	5	0.580	0.1907	4.0x10 ⁸	6.88	0.43	0.115	0.0	0.0	0.0	0.0	0.0
5	6	1.056	0.348	7.2x10 ⁸	6.18	0.38	0.178	0.0	0.0	0.0	0.0	0.0
6	7	1.79	0.589	1.2x10 ⁹	7.05	0.32	0.329	0.0081	0.0	0.0	0.0	0.028
-----7.08-----Start Microfiltration-----												
7	8	2.50	0.822	1.5x10 ⁹	10.10	0.67	0.364	0.0091	0.0	0.0	0.0	0.034
8	9	3.44	1.149	2.5x10 ⁹	10.68	0.76	0.56	0.046	0.0	0.0	0.0	0.062
9	12	11.4	3.685	8.2x10 ⁹	9.69	0.82	1.35	0.06	0.0	0.0	0.0	0.120
10	14	17.7	5.821	1.3x10 ¹⁰	7.26	0.88	2.24	0.276	0.0415	0.0415	0.170	0.194
11	16	25.4	8.354	1.5x10 ¹⁰	5.24	0.74	3.17	0.564	0.157	1.53	0.518	0.544
12	18	29.2	9.603	1.1x10 ¹⁰	4.12	0.74	3.34	0.710	0.248	2.33	0.718	0.712
13	20	34.4	11.31	1.2x10 ¹⁰	3.91	0.75	--	--	--	--	--	--
14	21	37.8	12.43	1.2x10 ¹⁰	3.10	0.82	3.51	0.673	0.215	3.54	0.923	0.868



APPENDIX IV

Level Control Loop Start-Up Procedures and Schematic Diagram

Preliminary Procedures

1. Calibrate the level transmitter as described in the transmitter operating manual using the actual fermentation media. Transmitter should be set for low level fail safe.

2. Connect all process piping and wiring as shown in Figures 8 and A6.

Start-Up Procedure

1. All controls and switches should be in the following positions at this point:

- | | | |
|--------------------------------|--|----------------------------------------------|
| (a) FEED PUMP | | |
| POWER | | - OFF |
| (b) CROSS FLOW PUMP | | |
| POWER | | - OFF |
| LOCAL/REMOTE | | - REMOTE |
| FWD/REV | | - DETERMINE DIRECTION
FROM PROCESS PIPING |
| (c) CONTROLLER | | |
| POWER | | - OFF (UNPLUGGED) |
| SET-POINT | | - 60 (NOT CRITICAL) |
| MAN/AUTO | | - MANUAL |
| PROPORTIONAL
GAIN (K_C) | | - 1.6 |
| RESET ($1/\tau_I$) | | - 1.2 hr^{-1} |
| RATE (τ_D) | | - 0.011 hr |



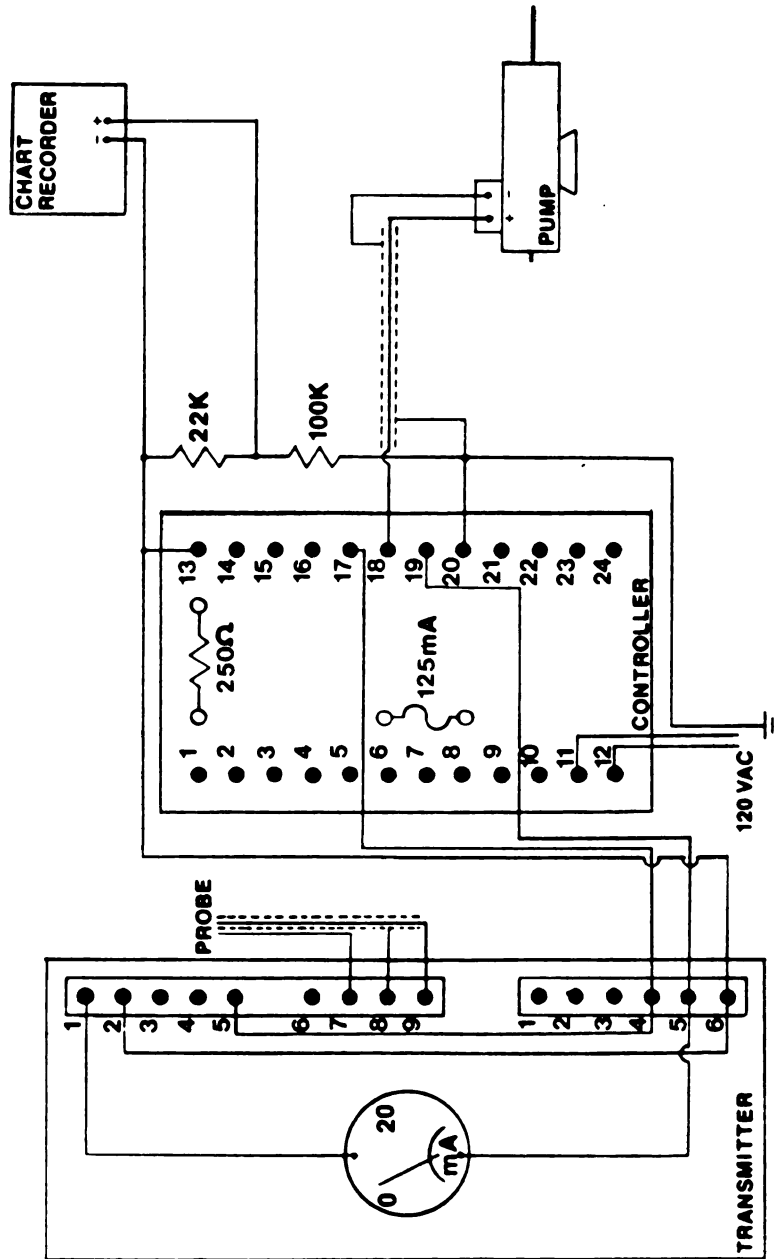


Figure A6. Level Control Loop Schematic Diagram



(d) FILTRATE THROTTLING
VALVE

- CLOSED

2. Turn on power to crossflow pump and controller.

This activates the entire control loop. Pump will not be turning.

3. Using the + button on the controller, hold down until pump turns at 250 rpm.

4. After the filtration loop is filled with liquid, adjust setpoint until all error lamps are off. (This will occur at or near a setpoint valve equal to the percent reading on the transmitter ammeter.)

5. Turn on the feed pump and set the desired flow rate. Open the filtrate throttling valve so that the filtrate flow rate appears to equal the feed rate.

6. Observe the level in the fermentor making adjustments on the throttling valve as needed*. When the system looks like it is operating satisfactorily, switch to automatic on the controller.

7. If the system settles in above or below the original level adjust the setpoint appropriately to increase or decrease the level*.

8. During the course of a run the pump speed will generally increase as the membrane becomes fouled. When full speed is reached, open the throttling valve slightly. This will allow the pump to slow down.

* Any changes made in the system should be small with a sufficiently long waiting period to allow these changes to settle out.



Appendix V

Computer Program and Output

Table A6. Computer Program and Simulated Results

```

1 PROGRAM MODEL
2 COMMON KS, MUMAX, BETA, ALPHAS, ALPHA, GAMMA
3 REAL MUMAX, KS, MC, NF, NFN
4 MC=3.74E-13
5 I=0
6 TSTOP=21.0
7
8 C READ KINETIC PARAMETERS
9 READ(10)MUMAX,KS,BETA,ALPHAS,ALPHA,GAMMA
10 FORMAT(4G10.6,2G10.6)
11 C READ INITIAL CONDITIONS
12 READ(10,END=70)TS,XF,SF,AF,PF,NF
13 I=I+1
14 C PRINT TABLE HEADINGS
15 WRITE(1,901)
16 WRITE(1,902)
17 WRITE(1,903)
18 WRITE(1,904)
19 WRITE(1,905)
20 T=0.0
21 NPRINT=500
22 KOUNT=NPRINT
23 DH=0.0
24 DT=0.001
25 AFO=0.0
26 SFO=0.0
27 PFO=0.0
28 C PRINT EVERY HALF HOUR
29 40 IF(KOUNT.EQ.NPRINT)THEN
30 WRITE(1,50)T,XF,NF,SF,AF,PF
31 FORMAT(F17.1,F10.3,E11.2,F9.3,F9.3,F11.3)
32 KOUNT=0
33 END IF
34 C START MICROFILTRATION AT T=TS
35 IF(DH.NE.0.0.OR.T.LT.TS) GO TO 60
36 READ(10)SFO,AFO,DH,TSTOP
37 TAU=1./DH
38 WRITE(1,906)TS,TAU
39 WRITE(1,905)
40 C 60 CALL KINETIC(SF,XF,RG,RS,RA,RP)
41 PREDICTOR EQUATIONS
42 XFN=XF+RG*DT
43 NFN=NF+RG/MC*DT/1000.
44 SFN=SF+(RS+DH*(SFO-SF))*DT
45 AFN=AF+(RA+DH*(AFO-AF))*DT
46 PFN=PF+(RP+DH*(PFO-PF))*DT
47 C CALL KINETIC(SFN,XFN,RSN,RAN,RPN)
48 CORRECTOR EQUATIONS
49 XF=XF+(RG+RGN)/2.*DT
50 NF=NF+(RG+RGN)/2./MC*DT/1000.
51 SF=SF+((RS+DH*(SFO-SF)+RSN+DH*(SFO-SFN))/2.)*DT
52 AF=AF+((RA+DH*(AFO-AF)+RAN+DH*(AFO-AFN))/2.)*DT
53 PF=PF+((RP+DH*(PFO-PF)+RPN+DH*(PFO-PFN))/2.)*DT
54 KOUNT=KOUNT+1
55 T=T+DT
56 C IF T=TSTOP GO TO NEXT EXPERIMENT
57 IF(T.GT.TSTOP) GO TO 20
58 GO TO 40
59 70 STOP
60 901 FORMAT('1',9X,'EXPERIMENT',I1)
61 902 FORMAT('0',12X,'TIME',7X,'XF',8X,'NF',8X,'SF',8X,'AF',8X,'PF')
62 903 FORMAT('13X',(HR)',5X,(G/L) (CELLS/ML) (G/L)',5X,(G/L),5X,
63 (G/L))
64 904 FORMAT('0',34X,'BATCH GROWTH')
65 905 FORMAT('0',)
66 906 FORMAT('0',F16.1,' START MICROFILTRATION - RESIDENCE TIME= ',
67 CF4.2,' HR')
68 END

```



Table A6 (cont'd).

```
1      SUBROUTINE KINETIC(S,X, RG,RS,RA,RP)
2      COMMON KS,MUMAX,BETA,ALPHAS,ALPHAA,GAMMA
3      REAL MUMAX,KS
4      IF(S.LE.O.) GO TO 10
5      RG=MUMAX*(S/(S+KS))*X
6      RS=-ALPHAS*RG-BETA*X
7      RA=-ALPHAA*RG
8      RP=-GAMMA*RS
9      RETURN
10     10 RS=O.
11        RG=O.
12        RA=O.
13        RP=O.
14        RETURN
15     END
```

Table A6 (cont'd).

EXPERIMENT 1					
TIME (HR)	XF (G/L)	NF (CELLS/ML)	SF (G/L)	AF (G/L)	PF (G/L)
BATCH GROWTH					
0.0	.012	.26E+08	8.000	.890	0.000
.5	.015	.35E+08	7.988	.889	.002
1.0	.019	.46E+08	7.973	.888	.005
1.5	.024	.60E+08	7.954	.887	.008
2.0	.031	.78E+08	7.930	.885	.013
2.5	.040	.10E+09	7.898	.883	.019
3.0	.051	.13E+09	7.857	.880	.026
3.5	.065	.17E+09	7.806	.876	.036
4.0	.084	.22E+09	7.739	.871	.048
4.5	.108	.28E+09	7.654	.865	.063
5.0	.138	.36E+09	7.545	.857	.083
5.5	.177	.47E+09	7.404	.847	.109
6.0	.227	.60E+09	7.225	.834	.142
6.5	.290	.77E+09	6.995	.817	.184
7.0	.372	.99E+09	6.700	.796	.238
7.5	.477	.13E+10	6.322	.769	.307
8.0	.611	.16E+10	5.839	.734	.396
8.5	.783	.21E+10	5.219	.689	.509
9.0	1.003	.27E+10	4.427	.632	.654
9.5	1.284	.34E+10	3.414	.559	.839
10.0	1.641	.44E+10	2.126	.466	1.075
10.5	2.086	.56E+10	.521	.351	1.369
11.0	2.227	.60E+10	-.000	.314	1.464
11.5	2.227	.60E+10	-.000	.314	1.464
12.0	2.227	.60E+10	-.000	.314	1.464
12.5	2.227	.60E+10	-.000	.314	1.464
13.0	2.227	.60E+10	-.000	.314	1.464
13.5	2.227	.60E+10	-.000	.314	1.464
14.0	2.227	.60E+10	-.000	.314	1.464
14.5	2.227	.60E+10	-.000	.314	1.464
15.0	2.227	.60E+10	-.000	.314	1.464
15.5	2.227	.60E+10	-.000	.314	1.464
16.0	2.227	.60E+10	-.000	.314	1.464
16.5	2.227	.60E+10	-.000	.314	1.464
17.0	2.227	.60E+10	-.000	.314	1.464
17.5	2.227	.60E+10	-.000	.314	1.464
18.0	2.227	.60E+10	-.000	.314	1.464
18.5	2.227	.60E+10	-.000	.314	1.464
19.0	2.227	.60E+10	-.000	.314	1.464
19.5	2.227	.60E+10	-.000	.314	1.464
20.0	2.227	.60E+10	-.000	.314	1.464
20.5	2.227	.60E+10	-.000	.314	1.464
21.0	2.227	.60E+10	-.000	.314	1.464

Table A6 (cont'd).

EXPERIMENT 2					
TIME (HR)	XF (G/L)	NF (CELLS/ML)	SF (G/L)	AF (G/L)	PF (G/L)
BATCH GROWTH					
0.0	.034	.54E+08	8.000	.620	0.000
.5	.044	.80E+08	7.965	.617	.006
1.0	.056	.11E+09	7.921	.614	.015
1.5	.072	.16E+09	7.864	.610	.025
2.0	.092	.21E+09	7.790	.605	.038
2.5	.118	.28E+09	7.697	.598	.056
3.0	.152	.37E+09	7.576	.589	.078
3.5	.195	.48E+09	7.422	.578	.106
4.0	.249	.63E+09	7.224	.564	.142
4.5	.320	.82E+09	6.971	.546	.188
— 4.5 - START MICROFILTRATION - RESIDENCE TIME= 4.15 HR —					
5.0	.410	.11E+10	6.781	.538	.223
5.5	.525	.14E+10	6.527	.525	.270
6.0	.673	.18E+10	6.191	.506	.331
6.5	.863	.23E+10	5.752	.478	.411
7.0	1.105	.29E+10	5.182	.441	.516
7.5	1.415	.37E+10	4.446	.391	.650
8.0	1.812	.48E+10	3.500	.326	.823
8.5	2.316	.62E+10	2.293	.241	1.044
9.0	2.949	.78E+10	.785	.135	1.320
9.5	3.406	.91E+10	.019	.086	1.460
10.0	3.642	.97E+10	.017	.094	1.461
10.5	3.876	.10E+11	.016	.103	1.461
11.0	4.107	.11E+11	.014	.111	1.461
11.5	4.335	.12E+11	.013	.119	1.462
12.0	4.560	.12E+11	.012	.127	1.462
12.5	4.783	.13E+11	.011	.134	1.462
13.0	5.002	.13E+11	.011	.142	1.462
13.5	5.219	.14E+11	.010	.149	1.462
14.0	5.433	.14E+11	.009	.156	1.462
14.5	5.645	.15E+11	.009	.163	1.462
15.0	5.853	.16E+11	.008	.170	1.462
15.5	6.060	.16E+11	.008	.176	1.463
16.0	6.263	.17E+11	.007	.183	1.463
16.5	6.464	.17E+11	.007	.189	1.463



Table A6 (cont'd).

EXPERIMENT 3

TIME (HR)	XF (G/L)	NF (CELLS/ML)	SF (G/L)	AF (G/L)	PF (G/L)
— BATCH GROWTH —					
0.0	.029	.60E+08	8.200	.800	.014
.5	.037	.82E+08	8.171	.798	.019
1.0	.047	.11E+09	8.134	.795	.026
1.5	.060	.14E+09	8.086	.792	.035
2.0	.077	.19E+09	8.025	.787	.046
2.5	.099	.25E+09	7.946	.782	.061
3.0	.127	.32E+09	7.845	.774	.079
3.5	.163	.42E+09	7.716	.765	.103
4.0	.209	.54E+09	7.551	.753	.133
4.5	.268	.70E+09	7.339	.738	.172
5.0	.343	.90E+09	7.067	.718	.221
— 5.3 — START MICROFILTRATION - RESIDENCE TIME = 2.94 HR —					
5.5	.440	.12E+10	6.799	.691	.267
6.0	.563	.15E+10	6.575	.659	.301
6.5	.722	.19E+10	6.270	.623	.350
7.0	.925	.25E+10	5.865	.582	.419
7.5	1.185	.32E+10	5.334	.534	.512
8.0	1.518	.40E+10	4.644	.476	.634
8.5	1.944	.52E+10	3.754	.405	.794
9.0	2.486	.66E+10	2.614	.316	1.000
9.5	3.171	.85E+10	1.177	.208	1.261
10.0	3.836	.10E+11	.029	.123	1.469
10.5	4.182	.11E+11	.025	.127	1.468
11.0	4.524	.12E+11	.021	.130	1.467
11.5	4.861	.13E+11	.019	.134	1.467
12.0	5.195	.14E+11	.017	.139	1.466
12.5	5.524	.15E+11	.016	.144	1.466
13.0	5.849	.16E+11	.014	.149	1.465
13.5	6.170	.16E+11	.013	.154	1.465
14.0	6.487	.17E+11	.012	.160	1.464
14.5	6.800	.18E+11	.011	.165	1.464
15.0	7.109	.19E+11	.010	.171	1.464
15.5	7.414	.20E+11	.010	.176	1.464
16.0	7.715	.21E+11	.009	.182	1.464
16.5	8.013	.21E+11	.009	.187	1.464
17.0	8.307	.22E+11	.008	.193	1.463
17.5	8.598	.23E+11	.008	.199	1.463
18.0	8.884	.24E+11	.007	.204	1.463
18.5	9.168	.24E+11	.007	.210	1.463
19.0	9.447	.25E+11	.007	.215	1.463
19.5	9.723	.26E+11	.006	.221	1.463
20.0	9.996	.27E+11	.006	.226	1.463
20.5	10.266	.27E+11	.006	.232	1.463



Table A6 (cont'd).

EXPERIMENT 4					
TIME (HR)	XF (G/L)	NF (CELLS/ML)	SF (G/L)	AF (G/L)	PF (G/L)
BATCH GROWTH					
0.0	.039	.72E+08	8.200	.530	0.000
.5	.049	.10E+09	8.161	.527	.007
1.0	.063	.14E+09	8.111	.524	.016
1.5	.081	.19E+09	8.046	.519	.028
2.0	.104	.25E+09	7.964	.513	.043
2.5	.133	.33E+09	7.858	.505	.063
3.0	.171	.43E+09	7.723	.496	.087
3.5	.219	.56E+09	7.549	.483	.119
4.0	.281	.72E+09	7.327	.467	.160
4.5	.360	.93E+09	7.041	.446	.212
5.0	.462	.12E+10	6.676	.420	.279
— 5.1 — START MICROFILTRATION - RESIDENCE TIME = 1.58 HR —					
5.5	.592	.16E+10	8.447	.607	.288
6.0	.759	.20E+10	9.977	.770	.305
6.5	.973	.26E+10	10.945	.878	.344
7.0	1.248	.33E+10	11.462	.943	.407
7.5	1.601	.42E+10	11.596	.974	.497
8.0	2.053	.55E+10	11.385	.973	.620
8.5	2.633	.70E+10	10.834	.944	.782
9.0	3.377	.90E+10	9.923	.886	.993
9.5	4.330	.12E+11	8.608	.797	1.266
10.0	5.551	.15E+11	6.818	.672	1.617
10.5	7.112	.19E+11	4.456	.505	2.066
11.0	9.091	.24E+11	1.436	.289	2.632
11.5	10.813	.29E+11	.049	.200	2.894
12.0	12.145	.32E+11	.039	.214	2.903
12.5	13.460	.36E+11	.032	.228	2.909
13.0	14.758	.39E+11	.027	.242	2.914
13.5	16.040	.43E+11	.023	.256	2.917
14.0	17.306	.46E+11	.021	.270	2.919
14.5	18.557	.50E+11	.018	.283	2.921
15.0	19.791	.53E+11	.016	.296	2.922
15.5	21.011	.56E+11	.015	.309	2.923
16.0	22.215	.59E+11	.014	.322	2.924
16.5	23.405	.63E+11	.013	.335	2.925
17.0	24.580	.66E+11	.012	.348	2.925
17.5	25.740	.69E+11	.011	.360	2.925
18.0	26.886	.72E+11	.010	.372	2.926
18.5	28.017	.75E+11	.010	.384	2.926
19.0	29.135	.78E+11	.009	.396	2.926

Table A6 (cont'd).

11/02/83 MSU HUSTLER 2 LSD 52.49 11/22/83 CYBER751
 15.02.08.1854689
 15.02.08.JOE READ - 11/02/83 .25.01.49.
 15.02.08.GPULKE, JC19.
 15.02.09.LAST ACCESS - B 14.53 11/02/83
 15.02.09.RUNS - 0871 PPGOL AR BALANCE \$ 0063.79
 15.02.09.JO0096 CARDS READ VALUE \$000000.14
 15.02.09.RP CCL CBL CCCCJJC.002 MAXFL 026300
 15.02.09.CP-PP SEC. .080- .021 \$.00
 15.02.09.FTNS.08.
 15.02.21. 64700 CM STORAGE USED.
 15.02.21. J.221 CP SECONDS COMPILATION TIME.
 15.02.21.RP 0000077 CCCCJJC.3076 MAXFL .60700
 15.02.21.CP-PP SEC. .221- 9.343 \$.22
 15.02.26.LGC.
 15.02.27.EXEC BEGUN.15.02.27.
 15.03.13.STOP
 15.03.13. 24200 MAXIMUM EXECUTION FL.
 15.03.13. 3.962 CP SECONDS EXECUTION TIME.
 15.03.13.MAX FILES 006 MAX PRUS 0001000.
 15.03.13.RP 0000028 CCCCJJC.002 MAXFL 034000
 15.03.13.PP 14.152 SEC.
 15.03.13.CP USE 4.424 SEC VALUE \$.86
 15.03.13.PP USE 1.170 SEC VALUE \$.03
 15.03.13.CM USE 1.923 M-H VALUE \$.46
 15.03.13.TOTAL COMPITE VALUE AT RG2 \$ 1.34
 15.03.51.000009 PAGES PRINT. 000305 LINES PRINT. FOR \$ 000.33

LITERATURE CITED



LITERATURE CITED

- Aiba, S., Shoda, M., and Nagatani, M., "Kinetics of Product Inhibition in Alcohol Fermentation," Biotechnology and Bioengineering, 10, 845 (1968).
- Amarasingham, C. R. and Davis, B. D., "Regulation of α -Ketoglutarate Dehydrogenase Formation of *Escherichia coli*," Journal of Biological Chemistry, 240, 3664 (1965).
- Andrews, J. F., "A Mathematical Model for the Continuous Culture of Microorganisms Utilizing Inhibiting Substrates," Biotechnology and Bioengineering, 10, 707 (1968).
- Bailey, J. E., and D. F. Ollis. Biochemical Engineering Fundamentals. McGraw-Hill: 1977.
- Beck, C., and von Meyenberg, H. K., "Enzyme Pattern and Aerobic Growth of *Saccharomyces cerevisiae* Under Various Degrees of Glucose Limitation," Journal of Bacteriology, 96, 479 (1968).
- Bijkerk, H. E. and Hall, R. J., "A Mechanistic Model of Aerobic Growth of *Saccharomyces cerevisiae*," Biotechnology and Bioengineering, 24, 267 (1977).
- Bolivar, F., Rodriques, R. L., Betlach, M. C., and Boyer, H. W., "Construction and Characterization of New Cloning Vehicles I. Ampicillin-Resistance Derivatives of the Plasmid pMB9," Gene, 2, 75 (1977a).
- Bolivar, F., Rodriguez, R. L., Greene, P. J. Betlach, M. C., Heyneker, H. L., Boyer, H. W., Crosa, J. H., and Falkow, S., "Construction and Characterization of New Cloning Vehicles II. A Multipurpose Cloning System," Gene, 2, 95 (1977b).
- Bolivar, F., and Backman, K., "Plasmids of *Escherichia coli* as Cloning Vectors," Methods in Enzymology, 68, 245 (1979).
- Boyer, H. W. and Roulland-Dussoix, D., "A Complementation Analysis of the Restriction and Modification of DNA in *Escherichia coli*," Journal of Molecular Biology, 41, 459 (1969).
- Charley, R. C., Fein, J. C., Lavers, B. H., Lawford, H. G., and Lawford, G. L., "Optimization of Process Design for Continuous Ethanol Production in *Zymomonas mobilis* ATCC 29191," Biotechnology Letters, 5, 169 (1983).



- Chesney, A. M., "The Latent Period in the Growth of Bacteria," J. of Exp. Med., 24, 387 (1916).
- Coulman, G. A., Stieber, R. W., and Gerhardt, P., "Dialysis Continuous Process for Ammonium-Lactate Fermentation of Whey: Mathematical Model and Computer Simulation," Applied and Environmental Microbiology, 34, 725 (1977).
- Doelle, H. W., Ewings, K. N., and Hollywood, N. W., "Regulation of Glucose Metabolism in Bacterial Systems," Advances in Biochemical Engineering, 23, 1 (1982).
- Doelle, H. W., Hollywood, N., and Westwood, A. W., "Effect of glucose concentration in a number of enzymes involved in the aerobic and anaerobic utilization of glucose in turbidostat cultures of *Escherichia coli*," Microbios, 9, 221 (1974).
- Dostálek, M. and Häggstrom, M., "A Filter-Fermentor-Apparatus and Control Equipment," Biotechnology and Bioengineering, 24, 2077 (1982).
- Dubois, M., Gilles, K. A., Hamilton, J. K., Rebers, P. A., and Smith, F., "Colorimetric Method for Determination of Sugars and Related Substances," Analytical Chemistry, 28, 350 (1955).
- Endo, I., Nagamune, F., and Inoue, I., "Start-up of the Chemostat Culture," Annals of the New York Academy of Sciences, 369, 245 (1981).
- Faber, M., "Meeting Report: Cornell Scientists Clone, Express Cellulase Genes in *E. coli*," Biotechnology, 1, 139 (1983).
- Franson, M. A. (ed). Standard Methods for the Examination of Water and Wastewater. 14th edition. American Public Health Association: 1976.
- Gaden, E. L., "Fermentation Process Kinetics," Journal of Biochemical and Microbiological Technology and Engineering, 1, 413 (1959).
- Gerhardt, P., R. G. E. Murphy, R. N. Costilow, E. W. Nester, W. A. Wood, N. R. Krieg, G. B. Phillips. Manual of Methods for General Bacteriology. American Society for Microbiology: 1981.
- Henry, J. D. and Allred, R. C., "Concentration of Bacterial Cells by Cross Flow Filtration," Developments in Industrial Microbiology, 13, 177 (1972).
- Herbert, D., Elsworth, R., and Telling, R. C., "The Continuous Culture of Bacteria; a Theoretical and Experimental Study," Journal of General Microbiology, 14, 601 (1956).



- Hollywood, N., and Doelle, H. W., "Effect of specific growth rate and glucose concentration on growth and glucose metabolism of *Escherichia coli* K-12," Microbios, 17, 23 (1976).
- Holzberg, I., Finn, R. K., and Steinkraus, K. H., "A Kinetic Study of the Alcohol Fermentation of Grape Juice," Biotechnology and Bioengineering, 9, 413 (1967).
- Ingraham, J. L., O. Maaloe, F. C. Neidhardt. Growth of the Bacterial Cell. Sihauer Associates, Inc.: 1983.
- Johnson, M., "Isolation and Properties of a Pure Yeast Poly-peptidase," Journal of Biological Chemistry, 137, 575 (1941).
- Johnson, R. R., Balwani, T. L., Johnson, L. J., McClure, K. E., and Dehority, B. A., "Corn Plant Maturity. II. Effect on *in vitro* Cellulose Digestibility and Soluble Carbohydrate Content," J. of Animal Science, 25, 617 (1956).
- Kossen, N. W. F., "Mathematical Modelling of Fermentation Processes: Scope and Limitations," Symp. Soc. Gen. Microbiology, 29, 327 (1979).
- Landwall, P. and Holme, F., "Removal of Inhibitors by Dialysis Culture," Journal of General Microbiology, 103, 345 (1977).
- Levenspiel, O., "The Monod Equation: A Revisit and a Generalization to Product Inhibition Situations," Biotechnology and Bioengineering, 22, 1671 (1980).
- Lodge, R. M. and Hinshelwood, C. N., "The Lag Phase of *Bact. Lactis Aerogenes*," J. Chem. Soc., 213 (1943).
- Luedeking, R. and Piret, E. L., "A Kinetic Study of the Lactic Acid Fermentation. Batch Process at Controlled pH," Journal of Biochemical and Microbiological Technology and Engineering, 1, 393 (1959).
- Marr, A. G., Nilson, E. H., and Clark, D. J., "The Maintenance Requirement of *Escherichia coli*," Annals of the New York Academy of Science, 122, 536 (1963).
- Mateles, R. I., Ryu, D. Y., and Yasuda, T., "Measurement of Unsteady State Growth of Micro-organisms," Nature, 208, 263 (1965).
- Monod, J., "The Growth of Bacterial Cultures," Ann. Review of Microbiology, 3, 371 (1949).

- Montgomery, R., "Further studies of the phenol-sulfuric acid reagent for carbohydrates," Biochim. Biophys. Acta, 48, 591 (1961).
- Pamment, N. B. and Hall, R. J., "Absence of External Causes of Lag in *Saccharomyces cerevisiae*," J. of Gen. Microbiology, 105, 297 (1978).
- Pamment, N. B., Hall, R. J., and Barford, J. P., "Mathematical Modeling of Lag Phases in Microbial Growth," Biotechnology and Bioengineering, 20, 349 (1978).
- Penfold, W. J., "On the Nature of Bacterial Lag," J. of Hygiene, 14, 215 (1914).
- Peringer, P., Blachere, H., Corrieu, G., and Lane, A. G., "Mathematical Model of the Kinetics of Growth of *Saccharomyces cerevisiae*," Biotechnology and Bioengineering Symposium, 4, 27 (1973).
- Peringer, P., Blachere, H., Corrieu, G., and Lane, A. G., "A Generalized Mathematical Model for the Growth Kinetics of *Saccharomyces cerevisiae* with Experimental Determination of Parameters," Biotechnology and Bioengineering, 16, 431 (1974).
- Pirt, S. J., and Kurowski, W. M., "An Extension of the Theory of the Chemostat with Feedback of Organisms. Its Experimental Realization with a Yeast Culture," Journal of General Microbiology, 63, 357 (1970).
- Repaske, R., Repaske, A. C., and Mayer, R. D., "Carbon Dioxide Control of Lag Period and Growth of *Streptococcus sanguis*," J. of Bacteriology, 117, 652 (1974).
- Rogers, P. L., Lu, K. J., Shotnicki, M. L., and Tribe, D. E., "Ethanol Production by *Zymomonas mobilis*," Advances in Biochemical Engineering, 23, 37 (1982).
- Sortland, L. D. and Wilke, C. R., "Growth of *Streptococcus faecalis* in Dense Culture," Biotechnology and Bioengineering, 11, 805 (1969).
- Stanier, B. Y., E. A. Adelberg, J. Ingraham, The Microbial World, 4th edition, Prentice-Hall: 1976.
- Stieber, R. W., and Gerhardt, P., "Continuous Process for Ammonium-lactate Fermentation of Deproteinized Whey," Journal of Dairy Science, 62, 1558 (1979).
- Supelco, Inc., "Extraction Procedures for GC Analysis of Culture By-products for Volatile Acids and Alcohols," Supplement to Bulletin 748G, 1975.

- Swanson, C. H., Aris, R., Fredrickson, A. G., and Tsuchija, H. M., "Bacterial Growth as an Optimal Process," J. of Theo. Biology, 12, 220 (1966).
- Tanny, G. B., Merilman, D., and Pistole, T., "Improved Filtration Technique for Concentrating and Harvesting Bacteria," Applied and Environmental Microbiology, 40, 269 (1980).
- Watson, D. C., and Berry, D. R., "Use of an Exchange Filtration Technique to Obtain Synchronous Sporulation in an Extended Batch Fermentation," Biotechnology and Bioengineering, 21, 213 (1979).
- Yang, R. D., and Humphrey, A. E., "Dynamic and Steady State Studies of Phenol Biodegradation in Pure and Mixed Cultures," Biotechnology and Bioengineering, 17, 1211 (1975).

MATERIAL BIBLIOGRAPHY

Material Bibliography

1M	American Instrument Company, Inc. Silver Springs, Maryland	Peristaltic pump
2M	Beckman Instruments Inc. Fullerton, California	Spectrophotometer Model DB-G
3M	Cole-Parmer Instrument Co. Chicago, Illinois	Masterflex Variable Speed System Cat. No. 7549-19
4M	Difco Laboratories Detroit, Michigan	Plate Count Agar
5M	Drexelbrook Engineering Co. Horsham, Pennsylvania	Level Transmitter Model YC 508-25-2
6M	Gelman Sciences, Inc. Ann Arbor, Michigan	Acroflux Capsule
7M	Leeds and Northrup North Wales, Pennsylvania	Autoclavable pH electrodes
8M	Leeds and Northrup North Wales, Pennsylvania	Current controller Centry Model 440- -1-20-33-51-A104
9M	Linear Instrument Corporation Reno, Nevada	Chart Recorder Model 141
10M	New Brunswick Scientific Company New Brunswick, New Jersey	Microferm fermentor
11M	New Brunswick Scientific Company New Brunswick, New Jersey	pH Controller Model pH-40
12M	Sigma Chemical Company St. Louis, Missouri	Antifoam A concentrate
13M	Sigmamotor Middleport, New York	Peristaltic pump Model T-6S
14M	Supelco, Inc. Bellefonte, Pennsylvania	Volatile Acid Standard Mix
15M	Supelco, Inc. Bellefonte, Pennsylvania	Column Packing SP-1000 on 100/120 Chromosorb W AW

16M	Supelco, Inc. Bellefonte, Pennsylvania	Non-volatile Acid Mix
17M	Supelco, Inc. Bellefonte, Pennsylvania	Column Packing 15% DEGS on 80/100 Chromosorb W AW
18M	Varian Associates Walnut Creek, California	Gas Chromatograph Series 1400
19M	Varian Associates Walnut Creek, California	Integrator CDS-111

MICHIGAN STATE UNIVERSITY LIBRARIES



3 1293 03061 2075